FUNCTIONAL AND PHARMACOLOGICAL IMPORTANCE OF THE COMPOSITE ATP BINDING SITE 1 IN CFTR CHLORIDE CHANNELS

A Dissertation presented to the Faculty of the Graduate School

University of Missouri-Columbia

In Partial Fulfillment

Of the Requirements for the Degree

Doctor of Philosophy

---

by

MING-FENG TSAI

Dr. Tzyh-Chang Hwang, Dissertation Supervisor

DECEMBER 2010

The undersigned, appointed by the Dean of the Graduate School, have examined the dissertation entitled

FUNCTIONAL AND PHARMACOLOGICAL IMPORTANCE OF THE COMPOSITE ATP BINDING SITE 1 IN CFTR CHLORIDE CHANNELS

Presented by Ming-Feng Tsai

A candidate for the degree of Doctor of Philosophy

And hereby certify that in their opinion it is worthy of acceptance.

Professor Tzyh-Chang Hwang

Professor Kevin Gillis

Professor Mark Milanick

Professor Luis Polo-Parada

Professor Xiaoqin Zou

ACKNOWLEDGEMENTS

In the past three years of my graduate career, there are many people who have made important contributions to my research work. It is because of all these helps that I can accumulate sufficient materials and gain necessary skills for composing this dissertation smoothly.

First and foremost I must thank TC Hwang, my advisor, for his guidance, patience, and instruction during these years. His directions help me tremendously in developing abilities necessary for pursuing an academic career, including those capabilities of critical thinking, effective presentation, and being independent.

I would like to extend my thanks to other members in my graduation committee, Kevin Gillis, Mark Milanick, Luis Polo-Parada, and Xiaoqin Zou, for attending my committee meetings and seminars as well as providing me valuable comments and advises during or after these events.

Many thanks to the members of the Hwang lab. It has always been a wonderful place to work. I especially thank Hiroyasu Shimizu, now an Associate Professor in Osaka Medical College, for working with me around the clock in my early days in the lab. The findings during that period set the groundwork for my following research. Collective thanks to each of the Hwang lab members: Min Li, Shenghui Hu, Cindy Chu, Silvia Bompadre, Zoia Kopeikin, Xiaohui Wang, Yonghong Bai, Haruna Miki, and

Kang-Yang Jih. I will miss the conversations about our lives, helping with each others problems, and all happy moments we have shared with.

I must not forget my beloved parents who always trust and support me for any of my major decisions in my life. Thanks for your endless love and providing me a warm and nurturing growing environment, where knowledge of all types are valued. Graciously, I thank my thoughtful and loving fiancée, Jian Yin. She has put up with my gluttony for work in the last two years and still loves me somehow. I thank her for always keeping me smile. Without her, the life here would not be so colorful.

Thanks for many friends I have made and professors I have had here at University of Missouri - Columbia. These people were instrumental in shaping my life as a scientist. Thank you all so much!

TABLE OF CONTENTS

LIST OF FIGURES

Figure **Page**

FUNCTIONAL AND PHARMACOLOGICAL IMPORTANCE OF THE COMPOSITE ATP BINDING SITE 1 IN CFTR CHLORIDE CHANNELS

Ming-Feng Tsai

Dr. Tzyh-Chang Hwang, Dissertation Supervisor

ABSTRACT

The cystic fibrosis transmembrane conductance regulator (CFTR) is a chloride ion channel whose defects cause the deadly genetic disease cystic fibrosis (CF). Like other ATP binding cassette (ABC) proteins, CFTR encompasses two cytoplasmic nucleotide binding domains (NBDs). Upon ATP binding, the two NBDs can coalesce into a head-to-tail dimer with ATP buried at two interfacial composite sites (sites 1 and 2). Although evidence suggests that gating of CFTR is mainly controlled by site 2, the role of site 1 remains less understood. I have used pyrophosphate as a probe or adopted a ligand exchange protocol to investigate ATP binding status in site 1 in real time. With these novel approaches, I have identified a "partial" NBD dimer state mediated by an ATP molecule tightly bound in site 1. A molecular model of CFTR gating was then established with opening and closing of CFTR coupled to the formation and partial separation of the NBD dimer. Moreover, I discovered several mutations that enhance ATP binding in site 1 and demonstrated that the activity of CF-associated mutant channels, ΔF508- and G551D-CFTR, can be significantly improved by these mutations, thus providing evidence that site 1 is a potential target for developing pharmaceutical reagents to treat patients with CF.

CHAPTER 1

INTRODUCTION

1-1. The Importance of CFTR as a Research Subject

The debilitating genetic disease cystic fibrosis (CF) is caused by dysfunctions of a chloride ion channel, cystic fibrosis transmembrane conductance regulator (CFTR) (Riordan et al., 1989). Chloride permeation through CFTR channels is necessary for normal physiological functions of epithelial cells lining tubular structures such as airways, pancreatic ducts, and sweat glands (Bradbury, 1999). In CF patients, the transepithelial anion flow is severely impaired, and subsequent defects in salt and water transport result in dehydrated mucus obstructing small airways. The resulting bacterial infections and destruction of the lung are usually the ultimate cause of mortality (Rowe and Miller, 2005). On the other extreme of the CFTR-related disease spectrum, increased activity of CFTR in the intestinal epithelia, often caused by bacterial toxins, results in secretory diarrhea which claims thousands of lives each year in developing countries (Sears and Kaper, 1996). *Thus, a thorough understanding of how CFTR channels work could have a broad impact on future development of therapeutics for treatment of CFTR-related diseases.*

When CFTR was first cloned in 1989, analysis of the amino acid sequence immediately placed CFTR as a member of the ATP binding cassette (ABC) protein

superfamily (Riordan et al., 1989). Among thousands of ABC proteins, only CFTR functions as an ion channel, while nearly all the remaining ABC proteins are transporters mediating active transports. Biochemical and structural advances in the study of ABC proteins have long provided a framework for us to investigate the molecular mechanism underlying the opening and closing (gating) of CFTR channels. On the other hand, *high resolution electrophysiological studies of CFTR at the single-molecule level also represent a unique opportunity to understand how other ABC proteins work.*

In the following chapters, a series of studies on CFTR channels are presented. The results led to the identification of a partial NBD dimer state, which represents the closed state upon CFTR gating. The existence of this state likely extends to a subset of ABC proteins to which CFTR belongs, and perhaps also to other members in the entire protein superfamily. Thus, it would be of great interest for scientists in the ABC protein field to investigate the functional relevance of this partial NBD dimer state. The experimental results also indicated that site 1 formed by NBDs can be a potential target for developing effective potentiators for CFTR channels. These findings with recent advances in determining NBD structures could pave the way for rational drug design to treat patients with CF in the future.

1-2. Overview of CFTR Structure-Function Relationship

The CFTR, like other ABC proteins, has a prototypical structure containing two nucleotide binding domains (NBD1 and NBD2) and two transmembrane domains

(TMD1 and TMD2), each formed typically by six membrane-spanning α-helices (Fig. 1-1). In addition to this core architecture, CFTR incorporates, between NBD1 and TMD2, a unique regulatory (R) domain, phosphorylation of which by protein kinase A is necessary for CFTR to function (Gadsby and Nairn, 1999).

All members in the ABC protein family, including CFTR, utilize the energy of ATP hydrolysis to perform their specific function. NBDs have evolved to harvest the free energy of ATP binding and hydrolysis to drive conformational changes associated with different functional states of ABC proteins. On the other hand, the structure of TMDs determines the physiological roles a particular ABC protein assumes. For example, as a chloride channel, the TMDs of CFTR are equipped with an anion-permeant pore for chloride movement across the membrane as well as a gate that opens and closes the permeation pathway.

One major breakthrough that allows CFTR investigators to get a glimpse of how ATP binding/hydrolysis events in NBDs are coupled to the function of CFTR is solving the high-resolution crystal structure of several full-length ABC transporters (Hollenstein et al., 2007; Oldham et al., 2008; Rees et al., 2009). It has been shown that the monomeric NBD1 and NBD2 in the nucleotide-free state can assemble into a dimer upon ATP binding, while subsequent ATP hydrolysis breaks the dimeric structure. Moreover, it is observed that the substrate binding site of the TMDs is exposed to different sides of the cell membrane in the ATP-bound or ATP-free states. Thus, these crystallographic data have led to a proposition that the ATP-fueled movements of NBDs (i.e. between monomeric and dimeric states) drive the

FIGURE 1-1

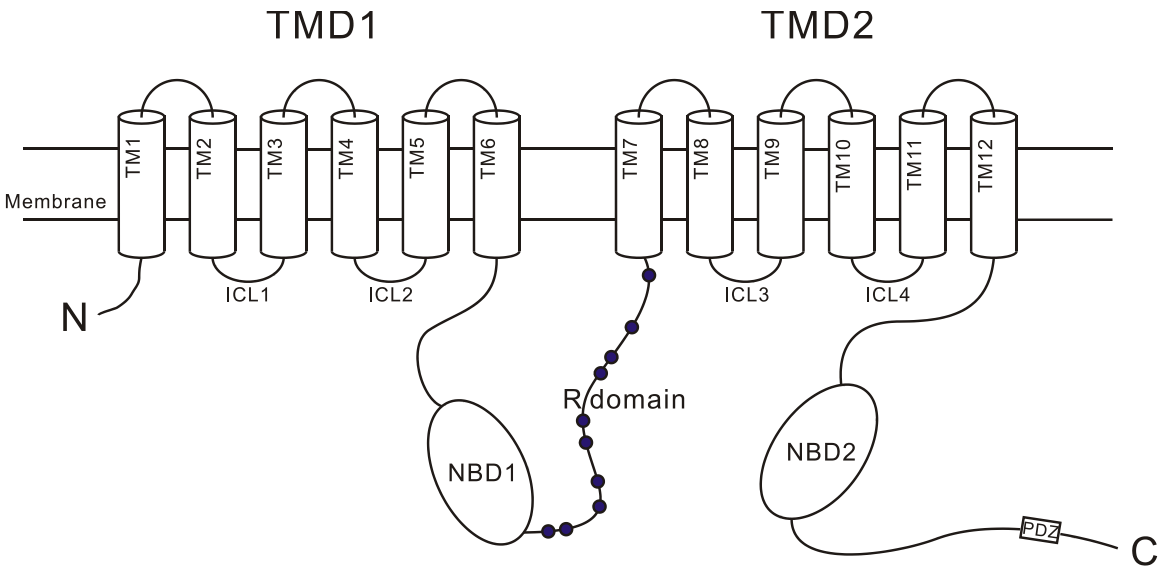

Figure 1-1. The topological model emphasizing the domain structure of a CFTR protein. Each transmembrane domain of CFTR contains transmembrane (TM) helices, intracellular (ICL) loops, and extracellular loops. Between NBD1 and TMD2 is the cytoplasmic R-domain, which contains multiple consensus sites (represented by black spheres) for PKA phosphorylation.

.

"alternating access" of ABC transporters' TMDs, allowing substrates to be transported from one side of the membrane to the other side (Fig. 1-2). Based on this idea as well as further electrophysiological and biochemical studies (Vergani et al., 2005; Mense et al., 2006; Gadsby et al., 2006), it has been proposed that the formation and separation of the NBD dimer are coupled to the repeated switch of CFTR's TMDs between open and closed pore conformations (Fig. 1-2).

1-3. CFTR as an Atypical ABC Protein: Structural Asymmetry between Two Composite Sites

The molecular model for ABC transporters' function (Fig. 1-2), however, should be applied to CFTR with additional cautions considering the fact that CFTR belongs to a subgroup of "atypical" or "asymmetrical" ABC proteins.

The NBDs for both classical and atypical ABC proteins share some common features. First, the monomeric NBDs can be divided into two subdomains. There is a larger core ("head") subdomain consisting of several ATP-interacting motifs (Walker motifs) that mediate ATP binding and hydrolysis. There is also a smaller helical ("tail") subdomain, containing the signature motif (consensus: LSGGQ), so-called because it is the hallmark of ABC proteins. Second, the two NBDs of an ABC protein are so arranged that the head subdomain from one NBD faces the tail subdomain from the other NBD. Upon ATP binding to the head subdomains, the two NBDs coalesce into a head-to-tail dimer with two ATP molecules buried at two

FIGURE 1-2

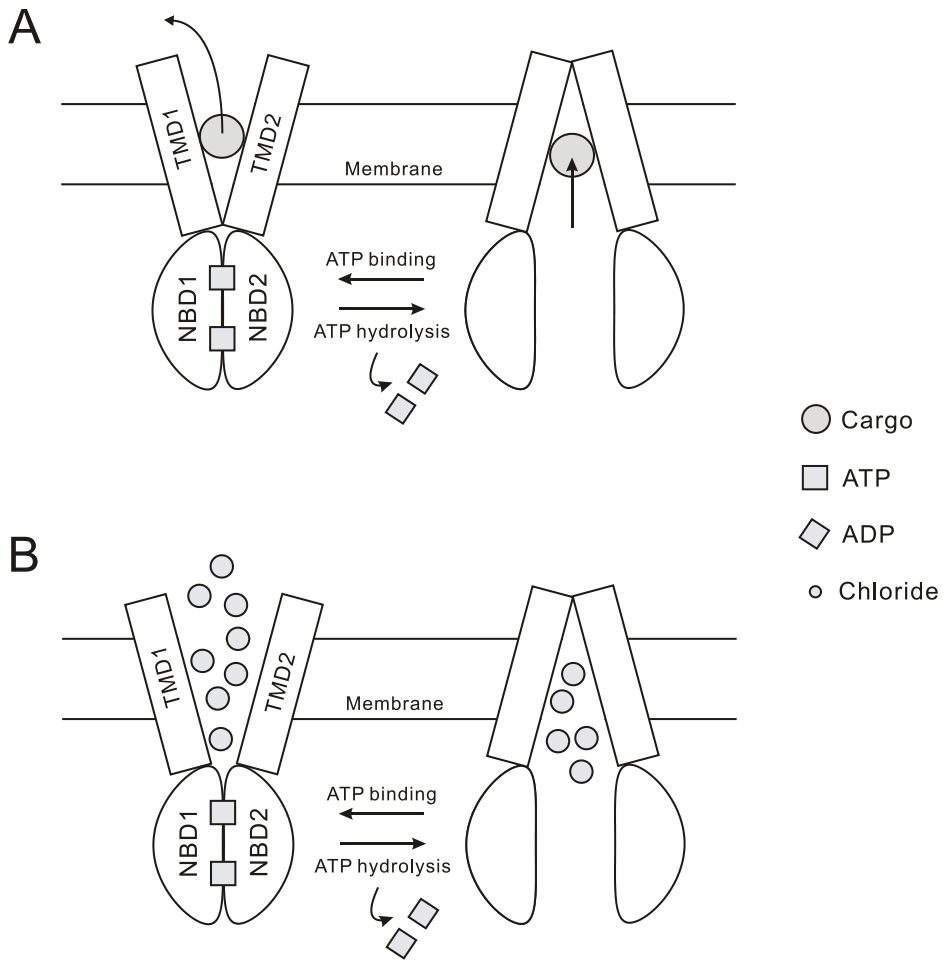

Figure 1-2. A structure based model of the transport mechanism for ABC proteins. **(A)** The formation and separation of the NBD dimer driven by ATP binding and hydrolysis are coupled to the outward- and inward-facing conformations of the TMDs, allowing the substance to bind from extracellular side and to be released to the cytoplasmic side of the cell membrane. **(B)** Similarly, it is proposed that NBDs switch between dimeric and monomeric states to open and close CFTR channels.

interfacial composite sites: site 1 formed by the head of NBD1 and the tail of NBD2 while site 2 formed by the head of NBD2 and the tail of NBD1 (Fig. 1-3).

Despite these similarities of CFTR and classical ABC proteins in basic NBD architecture and in the configuration of dimerization, a close inspection of the amino-acid sequence of CFTR's NBDs reveals significant deviations in some motifs from the consensus sequences of ABC proteins (Lewis et al., 2004). This property is not unique to CFTR but is also seen in other "atypical" ABC proteins in eukaryotes (Jha et al., 2004; Zhang et al., 2006; Park et al., 2008; Procko et al., 2009) and, less frequently, in bacteria (Lubelski et al., 2006). Strikingly, the deviations in almost all cases are "asymmetrically" restricted to only one composite site but not the other. Thus, one composite site will be formed exclusively by conserved motifs, while the other contains non-consensus substitutions in several motifs. For CFTR, site 1 harbors all non-consensus substitutions (Fig. 1-3). Two critical residues for ATP hydrolysis in NBD1's head subdomain are replaced by serine. Additionally, the consensus signature motif LSGGQ becomes LSHGH in NBD2's tail subdomain.

The expected consequence of these substitutions is a severely impaired ability for CFTR's site 1 to catalyze ATP hydrolysis. Thus, upon NBD dimerization, it's likely that only one interfacial ATP molecule (i.e. that bound in site 2) will be hydrolyzed rapidly, while the other may remain intact for a substantial amount of time. This line of thinking immediately leads to a possible presence of a single-ATP bound state, overlooked by the aforementioned molecular model (Fig. 1-2), where the NBDs of an ABC protein switch between a two-ATP bound dimeric state and a nucleotide-free

monomeric state. Thus intriguing questions rise. What is the NBD configuration of this single-ATP bound intermediate state? How stable is it? What is its functional role? How is it related to the molecular model (Fig. 1-2) described above?

1-4. Methods to Investigate the Single-ATP Bound State

To answer these questions, the challenging tasks are to isolate, detect, and characterize the single-ATP bound intermediate. In this case, X-ray crystallography may not be the best approach as proteins are usually crystallized in most stable conformational states. Photolabelling experiments (Aleksandrov et al., 2002; Basso et al., 2003; Aleksandrov et al., 2008) have been employed to demonstrate an occlusion phenomenon of CFTR where 8-azido-ATP is observed to bind in NBD1 for tens of minutes. Nonetheless, potential pitfalls of these biochemical experiments include unknown functional and maturation status of the sampled CFTR protein, limited time resolution, and the difficulty of quantifying the efficiency of labeling. Electrophysiological methods, with the exceptional power of real-time recording of ion channel gating transitions, could be a promising approach to tackle these issues. However, the difficulty lies in the observation that opening and closing of CFTR mainly reflects molecular events in site 2 instead of ligand binding and unbinding in site 1 (Powe et al., 2002; Zhou et al., 2006). In other words, recording steady-state CFTR gating will provide limited information about ATP binding status in site 1, thus not allowing an assessment of the single ATP bound state.

That site 1 may have a longer ATP dwell time than site 2, due to substitutions in critical catalytic residues, indicates that the two composite sites of CFTR may have

FIGURE 1-3

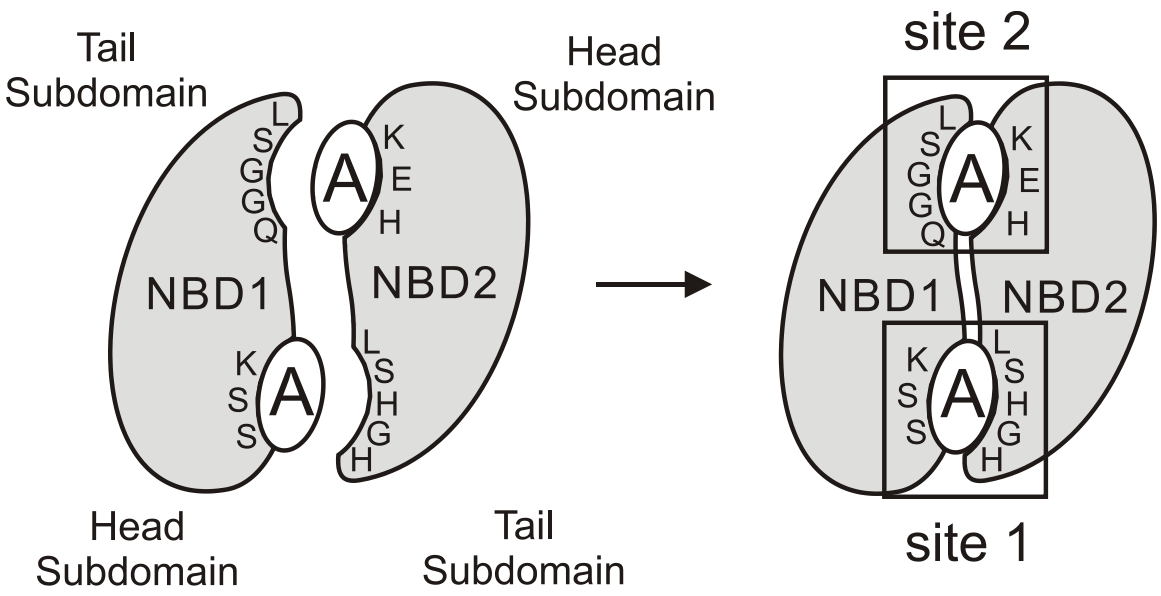

Figure 1-3. The formation of the head-to-tail dimer of atypical ABC proteins. A monomeric NBD can be divided into a head subdomain that binds ATP and a tail subdomain that contains the signature (LSGGQ) motif. Upon ATP binding the two NBDs can assemble into a head-to-tail dimer with ATP trapped at two interfacial composite sites, site 1 and site 2. Thus, each composite site is formed by the head of one NBD and the tail of the partner NBD. For atypical ABC proteins, there exist non-conserved substitutions in one composite. For instance, critical ATP-interacting motifs in CFTR's site 1 contains many substitutions, including a G → H and a Q → H mutations in NBD1's signature motif and a E → S mutation in NBD1's Walker B motif, which leads to impaired catalytic ability of site 1.

different relaxation times toward a new equilibrium upon breaking the steady-state condition. For example, removing the ATP solution from CFTR channels may result in rapid nucleotide releasing from site 2 but slow ATP dissociation from site 1. Similarly, changing the ligands supplied to CFTR channels may lead to a rapid ligand exchange in site 2 but a slower exchange in site 1. Acquiring the time period required for site 1 to reach a new equilibrium can theoretically give the ATP dwell time in site 1 and thus provides an estimation of the life-time (i.e. stability) of the single ATP bound intermediate state of CFTR. However, this could be technically challenging, as to measure the relaxation time by electrophysiological experiments, it's necessary to have a probe that reports the progress of site 1 toward a new equilibrium. For instance, upon removal of ATP, CFTR channels shut within 1 s due to rapid ATP hydrolysis in site 2. A special experimental design is thus needed to enable tracking the "invisible" dissociation of ATP from site 1.

In chapter 2, I present different modes of CFTR gating elicited by the inorganic pyrophosphate (PPi). I demonstrated that by binding to site 2, PPi induces short ($\tau \sim 1$ s) openings in the absence of ATP but locks CFTR in the open state ($\tau \sim 30$ s) when site 1 is pre-occupied by an ATP molecule. This ability of PPi to differentiate the presence or absence of ATP in site 1 allows me to monitor the releasing of ATP from site 1 by applying PPi at different time points after CFTR channels are closed upon withdrawal of ATP. Interestingly, in patches containing hundreds of channels, the number of closed channels being locked open by PPi decreased as the washout time was prolonged, suggesting that fewer channels have ATP remained bound in site 1. Fitting the number of channels responding robustly to PPi with a single

exponential function yielded a time constant of ~25 s, a number that estimates how long ATP can stay bound in site 1 when site 2 is vacant. Thus, this set of experiment demonstrated that the single ATP-bound intermediate state is extremely stable.

In chapter 3, a ligand exchange experiment was developed as an independent approach to investigate ATP binding status in site 1. In this experimental design, the steady state gating of CFTR by ATP was suddenly interrupted by changing the ligand to PATP, a high affinity ATP analogue. It has been shown that PATP accelerates openings of CFTR by interacting with site 2 while stabilizes the open state by binding to site 1 (Zhou et al., 2005; Tsai et al., 2009). Thus, it's expected that upon ATP/PATP exchange, the opening rate of CFTR will increase immediately while the open time will become longer only after the tightly-bound ATP molecule dissociates from site 1. This was indeed the case and I observed that it took an average of ~50 s for PATP to increase CFTR open time, indicating that ATP is able to occupy site 1 for tens of seconds without dissociation. Therefore, the experiment again confirmed the existence of a stable intermediate state with one ATP bound in CFTR's NBDs.

1-5. A New Molecular Model for CFTR Gating

Having demonstrated the extra-stable single ATP bound intermediate of CFTR, now the stage has been set to pose the question: What's the configuration of NBDs at this state? Although crystallographic studies have revealed a two-ATP bound dimeric state and a nucleotide-free monomeric state of NBDs, neither of the two conformations appears to provide a satisfactory structural basis. For instance, if the

NBDs assume a dimeric structure with only one ATP bound in site 1, this will effectively prevent ATP from reaching the vacant site 2. On the other hand, if the NBDs rest monomerically, it's also difficult to imagine that an ATP molecule can remain stayed in the exposed ATP binding site of monomeric NBDs (Lewis et al., 2004; Lewis et al., 2005) for tens of seconds. Thus, we hypothesized that the single ATP bound state represents a "partial" NBD dimer, where the interface between two NBDs is partially closed to lock an ATP molecule in site 1 while is partially open to facilitate ligand exchange in site 2 (Fig. 1-4). It follows that the two NBDs of CFTR seldom separate completely into the monomeric resting state.

The hypothesis that the NBD interface of CFTR remains at least partially closed to trap an ATP molecule in site 1 for tens of seconds can be tested by mutating residues in the two NBD subdomains that constitute site 1 (i.e. the tail subdomain of NBD2 and the head subdomain of NBD1). This maneuver is expected to alter the dissociation rate of the tightly bound ATP molecule if both subdomains are necessary for CFTR to retain ATP in site 1. Indeed, in chapters 2 and 3, using the same experimental protocols as described in section 1-4, I provided evidence that ATP binding in site 1 became much unstable when the interactions between ATP and either NBD1's ATP-interacting motifs or NBD2's signature motif were disrupted.

There is strong evidence that ATP-elicited opening of CFTR is coupled to the dimerization of NBDs (Vergani et al., 2005; Mense et al., 2006). It's also known that closure of CFTR is caused by hydrolysis of ATP in site 2 (Gadsby et al., 2006; Chen and Hwang, 2008). As this opening-closing cycle of CFTR is completed within 1

FIGURE 1-4

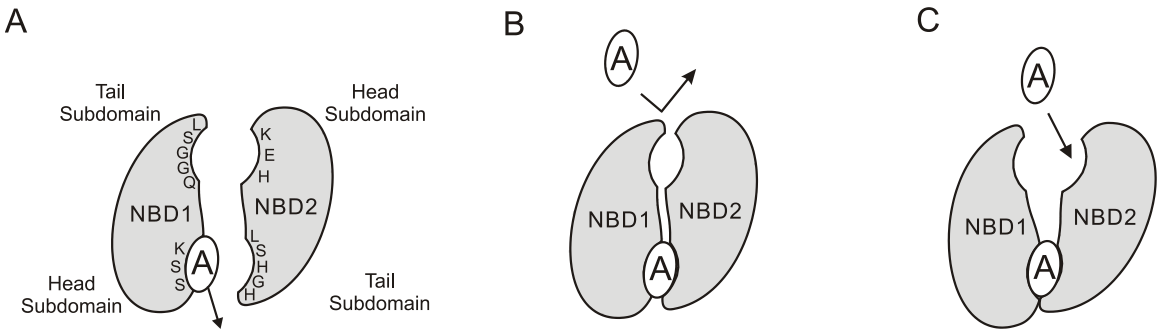

Figure 1-4. Cartoons illustrating the partial dimer state hypothesis. (A) It's counterintuitive to relate the single ATP bound state to the monomeric state of NBDs observed in crystal structures, as the exposed ATP binding site is unlikely to bind an ATP molecule for tens of seconds. **(B)** It's also problematic to assume a dimeric configuration for the single-ATP bound intermediate as this dimeric structure will prevent ATP from binding to site 2. **(C)** The existence of a partial NBD dimer would allow stable ATP binding to occur in site 1 and at the same time also enable ligand exchange to take place in NBD2.

second, much shorter than the ATP dwell time in site 1, my results suggest that the NBD dimer is not completely separated upon channel closure, since the ATP molecule bound in site 1 can keep two NBDs connected together. Therefore, I reached the conclusion that opening and closing of CFTR should be coupled to the formation and "partial" separation of the NBD dimer (Fig. 1-5). It's noted that this movement of NBDs is much less than that suggested by crystallographic studies (Fig. 1-2), where complete separation of two NBDs for several angstrom is required for a functional cycle of an ABC protein.

Here, an intriguing question is whether the molecular model of CFTR's functional cycle can be applied to other ABC proteins, most of which are membrane transporters. For atypical ABC proteins, including the human multiple drug resistance proteins (MRPs or ABCC1-6), sulfonylurea receptors (SURs or ABCC8-9), and transporters for antigen processing (TAPs or ABCB2-3), the ability of site 1 to catalyze ATP hydrolysis, similar to CFTR, is severely impaired (reviewed in Procko et al., 2009). If the ATP dwell time in site 1 is also longer than the duration of a functional cycle for these ABC proteins, it's conceivable that limited movements of NBDs are sufficient to drive the function of these proteins. For classical ABC proteins, an "alternating ATP hydrolysis" model for the P-glycoprotein (ABCB1) has been proposed based on a series of carefully-designed biochemical experiments, conducted long before the determination of ABC protein structures (Urbatsch et al., 1995). In this model, it's suggested that only one ATP molecule is hydrolyzed per transport cycle, thus implicating that the NBDs for P-glycoprotein may also not

separate completely during a functional cycle. More detailed discussions on this issue can be found in the discussion section in chapter 3.

Finally, I addressed the issue about how the new model of CFTR's function is related to the monomeric state of NBDs, demonstrated in crystallographic studies. With independent approaches elaborated in chapters 2 and 3, I was able to derive two conclusions. First, entering of CFTR into the resting state preferentially takes place when the channel is in the partial dimer state rather than in the dimeric state. Second, the complete separation of the stable partial dimer is a poorly reversible process. In other words, once reached the resting state, the CFTR channel has to enter the dimeric state through a pathway without the formation of a stable partial NBD dimer (Fig. 1-5). To this point, a novel and detailed model describing the structure-function relationship of CFTR has been established.

1-6. Mutations of CFTR Cause Cystic Fibrosis

More than 1500 mutations of the 1480-amino-acid CFTR protein have been reported to cause the disease cystic fibrosis (http://www.genet.sickkids.on.ca/cftr) by decreasing the membrane expression of CFTR proteins or by impairing channel functions. Among various CF mutations, ΔF508 constitutes ~90% of mutations in all CF cases and leads to a severe clinical phenotype. It's well known that the ΔF508 mutation prevents CFTR protein from reaching the membrane (Reviewed in Rowe et al., 2005). Moreover, most but not all studies indicate that human ΔF508-CFTR manifests a gating defect mainly caused by a decreased opening rate (Dalemans et

FIGURE 1-5

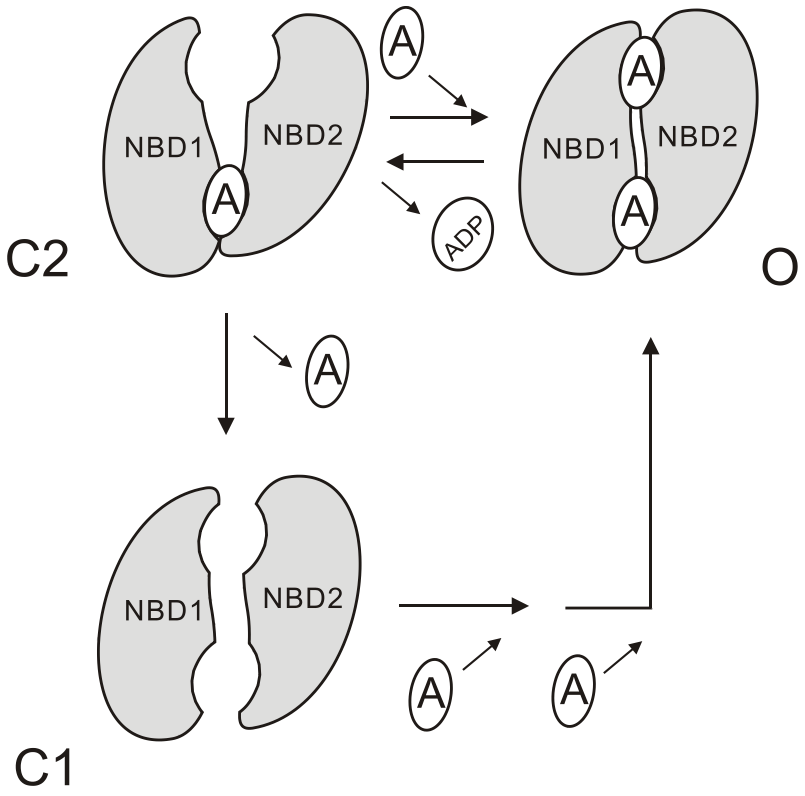

Figure 1-5. A new molecular model for CFTR gating (simplified version). In this model, opening and closing of CFTR is coupled to the formation and partial separation of the NBD dimer (C2 ↔ O). The CFTR channel can occasionally enter into the ATP-free monomeric state from the partial dimer state (C2 → C1). This step is poorly reversible and thus CFTR has to enter the open state through a different pathway (C1 →→ O). See more detail about this molecular model in chapter 3.

al., 1991; Denning et al., 1992; Li et al., 1993; Haws et al., 1996; Schultz et al., 1999; Wang et al., 2001; Ostedgaard et al., 2007; Miki et al., 2010). The exact mechanism for the ΔF508-induced functional and expressional defects, however, remains poorly understood.

G551D, the third most common CF-associated mutation, is located in NBD1's signature motif. This mutation does not affect protein expression but completely abolishes the ATP-dependent gating of CFTR and thus decreases the channel open probability by ~100-fold (Bompadre et al., 2007). In this case, the mechanism by which the mutation causes defective CFTR function is relatively clear. As discussed above, ATP-induced opening of CFTR is driven by dimerization of NBDs. Since the signature motif of NBD1 has to engage with the ATP molecule bound in NBD2's ATP-interacting motif upon NBD dimerization, a negatively-charged D551 side chain at this motif will likely clash with the also negatively charged phosphate groups of ATP, thus eliminating the possibility of the formation of a tight NBD dimer.

Due to the development of numerous cystic fibrosis therapies, the past two decades have witnessed a tremendous improvement of the life quality and expectancy of CF patients. However, as current therapies only treat symptoms but not the underlying defects of CFTR, CF remains an incurable disease to date. In this regard, identification of chemical compounds called correctors and potentiators has been the research focus for CFTR investigators in recent years. Searching for CFTR correctors, which rescue membrane expression of CFTR, presents a great challenge because of the complicated and multi-step nature of protein processing. On the

other hand, a greater amount of potentiators, which act to improve CFTR activity has been discovered (Verkman and Galietta, 2009). Among them, VX-770 is currently in phase III clinical trials for CF patients carrying the G551D mutation (Van Goor et al., 2009). Importantly, hidden behind the therapeutic indications are so far largely unexplored mechanisms by which the potentiators restore the function of mutant CFTR channels. A better understanding of these mechanisms could broaden our knowledge base about how CFTR gating can be regulated and potentially benefits future design of new pharmaceuticals.

1-7. From a Nucleotide Potentiator to the Identification of a Potentiation Mechanism for WT- and CF-Associated CFTR

Our group has previously reported that PATP is a potentiator of G551D-CFTR and this ATP analogue binds to NBD1's head subdomain to increase the channel activity (Bompadre et al., 2008). It's noted that this observation is in fact quite puzzling as ATP can also bind to NBD1's head but has virtually no effect on G551D channels. We thus asked the question: what is the factor that determines whether a nucleotide can potentiate G551D channels or not? Given that PATP has a higher apparent affinity than ATP to gate CFTR (Zhou et al., 2005), one possibility is that it's the high affinity to NBD1 that grants a ligand the ability to activate G551D channels. This hypothesis seems counterintuitive at first glance as we've discussed that site 1, constituted by NBD1's head and NBD2's tail, can already bind ATP tightly. However, when the ligand exchange experiment (see 1-4 and chapter 3) was carried out with

G551D-CFTR, it was noticed that site 1 of this mutant has a drastically decreased capability to retain ATP compared with that of WT-CFTR. Interestingly, it was also found that PATP stayed in site 1 of G551D-CFTR for a substantially longer time than ATP. These observations appear to be in support of our hypothesis, which predicts that enhancing ligand affinity in site 1 should lead to ATP-dependent activity of G551D-CFTR.

To test this prediction, we mutated several amino-acid residues in either NBD1's head or NBD2's tail with the guidance of crystal structures, intending to help G551D channels to bind ATP more tightly in site 1. In chapter 4, using the methods described in section 1-4 and chapters 2 & 3, I was able to evaluate the effects of these mutations. It turned out that three (W401Y, W401F, and H1348G) of them are capable of enhancing ATP-site 1 interactions for WT-CFTR channels and these gain-of-function mutations indeed drastically improve the function of G551D-CFTR with ATP-dependent activity at least partially restored. Therefore, I can conclude that optimizing ligand-site 1 interactions could serve as a strategy to ameliorate the functional defects of G551D channels.

The finding that site 1-ATP interactions can be further optimized even for WT-CFTR implicates that the same strategy to augment the activity of G551D-CFTR may also be applicable to WT-CFTR and other CF-associated mutants, like ΔF508-CFTR. In chapter 4, I show that this is indeed the case and discuss in more detail the mechanism by which a tight ATP binding in site 1 potentiates CFTR channels. In

closing, our results demonstrate for the first time a clear molecular target that could serve as the site for the action of a CFTR potentiator.

1-8. Conclusion

Here, in addition to a basic introduction to CFTR structure and function, I have outlined the thinking flow for a series of studies that were initiated from the development of new methods to investigate CFTR's site 1 (1-4), continued by the establishment of a new model for CFTR gating (1-5), and finally ended with the identification of a molecule target for developing pharmaceuticals to treat cystic fibrosis (1-7). I expect that through this chapter, the readers could gain a more descent understanding about not only the rationale behind the experimental design in the following chapters but also the relation between them.

In the following chapters, I will elaborate the idea described in this introductory chapter. It's noted that the content of chapters 2 and 3 are from two of my recently published papers in the Journal of General Physiology (Tsai et al., 2009 & Tsai et al., 2010). According to the journal policy, the copyright of all materials published in JGP remains with the authors.

1-9. References

Aleksandrov, L., A. Aleksandrov, and J.R. Riordan. 2008. Mg2+ -dependent ATP occlusion at the first nucleotide-binding domain (NBD1) of CFTR does not require the second (NBD2). *Biochem J*. 416:129-136.

Aleksandrov, L., A.A. Aleksandrov, X.B. Chang, and J.R. Riordan. 2002. The First Nucleotide Binding Domain of Cystic Fibrosis Transmembrane Conductance Regulator Is a Site of Stable Nucleotide Interaction, whereas the Second Is a Site of Rapid Turnover. *J Biol Chem*. 277:15419-15425.

Basso, C., P. Vergani, A.C. Nairn, and D.C. Gadsby. 2003. Prolonged nonhydrolytic interaction of nucleotide with CFTR's NH2-terminal nucleotide binding domain and its role in channel gating. *J Gen Physiol*. 122:333-348.

Bompadre, S.G., M. Li, and T.C. Hwang. 2008. Mechanism of G551D-CFTR (cystic fibrosis transmembrane conductance regulator) potentiation by a high affinity ATP analog. *J Biol Chem*. 283:5364-5369.

Bompadre, S.G., Y. Sohma, M. Li, and T.C. Hwang. 2007. G551D and G1349D, two CF-associated mutations in the signature sequences of CFTR, exhibit distinct gating defects. *J Gen Physiol*. 129:285-298.

Bradbury, N.A. 1999. Intracellular CFTR: localization and function. *Physiol Rev*. 79:S175-191.

Chen, T.Y., and T.C. Hwang. 2008. CLC-0 and CFTR: chloride channels evolved from transporters. *Physiol Rev*. 88:351-387.

Dalemans, W., P. Barbry, G. Champigny, S. Jallat, K. Dott, D. Dreyer, R.G. Crystal, A. Pavirani, J.P. Lecocq, and M. Lazdunski. 1991. Altered chloride ion channel kinetics associated with the delta F508 cystic fibrosis mutation. *Nature*. 354:526-528.

Denning, G.M., M.P. Anderson, J.F. Amara, J. Marshall, A.E. Smith, and M.J. Welsh. 1992. Processing of mutant cystic fibrosis transmembrane conductance regulator is temperature-sensitive. *Nature*. 358:761-764.

Gadsby, D.C., and A.C. Nairn. 1999. Control of CFTR channel gating by phosphorylation and nucleotide hydrolysis. *Physiol Rev*. 79:S77-S107.

Gadsby, D.C., P. Vergani, and L. Csanady. 2006. The ABC protein turned chloride channel whose failure causes cystic fibrosis. *Nature*. 440:477-483.

Haws, C.M., I.B. Nepomuceno, M.E. Krouse, H. Wakelee, T. Law, Y. Xia, H. Nguyen, and J.J. Wine. 1996. Delta F508-CFTR channels: kinetics, activation by forskolin, and potentiation by xanthines. *Am J Physiol*. 270:C1544-1555.

Hollenstein, K., R.J. Dawson, and K.P. Locher. 2007. Structure and mechanism of ABC transporter proteins. *Curr Opin Struct Biol*. 17:412-418.

Jha, S., N. Dabas, N. Karnani, P. Saini, and R. Prasad. 2004. ABC multidrug transporter Cdr1p of Candida albicans has divergent nucleotide-binding domains which display functional asymmetry. *FEMS Yeast Res*. 5:63-72.

Lewis, H.A., S.G. Buchanan, S.K. Burley, K. Conners, M. Dickey, M. Dorwart, R. Fowler, X. Gao, W.B. Guggino, W.A. Hendrickson, J.F. Hunt, M.C. Kearins, D. Lorimer, P.C. Maloney, K.W. Post, K.R. Rajashankar, M.E. Rutter, J.M. Sauder, S. Shriver, P.H. Thibodeau, P.J. Thomas, M. Zhang, X. Zhao, and S. Emtage. 2004. Structure of nucleotide-binding domain 1 of the cystic fibrosis transmembrane conductance regulator. *EMBO J*. 23:282-293.

Lewis, H.A., X. Zhao, C. Wang, J.M. Sauder, I. Rooney, B.W. Noland, D. Lorimer, M.C. Kearins, K. Conners, B. Condon, P.C. Maloney, W.B. Guggino, J.F. Hunt, and S. Emtage. 2005. Impact of the deltaF508 mutation in first nucleotide-binding domain of human cystic fibrosis transmembrane conductance regulator on domain folding and structure. *J Biol Chem*. 280:1346-1353.

Li, C., M. Ramjeesingh, E. Reyes, T. Jensen, X. Chang, J.M. Rommens, and C.E. Bear. 1993. The cystic fibrosis mutation (delta F508) does not influence the chloride channel activity of CFTR. *Nat Genet*. 3:311-316.

Lubelski, J., R. van Merkerk, W.N. Konings, and A.J. Driessen. 2006. Nucleotide-binding sites of the heterodimeric LmrCD ABC-multidrug transporter of Lactococcus lactis are asymmetric. *Biochemistry*. 45:648-656.

Mense, M., P. Vergani, D.M. White, G. Altberg, A.C. Nairn, and D.C. Gadsby. 2006. In vivo phosphorylation of CFTR promotes formation of a nucleotide-binding domain heterodimer. *EMBO J*. 25:4728-4739.

Miki, H., Z. Zhou, M. Li, T.C. Hwang, and S.G. Bompadre. 2010. Potentiation of disease-associated CFTR mutants by hydrolyzable ATP analogs. *J Biol Chem*.

Oldham, M.L., A.L. Davidson, and J. Chen. 2008. Structural insights into ABC transporter mechanism. *Curr Opin Struct Biol*. 18:726-733.

Ostedgaard, L.S., C.S. Rogers, Q. Dong, C.O. Randak, D.W. Vermeer, T. Rokhlina, P.H. Karp, and M.J. Welsh. 2007. Processing and function of CFTR-DeltaF508 are species-dependent. *Proc Natl Acad Sci U S A*. 104:15370-15375.

Park, S., B.B. Lim, C. Perez-Terzic, G. Mer, and A. Terzic. 2008. Interaction of asymmetric ABCC9-encoded nucleotide binding domains determines KATP channel SUR2A catalytic activity. *J Proteome Res*. 7:1721-1728.

Powe, A.C., Jr., L. Al-Nakkash, M. Li, and T.C. Hwang. 2002. Mutation of Walker-A lysine 464 in cystic fibrosis transmembrane conductance regulator reveals functional interaction between its nucleotide-binding domains. *J Physiol*. 539:333-346.

Procko, E., M.L. O'Mara, W.F. Bennett, D.P. Tieleman, and R. Gaudet. 2009. The mechanism of ABC transporters: general lessons from structural and functional studies of an antigenic peptide transporter. *FASEB J*. 23:1287-1302.

Rees, D.C., E. Johnson, and O. Lewinson. 2009. ABC transporters: the power to change. *Nat Rev Mol Cell Biol*. 10:218-227.

Riordan, J.R., J.M. Rommens, B. Kerem, N. Alon, R. Rozmahel, Z. Grzelczak, J. Zielenski, S. Lok, N. Plavsic, J.L. Chou, and et al. 1989. Identification of the cystic fibrosis gene: cloning and characterization of complementary DNA. *Science*. 245:1066-1073.

Rowe, S.M., S. Miller, and E.J. Sorscher. 2005. Cystic fibrosis. *N Engl J Med*. 352:1992-2001.

Schultz, B.D., R.A. Frizzell, and R.J. Bridges. 1999. Rescue of dysfunctional deltaF508-CFTR chloride channel activity by IBMX. *J Membr Biol*. 170:51-66.

Sears, C.L., and J.B. Kaper. 1996. Enteric bacterial toxins: mechanisms of action and linkage to intestinal secretion. *Microbiol Rev*. 60:167-215.

Tsai, M.F., H. Shimizu, Y. Sohma, M. Li, and T.C. Hwang. 2009. State-dependent modulation of CFTR gating by pyrophosphate. *J Gen Physiol*. 133:405-419.

Urbatsch, I.L., B. Sankaran, J. Weber, and A.E. Senior. 1995. P-glycoprotein is stably inhibited by vanadate-induced trapping of nucleotide at a single catalytic site. *J Biol Chem*. 270:19383-19390.

Van Goor, F., S. Hadida, P.D. Grootenhuis, B. Burton, D. Cao, T. Neuberger, A. Turnbull, A. Singh, J. Joubran, A. Hazlewood, J. Zhou, J. McCartney, V. Arumugam, C. Decker, J. Yang, C. Young, E.R. Olson, J.J. Wine, R.A. Frizzell, M. Ashlock, and P. Negulescu. 2009. Rescue of CF airway epithelial cell function in vitro by a CFTR potentiator, VX-770. *Proc Natl Acad Sci U S A*. 106:18825-18830.

Vergani, P., S.W. Lockless, A.C. Nairn, and D.C. Gadsby. 2005. CFTR channel opening by ATP-driven tight dimerization of its nucleotide-binding domains. *Nature*. 433:876-880.

Verkman, A.S., and L.J. Galietta. 2009. Chloride channels as drug targets. *Nat Rev Drug Discov*. 8:153-171.

Wang, F., S. Zeltwanger, S. Hu, and T.C. Hwang. 2000. Deletion of phenylalanine 508 causes attenuated phosphorylation-dependent activation of CFTR chloride channels. *J Physiol*. 524 Pt 3:637-648.

Zhang, D.W., G.A. Graf, R.D. Gerard, J.C. Cohen, and H.H. Hobbs. 2006. Functional asymmetry of nucleotide-binding domains in ABCG5 and ABCG8. *J Biol Chem*. 281:4507-4516.

Zhou, Z., X. Wang, M. Li, Y. Sohma, X. Zou, and T.C. Hwang. 2005. High affinity ATP/ADP analogues as new tools for studying CFTR gating. *J Physiol*. 569:447-457.

Zhou, Z., X. Wang, H.Y. Liu, X. Zou, M. Li, and T.C. Hwang. 2006. The two ATP binding sites of cystic fibrosis transmembrane conductance regulator (CFTR) play distinct roles in gating kinetics and energetics. *J Gen Physiol*. 128:413-422.

CHAPTER 2

STATE DEPENDENT MODULATION OF CFTR GATING BY PYROPHOSPHATE

2-1. Abstract

Cystic fibrosis transmembrane conductance regulator (CFTR) is an ATP-gated chloride channel. ATP-induced dimerization of CFTR's two nucleotide binding domains (NBDs) has been shown to reflect the channel open state; whereas hydrolysis of ATP is associated with channel closure. Pyrophosphate (PPi), like non-hydrolytic ATP analogs, is known to lock open the CFTR channel for tens of seconds when applied with ATP. In the current study, we demonstrate that PPi by itself opens the CFTR channel in a Mg^{2+} dependent manner long after ATP is removed from the cytoplasmic side of excised membrane patches. However, the short-lived open state ($\tau \sim 1.5$ s) induced by MgPPi suggests that MgPPi alone does not support a stable NBD dimer configuration. Surprisingly, MgPPi elicits long-lasting opening events ($\tau \sim 30$ s) when administrated shortly after the closure of ATP-opened channels. These results indicate the presence of two different closed states (C_1 and C_2) upon channel closure and a state-dependent effect of MgPPi on CFTR gating. The relative amount of channels entering MgPPi-induced long-open bursts during the ATP washout phase decreases over time, indicating a time-dependent dissipation of the closed state (C_2) that can be locked open by MgPPi. The stability of the C_2 state is

enhanced when the channel is initially opened by N^6-phenylethyl-ATP, a high affinity ATP analogue, but attenuated by W401G mutation, which likely weakens ATP binding to NBD1, suggesting that an ATP molecule remains bound to the NBD1 site in the C_2 state. Taking advantage of the slow opening rate of Y1219G-CFTR, we are able to identify a C_2-equivalent state (C_2*) which exists before the channel in the C_1 state is opened by ATP. This closed state responds to MgPPi much more inefficiently than the C_2 state. Finally, we show that MgAMP-PNP exerts its effects on CFTR gating via a similar mechanism as MgPPi. Structural and functional significance of our findings is discussed.

2-2. Introduction

The cystic fibrosis transmembrane conductance regulator (CFTR), a member of the ATP-binding cassette (ABC) transporter superfamiliy (Riordan et al. 1989), is a phosphorylation-activated but ATP-gated chloride channel in epithelial cells. Mutations of the CFTR gene resulting in malfunction of this channel cause the lethal genetic disease cystic fibrosis. The CFTR protein incorporates two nucleotide binding domains (NBD1 and NBD2) that serve as the gating machinery to drive the conformational changes during gating transitions (reviewed in Gadsby et al., 2006; Chen and Hwang, 2008). Each NBD holds the Walker A and Walker B motifs that form the major constituents for interactions with ATP (Walker et al., 1982). There is compelling evidence that, similar to other ABC transporters (reviewed in Higgins and Linton, 2004), once ATP binds to the nucleotide-interacting motifs, the two

NBDs of CFTR approach each other to form a head-to-tail dimer with two ATP molecules sandwiched at the dimer interface and this intramolectular interaction in turn leads to opening of the channel (Vergani et al., 2005; Mense et al., 2006). Since a biochemically stable NBD dimer formation in other ABC transporters is observed only when ATPase activity is abolished (Moody et al., 2002; Smith et al., 2002), it is proposed that ATP hydrolysis causes fast separation of the two NBDs and thus results in closing of the CFTR channel.

The idea that ATP hydrolysis precedes channel closing is further supported by the observations that CFTR mutations whose ATPase activity is abrogated (e.g. K1250A, E1371S) (Ramjeesingh et al., 1999) can remain open for minutes (Gunderson and Kopito, 1995; Zeltwanger et al., 1999; Vergani et al., 2003; Bompadre et al., 2005b), and that channel closure is markedly delayed in the presence of non-hydrolyzable ATP analogue AMP-PNP (Hwang et al., 1994), or of inorganic phosphate analogue orthovanadate, which presumably forms a stable complex with the hydrolytic product ADP (Baukrowitz et al., 1994). Gunderson and Kopito (1994) reported that, similar to AMP-PNP or vanadate, pyrophosphate (PPi), although fails to open the channel by itself, can 'lock' the CFTR channel into a prolonged open state in the presence of ATP. Carson et al. (1995) confirmed and expanded this observation by showing that PPi also strongly potentiates CF-associated mutations ΔF508 and G551S.

Data from several laboratories have suggested that PPi exerts its effect via binding to the ATP binding site at NBD2. First, several NBD2 mutations but not

corresponding NBD1 mutations (Gunderson and Kopito, 1995; Cotton et al., 1996; Berger et al., 2002) abolish PPi stimulation. Second, PPi fails to enhance the activity of murine CFTR and replacing human NBD2 with the equivalent region of murine CFTR also abolishes the effect of PPi (Lansdell et al., 1998; Scott-Ward et al., 2007). However, the idea that NBD2 determines the PPi sensitivity cannot explain several other findings. For example, PPi, when applied in the absence of ATP, fails to lock open the channel (Gunderson and Kopito, 1994, Carson et al., 1995). Biochemical studies show that PPi paradoxically produces a concentration-dependent increase in 8-N_3ATP photolabeling of CFTR (Carson et al. 1995). Furthermore, several results suggest an involvement of NBD1 in PPi's action on CFTR gating. Csanady et al. (2005) reported that deletion of the N-terminal regulatory insertion in NBD1 somewhat weakens PPi's effect. Cai et al. (2006) showed that PPi cannot potentiate G1349D, a mutation at the signature sequence of NBD2, which forms the ATP binding pocket with the nucleotide interacting motifs of NBD1. These observations can be nicely explained if one hypothesizes that ATP binding at NBD1 primes the CFTR channel into an activated state that can be locked open by PPi (cf. Gunderson and Kopito, 1995). This hypothesis, however appealing, is short of direct evidence.

Since most of the experiments described above were carried out when ATP and PPi were applied together, it is difficult to assess whether PPi acts on an open state (c.f. Hwang et al., 1994) or a closed state (Gunderson and Kopito, 1995). We reasoned that if the open state reflects a stable NBD dimer (Vergani et al., 2005), it seems unlikely that PPi would have access to the nucleotide binding site buried at the dimer interface in an open channel configuration. Thus, it's more likely that PPi

acts on a closed state. Indeed, in the current study, we provide evidence that once leaving the ATP-induced open state, closed channels respond to PPi in a magnesium-dependent manner. We demonstrate that shortly after channel closure, MgPPi alone locks open a closed state (C_2), where one ATP molecule is not yet dissociated from the NBD1 site. This result echoes the hypothesis that ATP primes the channel by binding to NBD1.

There are multiple closed states in the gating cycle of CFTR. In this study, we are able to differentiate two more closed states (C_1 and C_2*) based on their different responses to MgPPi. The C_1 state exists long after channel closure and the binding of MgPPi to this state induces relatively short openings. The C_2* state is present before the channel is opened from the C_1 state by ATP. Although this C_2-equivalent state likely has one ATP molecule in the NBD1 site, it has a weaker response to MgPPi compared with the C_2 state. Functional and structural implications of our results will be discussed.

2-3. Material and methods

Cell Culture and Transient Expression System

Chinese hamster ovary (CHO) cells were grown at 37 ˚C and 5 % CO_2 in Dulbecco's Modified Eagle's Medium supplemented with 10% fetal bovine serum. The cDNA constructs of wild-type (WT) or mutant CFTR were cotransfected with pEGFP-C3 (CLONTECH Laboratories, Inc.) encoding the green fluorescence protein

using PolyFect transfection reagent (QIAGEN) according to the manufacturer's instruction. The transfected CHO cells were plated on sterile glass chips in 35 mm tissue culture dishes and incubated at 25 ˚C. Electrophysiological experiments were performed 2-5 days after transfection.

Electrophysiological Recordings

Before inside-out patch-clamp recordings, glass chips containing CHO cells transfected with various CFTR constructs, W401G, Y1219G, S1347G, E1371S, and WT-CFTR, were transferred to a continuously perfused chamber located on the stage of an inverted microscope (Olympus Corp. Japan). Patch-clamp pipettes were made from borosilicate capillary glass using a two-stage vertical puller (Narishige, Japan). The pipette tips were fire-polished with a homemade microforge to ~ 1 μm external diameter, resulting in a pipette resistance of 2 ~ 4 MΩ in the bath solution.

CFTR channel currents were recorded at room temperature with an EPC-10 patch-clamp amplifier, filtered at 100 Hz with an eight-pole Bessel filter (Warner Instrument Corp.) and captured onto a hard disk at a sampling frequency of 500 Hz. The membrane potential was held at -60 mV. At this membrane potential, downward deflections represent channel openings. However, we inverted the current direction for clearer data presentations.

All inside-out patch-clamp experiments were done with a fast solution exchange device, SF-77B (Warner Instrument Corp.), which can minimize the dead time of solution change to ~ 20 ms (Cortic et al., 2003). To test the dead time of our solution

exchange, we perfused two solutions with different concentrations of NaCl to the patch pipette. Exponential fit of the resulting current changes yielded a time constant of ~ 30 ms.

Chemicals and Composition of Solutions

The pipette solution contained (in mM): 140 N-methyl-D-glucamine chloride (NMDG-Cl), 2 $MgCl_2$, 5 $CaCl_2$, and 10 HEPES (pH 7.4 with NMDG). Cells were perfused with a bath solution containing (in mM): 145 NaCl, 5 KCl, 2 $MgCl_2$, 1 $CaCl_2$, 5 glucose, 5 HEPES and 20 sucrose (pH 7.4 with NaOH). After the establishment of an inside-out configuration, the patch was perfused with a standard perfusion solution (i.e. intracellular solution) containing (in mM): 150 NMDG-Cl, 2 $MgCl_2$, 10 EGTA and 8 Tris (pH 7.4 with NMDG).

MgATP, PPi (tetrasodium salt), and PKA were purchased from Sigma-Aldrich (St Louis, MO). AMP-PNP was obtained from Roche (Indianapolis, IN). N^6-(2-phenyltehyl)-ATP (P-ATP) was from Biolog Life Science Institute (Bremen, Germany). MgATP, PPi, and AMP-PNP were stored in 250 mM stock solution at -20 ˚C. P-ATP stock solution was 10 mM and was stored at -80 ˚C. The [PKA] used in this study was 25 U ml^{-1}. All nucleotides and PPi were diluted in the perfusion solution to the concentrations as indicated in the figures and the pH was adjusted to 7.4 with NMDG. When NaAMP-PNP or NaPPi was used, the same concentration of $MgSO_4$ was added unless indicated otherwise.

When high concentrations of Mg^{2+} and NaPPi (> 5 mM) were mixed rapidly, precipitations occur immediately in spite of continuous stirring of the solution. The substances were in a form of amorphous glass-like granules occurring in large number under the microscope. However, when Mg^{2+} and NaPPi were mixed slowly, the formation of precipitations was much slower, allowing us to test the effects of a wider range of [PPi] (2 ~ 15 mM) on CFTR gating. To minimize a decrease of effective [PPi] due to precipitations, PPi solutions were used no more than 4 hours after preparation. In addition, whenever possible, we preferred using PPi concentration < 5 mM (e.g., 2 mM) to avoid this problem.

Data Analysis and Statistics

Steady-state macroscopic current amplitude was measured using Igor Pro program (version 4.07, Wavemetrics, Lake Oswego, OR). The baseline current was subtracted before the data was used for presentation. To estimate channel open time, we derived time constants from macroscopic relaxations upon removal of CFTR ligands. Current relaxations were fitted with single or double exponential functions using a Levenberg-Marquardt based algorithm within the Igor Pro program. Due to the limitation of the program, a current decay trace of two components may not be resolvable by a double exponential fit when one component has relatively small fractional amplitude (e.g. Fig. 3 B and Fig. 4). In this case, single exponential fitting was used to estimate the time constant of the dominant component.

All results are presented as means ± SEM.; n represents the number of experiments. Student's *t*-test or paired t-test was performed with Sigmaplot (version 8.0, SPSS Science, Chicago, IL). $P < 0.05$ was considered significant.

2-4. Results

MgPPi Supports WT-CFTR Gating in the Absence of ATP

It is reported that the non-hydrolytic ATP analogue AMP-PNP by itself can slightly increase CFTR channel activity (Aleksandrov et al., 2000; Vergani et al., 2003; see below). We first tested whether PPi has a similar effect in supporting CFTR gating. Macroscopic current was activated by cytoplasmic application of PKA catalytic subunit plus 2 mM ATP in inside-out patches containing hundreds of WT channels (Fig. 2-1A). Subsequent withdrawal of ATP resulted in a fast current decay that can be fitted with a single exponential function with a time constant of 0.42 ± 0.03 s (Fig. 2-1B, n = 12). Three minutes after ATP removal, patches were exposed to a range of [PPi] supplemented with the same concentration of Mg^{2+}. MgPPi could increase the current in a concentration-dependent manner in the complete absence of ATP (Fig. 2-1A). The dose-response relationship for the effect of MgPPi is obtained by normalizing the macroscopic currents induced by different concentrations of MgPPi to that by 2 mM ATP (Fig. 2-2B, red line).

For each MgPPi concentration, current traces after MgPPi removal from at least six patches were summed to give ensemble current relaxations (Fig. 2-1B). The

FIGURE 2-1

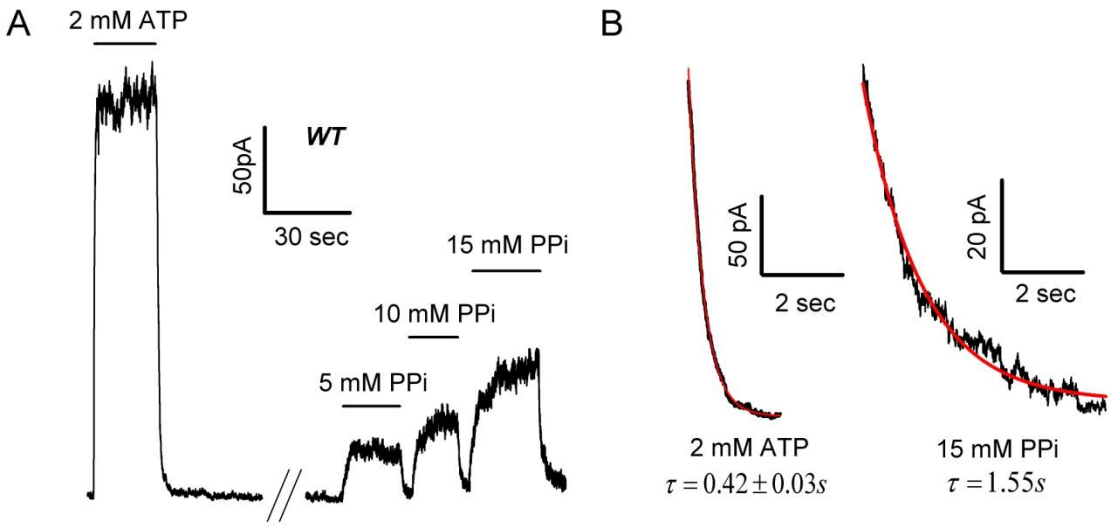

Figure 2-1. The effect of magnesium pyrophosphate on WT-CFTR. (A) A recording of WT-CFTR channels in an excised inside-out membrane patch. The channels were activated with 2 mM ATP + 25 U / ml PKA (not shown). After phosphorylation-dependent activation, application and removal of ATP result in rapid current rise and decay respectively. Three minutes after washout of ATP, channels were opened by different concentration of PPi plus Mg^{2+}. 15 mM PPi supplemented with 15 mM MgPPi seems still unable to saturate the macroscopic current. **(B)** Macroscopic current decay after ATP withdrawal (left) and the ensemble current relaxation after washout of 15 mM MgPPi (right). Channels opened by MgPPi appear to close more slowly than those opened by ATP.

relaxation time courses can be fitted with a single exponential function with a similar time constant ($\tau \sim 1.5$ s) for all MgPPi concentrations tested, suggesting that the open time for MgPPi-activated channels is longer than that of ATP-opened channels. However, since the channel open time is independent of [MgPPi] concentration, a higher concentration of MgPPi should increase the channel open probability mainly by increasing the opening rate. It is noted here that compared to ATP, which maximally activates CFTR at low millimolar concentrations (Zeltwanger et al., 1999), 15 mM MgPPi, the highest concentration tested, was still not able to saturate the current (Fig. 2-2B). These results indicate that although MgPPi indeed can increase the open probability of CFTR, its potency is far lower than ATP.

Our observation that MgPPi alone can support CFTR gating contradicts previous reports (Gundeson and Kopito, 1994; Carson et al., 1995) that PPi by itself is unable to open CFTR channels. We suspect that [Mg^{2+}] in the PPi solution may be the culprit since, unlike the current study, it is unclear if additional Mg^{2+} was added to the PPi solution in those reports. Fig. 2-2A shows a continuous current trace demonstrating that PPi's ability to increase channel activity indeed is dependent on Mg^{2+}. The current induced by 10 mM PPi with 10 mM Mg^{2+} is significantly higher than that with 10 mM PPi and 2 mM Mg^{2+} ($P < 0.01$). In fact, when [Mg^{2+}] in 10 mM and 15 mM PPi solutions was reduced to 2 mM, the ability of PPi in supporting channel gating was dramatically attenuated to that of 2 mM MgPPi (Fig. 2-2B, blue line), suggesting that it is MgPPi, not PPi, that activates CFTR. The observed difference is not due to the difference in total salt concentration since the result is essentially the same after adjusting all test solutions to the same salt concentration with NMDG-Cl

FIGURE 2-2

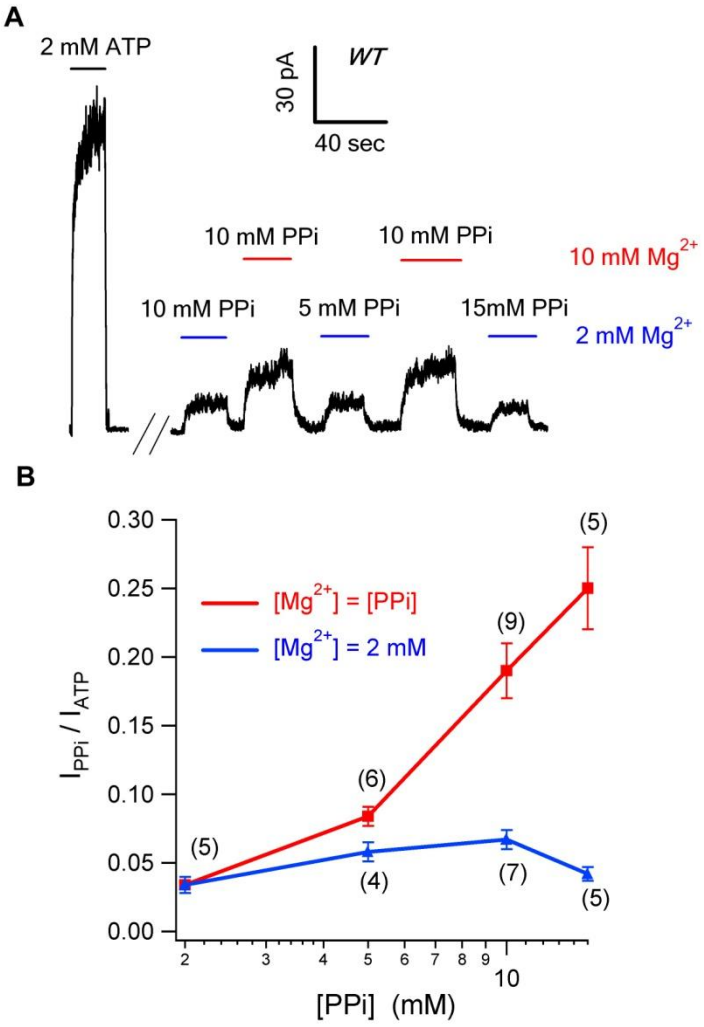

Figure 2-2. PPi opens WT-CFTR in a magnesium dependent manner. (A) WT-CFTR channels were exposed to a nucleotide-free solution for 3 minutes before they were treated with different combinations of [PPi] and [Mg^{2+}]. Raising PPi concentration fails to further increase channel activity if [Mg^{2+}] was not increased simultaneously. **(B)** Current elicited by PPi at different concentrations was normalized to the original ATP current. *Red line*: The PPi solution was supplement with the same concentration of Mg^{2+}. Blue line: [Mg^{2+}] in the PPi solution was fixed at 2 mM.

(data not shown). Unfortunately, the Mg^{2+}-dependence we identified in the current study also prevents us from testing the effect of higher concentrations of MgPPi (*e.g.* > 20 mM) due to the formation of precipitates (see *Materials and Methods*).

Different Closed States of WT-CFTR Revealed by MgPPi

It has been known for years that PPi, in the presence of ATP, 'locks' the channel in an open state with a macroscopic relaxation time constant in tens of seconds (Csanady et al., 2005). In Fig. 2-3A, we confirmed these results by showing that adding 10 mM MgPPi to 2 mM ATP further increased the macroscopic WT-CFTR current and the current decay upon removal of ATP and MgPPi follows a very slow time course with a time constant of 29.4 ± 4.04 s (n = 5). The difference in the relaxation time constant between MgPPi-opened channels ($\tau \sim 1.5$ s in Fig. 2-1B) and those opened by ATP plus MgPPi suggests a state-dependent modulation of CFTR gating by MgPPi. It appears that an exposure of the channel to ATP dramatically alters the effect of MgPPi.

To further explore this state-dependent modulation of CFTR gating, we modified our experimental protocol so that MgPPi was applied at different time points after the removal of ATP. Strikingly, we found that when 10 mM MgPPi was applied 20 seconds after ATP removal, instead of three minutes as in Fig. 2-1A, a significant amount of current was elicited (Fig. 2-3B, 65 ± 6% of ATP-activated current, n = 4). This PPi effect, similar to that described above (Fig. 2-2), is Mg^{2+} dependent (data not shown). After washout of MgPPi, the macroscopic current decayed slowly. Except for the very beginning of the current decay, the time course can be well fitted

with a single exponential function with a time constant of 29.98 ± 6.14 s (Fig. 2-3B, n = 4), indicating that many of those *closed* WT-CFTR channels were locked open by MgPPi alone! These results suggest that there are at least two different closed states (C_1 and C_2) following ATP removal and these two states can be differentiated by their distinct responses to MgPPi. When the channel is opened by MgPPi from the C_1 state, the open time is ~ 1.5 s as depicted in Fig. 1. In contrast, MgPPi locks open the channel with a time constant of ~30 s when it is in the C_2 state.

Transition of C_2 to C_1

Fig. 2-3C shows an experiment where 10 mM MgPPi was applied 40 seconds after nucleotide withdrawal. Compared to the result shown in Fig. 2-3B, 10 mM MgPPi induced a smaller current and its removal resulted in a clear biphasic current decay. The time course can be fitted with a double exponential function (Fig. 2-3C, inset), indicating the presence of two distinct open states. The time constant (32.46 ± 7.41s, n = 5) for the more stable open state is very similar to that of "locked open" channels shown above. However, the relative current amplitude (27 ± 2 % of ATP-induced current, n = 5) attributed to the locked open channels is significantly smaller than that shown in Fig. 2-3B when the washout time is 20 s, suggesting a slow dissipation of the C_2 closed state. In contrast, the less stable open state with a time constant of 1.86 ± 0.34 s (n = 5), very similar to the time constant for the MgPPi-opened channels after 3 minutes of ATP removal (Fig. 2-1A), made a distinguishable appearance in this condition (compare with Fig. 2-3B). Therefore,

FIGURE 2-3

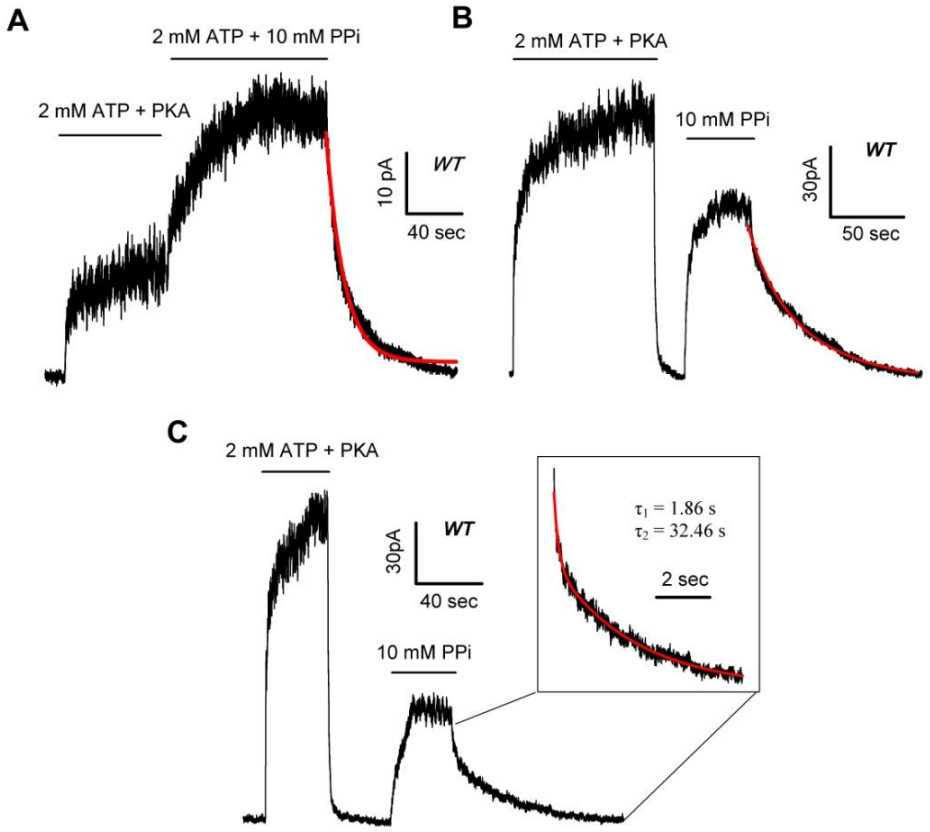

Figure 2-3. MgPPi locks open closed WT channels. (A) Steady state macroscopic current activated by 2 mM ATP plus PKA was further increased by a subsequent addition of 10 mM MgPPi. Red line represents single-exponential fit of the current relaxation upon removal of ATP and MgPPi. **(B)** MgPPi locks open closed channels shortly after removal of ATP. Note a 20-second time lapse between the removal of ATP and the application of MgPPi. **(C)** As the washout time was prolonged to 40 seconds, fewer channels were locked open by 10 mM MgPPi. Superimposed double exponential fit (red line) yields $\tau_1 = 1.86 \pm 0.34$ s, $\tau_2 = 32.46 \pm 7.41$ s (n = 5).

the longer the time lapse after ATP washout, the more channels were accumulated in the C_1 state upon which MgPPi acted to induce less stable openings.

To further elaborate this time-dependent alteration of C_1 and C_2 state distribution, we applied 10 mM MgPPi after WT channel, initially opened by ATP, was subsequently washed with nucleotide-free solution for different lengths of time. Except for the data obtained with a washout time < 20 s (see *Material and Methods* for details), the current relaxation after MgPPi removal was fitted with a double exponential function giving the fractional amplitude of slow and fast components. Fig. 2-4 plots the waiting time versus the two fractions of current induced by MgPPi relative to the original current in the presence of PKA and ATP. The left-hand Y axis represents the ratio of the current attributable to lock-open bursts at time *t* to that activated by ATP at time zero (red squares). This ratio decreases monotonically as the washout time was prolonged. In contrast, when the current resulted from short openings was normalized to ATP-induced current (Fig. 2-4, right-hand Y axis, blue squares), the ratio gradually increased and reached a plateau after 60 s of washout time.

Overall these data support the idea of a two-step channel closure scheme.

$$O \xrightarrow{\text{fast}} C_2 \xrightarrow{\text{slow}} C_1 \qquad \text{(scheme 1)}$$

FIGURE 2-4

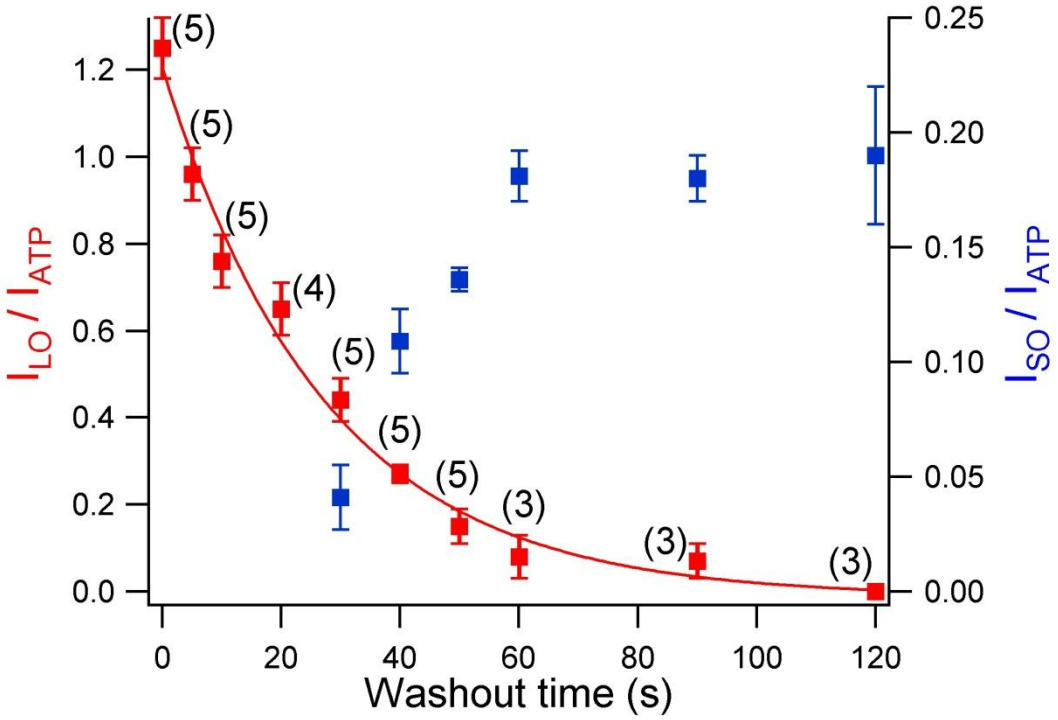

Figure 2-4. Time-dependent reopening of WT-CFTR by 10 mM MgPPi. MgPPi was applied at different time points after ATP washout. The current amplitude of the slow component (red squares, left Y-axis) and the fast component (blue squares, right Y-axis) derived from double exponential fitting were normalized to ATP current at t = 0. For t = 0 ~ 20 s, the fast component was too small to be resolved. Fitting the data points (red curve) by a single exponential function estimates the lifetime of the C_2 state to be 27.4 s.

The first step, O → C_2, is fast presumably because of a rapid hydrolysis of ATP and subsequent dissociation of the hydrolytic products. The second step, C_2 → C_1, is slow as MgPPi can lock open a significant number of channels even 20 seconds following washout of ATP. It should be noted here that this scheme may be oversimplified since there are likely other closed states in the channel closure process that we fail to identify due to the limitation of the current experimental design.

Assuming that MgPPi can efficiently lock open all channels in the C_2 state, in theory the lifetime of the C_2 state can be approximated by exponential fitting of the slow component of the current induced by MgPPi (red line in Fig. 2-4). Unfortunately, because of the slow current rise upon application of MgPPi (probably due to a low binding affinity of MgPPi), many channels in the C_2 state already dissipate without being locked open during the rising phase of MgPPi-induced current increase. Therefore, the time constant of 27.4 s derived from a single exponential fit of data points (red squares) in Fig. 2-4 can only be considered as a rough estimate of the lifetime of the C_2 state.

Possible Biochemical basis of the stable C_2 closed state

What makes C_1 and C_2 different closed states? We noticed that although a long washout of ATP finally results in a complete transition of the C_2 state to the C_1 state, re-application of ATP can once again bring channels back to the O state and subsequently the C_2 state (data not shown). Thus, the channel seems to have an

ability to remember the gating history for tens of seconds and if so, this long-lasting 'memory' likely comes from a prior exposure of the channels to ATP.

It has been shown that while the NBD2 of CFTR has a high nucleotide turnover rate, presumably due to its ATPase activity, ATP can be 'trapped' in NBD1 for a long time (Szabo et al., 1999; Aleksandrov et al., 2001, 2002; Basso et al., 2003). Using these biochemical data, Vergani et al. (2003) proposed that once ATP binds to the NBD1 site, it is occluded there; therefore during a gating cycle, when the channel closes, the ATP molecule remains bound at the NBD1 site. We wondered if the C_2 state described above may represent this elusive state defined based on biochemical data. If the C_2 state indeed has a bound ATP in NBD1, the effect of MgPPi on the C_2 state should meet two key predictions. First, with the NBD1 site occupied by ATP, MgPPi likely binds to NBD2 to lock open the channel. Reports from several different groups have already suggested that is the case (see *Introduction*). Thus, when MgPPi and ATP (or other nucleotides such as ADP) are applied together, they may compete for the NBD2 site. Second, the binding affinity of ATP or ATP analogue in NBD1 may affect the life time of the C_2 state.

To test whether MgPPi and ATP, when applied together, compete for a common binding site, we prepared solutions containing 2 mM MgPPi with various concentrations of ATP. In Fig. 2-5A, WT-CFTR channels in inside-out patches were first activated by PKA and 2 mM ATP. After the macroscopic current reached the steady state, subsequent application of 10 mM ATP plus 2 mM MgPPi further increased the current. Washout of this mixed solution resulted in a biexponential

current decay with a fast component reflecting ATP-induced open state ($\tau \sim 400$ ms) and a slow component ($\tau \sim 30$ s) representing channels in the lock-open state (c.f. Vergani et al., 2003). After the current reached the baseline, PKA and 2 mM ATP were applied again to ensure full phosphorylation of the channels. Once the channels were fully activated, 2 mM ATP and 2 mM MgPPi were applied. Note that not only is the steady state current with 2 mM ATP plus 2 mM MgPPi higher than that with 10 mM ATP plus 2 mM MgPPi, the current increase is also faster. In addition, the biphasic current decay after the removal of 2 mM ATP plus 2 mM MgPPi shows a noticeably smaller faction of the fast phase, indicating more channels enter the lock-open state (see the arrows in Fig. 2-5A). Thus, although MgPPi only locks open CFTR after the channel is primed by ATP, a higher [ATP] actually exerts an inhibitory effect. As summarized in Fig. 2-5B (red symbols), the fraction of the slow component decreased as the concentration of ATP was elevated. On the other hand, when [ATP] was fixed at 2 mM, an increased concentration of MgPPi led to a larger fraction of the slow component (see Fig. 2-5B, blue symbols). These results are consistent with the idea that ATP and MgPPi compete for a common binding site.

It seems counterintuitive that not all channels in the membrane patches are locked open in the presence of equal concentrations of ATP and MgPPi, when one considers the fact that the lock-open state ($\tau \sim 30$ s) is > 50 fold more stable than the regular open state ($\tau \sim 400$ ms). This phenomenon, however, can be readily explained by a proposition that ATP out-competes MgPPi in opening the channel. For example, when MgPPi and ATP are both at 2 mM, the slow component has a time constant $\tau_s = 26.9 \pm 1.56$ s (n = 12), while the time constant of the fast component

(τ_f) is 0.55 ± 0.06 s. From the fractional amplitude of the slow component (70.2 ± 3.7 %), we estimated that only 1 in every ~ 20 openings results in a lock-open event. This conclusion is probably not surprising as results from Zhou et al., (2006) suggested that the ring-ring stacking interaction (Lewis et al., 20005; cf. Lewis et al., 2004 and Thibodeau et al., 2005), which MgPPi is lacking, between the side chain of aromatic residues in NBDs (W401 in NBD1 or Y1219 in NBD2) and the adenine ring of ATP may play an important role in nucleotide binding. In fact, we have already shown above that MgPPi has a lower potency than ATP to open channel from the C_1-state.

If NBD2 is indeed the common binding site for ATP and MgPPi, one expects that removal of the side chain of Y1219 should diminish ATP's advantage in competing for the binding pocket. Fig. 2-5C shows that 2 mM MgPPi, when added to 2 mM ATP solution, dramatically increased the Y1219G-CFTR macroscopic current. Unlike the data for WT-CFTR (Fig. 2-5A), the current relaxation upon removal of ATP and MgPPi follows a monotonic decay with a time constant τ = 30.7 ± 4.5 s (n = 5), indicating that almost all Y1219G-CFTR channels have been locked open under this experimental condition. As a control, when a similar experiment was carried out for W401G. ATP still out-competes MgPPi as demonstrated by a large fraction of the fast component during current relaxation (data not shown).

Although scheme 1 depicts the first step of channel closure as a single step, as described above, this is likely an oversimplification. If this step indeed involves ATP hydrolysis and dissociation of the hydrolytic products as we speculated above, there

FIGURE 2-5

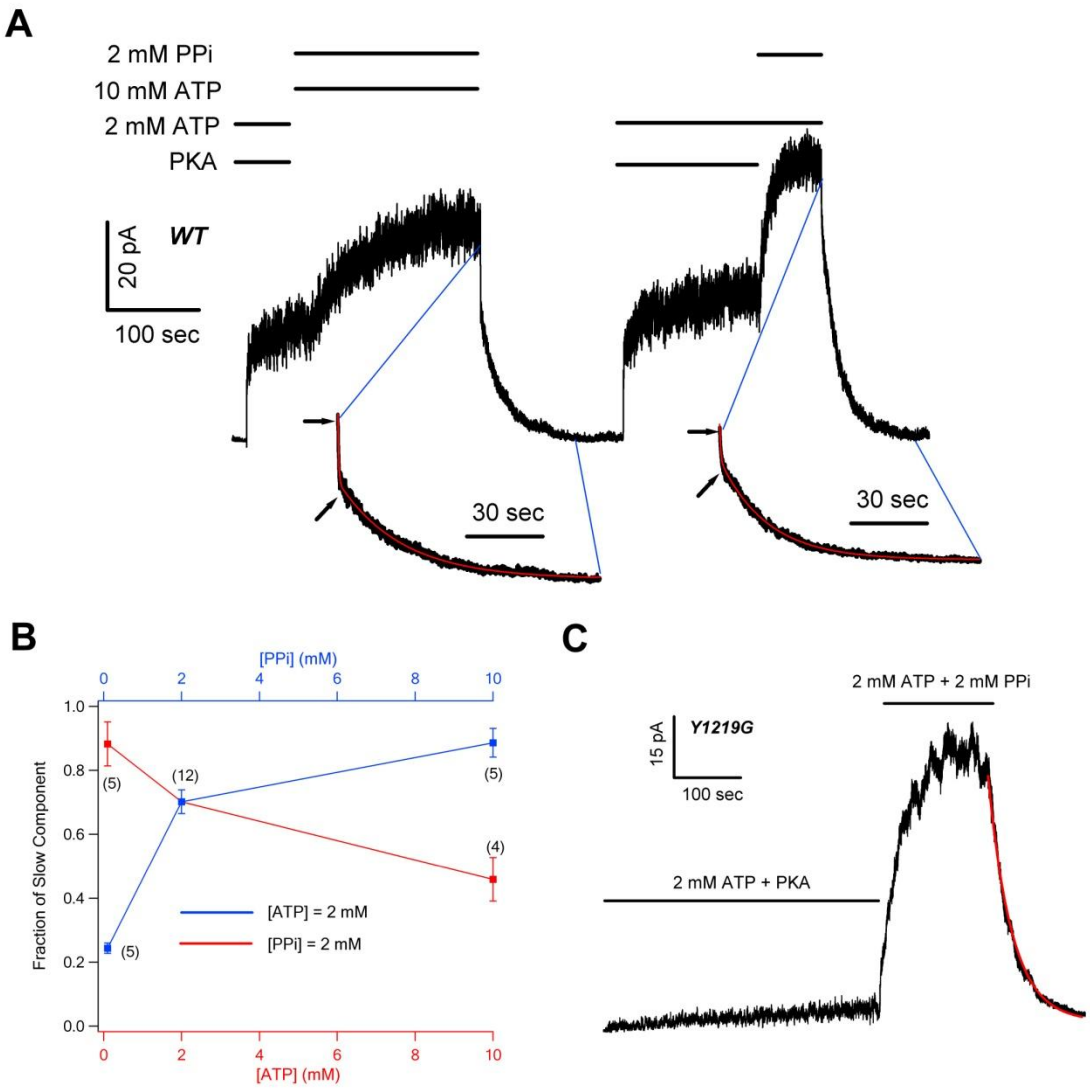
A
2 mM PPi
10 mM ATP
2 mM ATP
PKA
20 pA
WT
100 sec
30 sec
30 sec
B
[PPi] (mM)
0
2
4
6
8
10
1.0
0.8
0.6
0.4
0.2
0.0
Fraction of Slow Component
(5)
(12)
(5)
(4)
(5)
[ATP] = 2 mM
[PPi] = 2 mM
[ATP] (mM)
C
2 mM ATP + 2 mM PPi
15 pA
Y1219G
100 sec
2 mM ATP + PKA

Figure 2-5. ATP and MgPPi compete for a common binding site. (A) Steady state macroscopic current of WT-CFTR activated by 2 mM ATP and PKA was further increased by the application of 2 mM MgPPi + 2 mM ATP (right) or 2 mM MgPPi + 10 mM ATP (left). With lower [ATP] in the PPi solution, the current increase proceeds more rapidly (right). Fitting the current relaxation yields two time constants after the removal of 2 mM ATP plus 2 mM PPi (τ_1 = 0.55 ± 0.06 s, τ_2 = 26.9 ± 1.56 s, n = 12) or after 2 mM MgPPi + 10 mM ATP (τ_1 = 0.34 ± 0.03 s, τ_2 = 30.4 ± 3.1 s, n = 4). *Arrows* indicate the end of the fast component during current decay. **(B)** The fractional amplitude of the slow component under different combinations of [MgPPi] and [ATP]. Raising [ATP] (red line, lower X-axis) or reducing [PPi] (blue line, upper X-axis) decreases the fractional amplitude of the slow component. **(C)** Effects of PPi on Y1219G-CFTR. 2 mM ATP + PKA activated a small amount of current due to a reduced apparent affinity for ATP by the mutation. Upon application of 2 mM PPi plus 2 mM ATP, the current was greatly enhanced. The current decays monotonically with τ = 30.7 ± 4.5 s (n = 5).

must exist other closed state configurations. For example, one can imagine one closed state with ADP remained bound and the other closed state with an empty binding pocket. These two possible states can be differentiated by adding MgPPi in the presence of ADP. If ADP inhibits the effect of MgPPi as ATP, one can argue that the closed state where MgPPi acts should have an unoccupied NBD2. In Fig. 2-6A (n = 5), we show that a direct solution switch from 2 mM ATP to 2 mM MgPPi (a deadtime of ~ 20 ms) resulted in fast channel closure followed by a reopening of the channels. However, when the MgPPi solution was mixed with 5 mM ADP, the second-phase current rise was mostly abolished (summarized in Fig. 2-6B), indicating that ADP indeed inhibits the effect of MgPPi. It is known that ADP inhibits the ATP-dependent WT-CFTR activity (Anderson and Welsh, 1992; Gunderson and Kopito, 1994; Winter et al., 1994; Schultz et al., 1995) mainly by competing for NBD2 of CFTR (Bompadre et al., 2005a). Our results thus suggest that regardless whether NBD2 binding site is occupied by ATP that leads to channel opening, or by ADP which keeps the channel in a closed state with a bound ADP at the NBD2 site, MgPPi fails to exert its effects. We therefore propose that NBD2 is vacant when the channel is in the C_2 state.

Life Time of the C_2 State is Affected by the Nucleotide Biding Affinity in NBD1

Although the NBD2 site is vacant in the C_2 state, one ATP molecule may remain tightly bound at NBD1 to account for the long-lasting "memory" assumed by the C_2 state. We hypothesize that it is the dissociation of ATP at NBD1 that is responsible for the $C_2 \rightarrow C_1$ transition. This hypothesis predicts that a high affinity ATP analogue

FIGURE 2-6

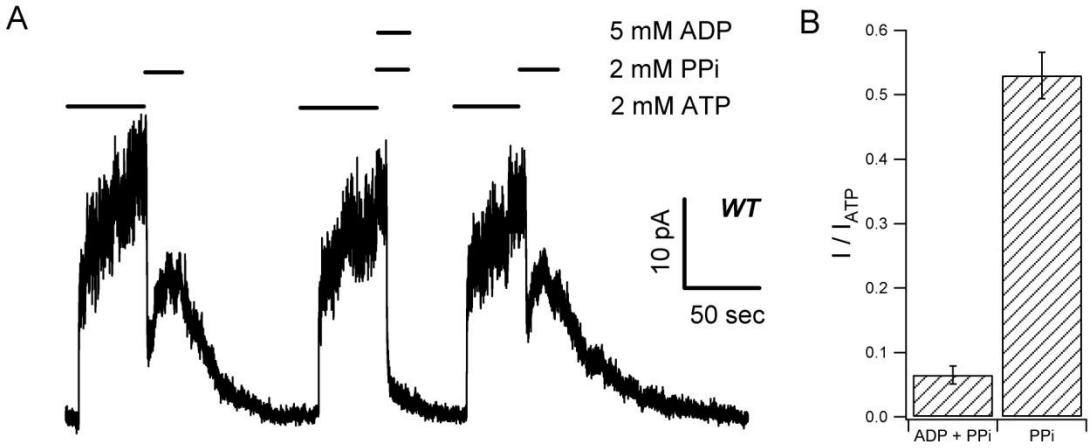

Figure 2-6. ADP inhibits the reopening of WT-CFTR by MgPPi. (A) WT channels were first opened by ATP. Once current reached steady state, a direct switch of the solution to MgPPi (dead time ~ 30 ms) results in a rapid decrease of the current followed by an increase of the current. In the same patch, the effect of MgPPi was dramatically reduced when applied together with 5 mM ADP. **(B)** Summary of data presented in (A). Steady state current induced by MgPPi or MgPPi + ADP was normalized to original ATP-dependent current. I_{MgPPi} / I_{ATP} = 0.53 ± 0.036 (n = 5); $I_{MgPPi\text{-}ADP}$ / I_{ATP} = 0.065 ± 0.014 (n = 5) ($P < 0.01$).

in NBD1 should slow down the dissipation of the C_2 state. To test this prediction, we used N^6-(2-phenylethyl)-ATP (P-ATP), which is 50-fold more potent than ATP (Zhou et al., 2005), to activate WT-CFTR. After macroscopic current was first elicited by the nucleotide at a saturating concentration (i.e. 2 mM ATP or 50 μM P-ATP), changing the perfusion solution directly to 2 mM MgPPi alone caused a rapid current decline due to channel closure through ATP hydrolysis and a subsequent current rise from the lock-open channels by MgPPi (Fig. 2-7A). We measured the ratio of the peak current induced by MgPPi (I_{PPi}) to the original nucleotide-activated current (I_N). It should be noted that since the open probabilities of WT-CFTR in the presence of ATP or P-ATP are 0.45 and 0.65 respectively (Zeltwanger et al., 1999; Zhou et al., 2006), a fair comparison of the two ratios (I_{PPi} /I_{ATP} and I_{PPi} /I_{PATP}) requires normalization of the open probability. We recalibrated the ratio using the following strategy. First we obtained the current level (I_N) reflecting all channels being in the open state by dividing I_{ATP} (or $I_{P\text{-}ATP}$) with the open probability (0.45 for I_{ATP}, and 0,65 for $I_{P\text{-}ATP}$). Then we divided the current generated by MgPPi (i.e., I_{PPi}) with I_N (the left-hand Y axis of Fig. 2-7C). This type of analysis more accurately portrays the actual number of channels entering the lock-open state under different conditions. As summarized in Fig. 2-7C, when the channels were first opened by P-ATP, 2 mM MgPPi locks open 49.3 ± 5.4 % (n = 4) of all channels in the patch. In contrast, when the channels were pretreated with ATP, only 19.5 ± 1.7 % (n = 5) of the channels were locked open.

We then used the same protocol to test the effect of MgPPi on the W401G mutation, which likely decreases the nucleotide binding affinity in NBD1 (Zhou et

FIGURE 2-7

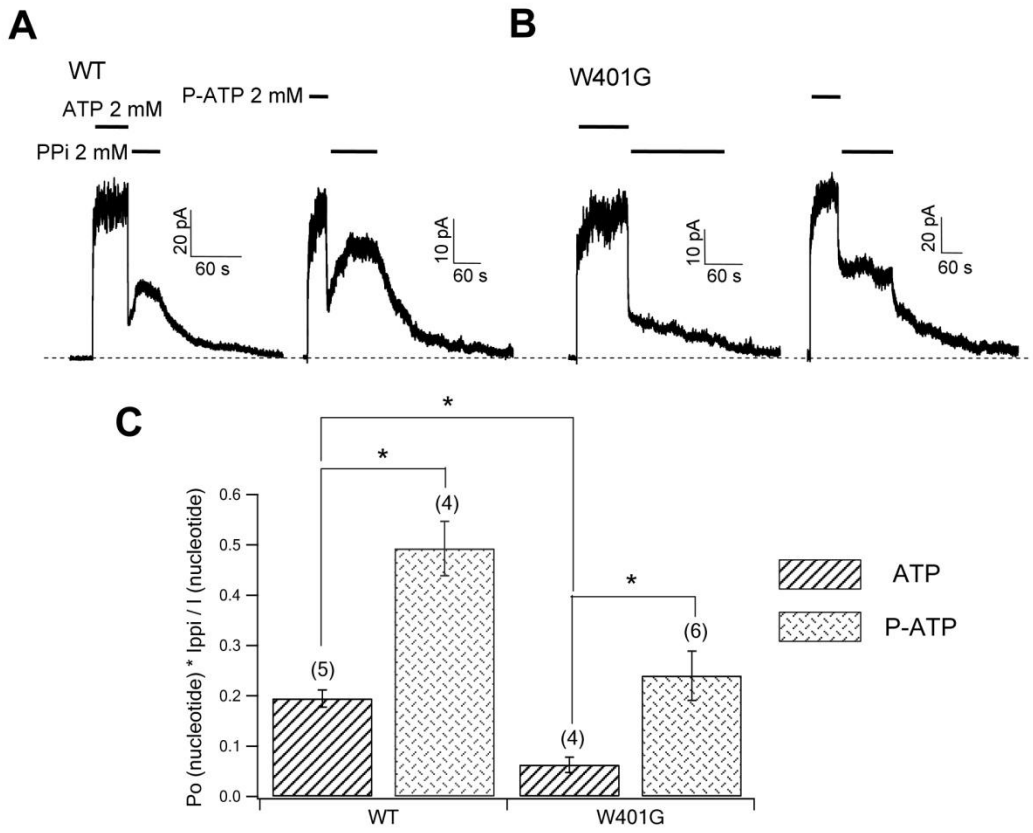

Figure 2-7. The effect of MgPPi can be modulated by altering the ligand-NBD1 interaction. (A) WT channels were exposed to 2 mM MgPPi solution immediately following washout of 2 mM ATP or 50 μM P-ATP. **(B)** The lock-open efficiency of MgPPi was reduced by the W401G mutation and P-ATP can partially restore the effectiveness of MgPPi on W401g-CFTR. **(C)** Summary of data presented in (A) and (B). *Asterisk*: $P < 0.01$.

al., 2006) because the imidazole ring of this tryptophan residue forms a ring-ring stacking interaction with the adenine ring of ATP in the crystal structure of human NBD1 (Lewis et al., 2005). As shown in Fig. 2-7B, changing the solution containing 2 mM ATP immediately to one with 2 mM PPi only locked open a small fraction of the channels (6.3 ± 1.9 % , n = 5). Previously, Zhou et al. (2006) showed that P-ATP may assume a tighter binding than ATP at NBD1 of W401G-CFTR. Indeed, opening of W401G-CFTR channels with P-ATP results in a higher fraction (24 ± 1.5 %, n = 5) of lock-open channels (Fig. 2-7B and C). Taken together, these data suggest that the binding affinity of nucleotide in NBD1 can affect the stability of the C_2 state. Interestingly, we also found that S1347G, a mutation at NBD2 signature sequence, which presumably forms the ATP binding pocket with NBD1's Walker A domain upon NBD dimer formation, greatly attenuates the stability of the C_2 state and this reduced stability can also be partly reversed by P-ATP (see supplemental Fig. 2-S1). More detailed interpretations of this result will be described in *Discussion*.

C_2 State Exists after the Channel is Opened by ATP

As described above, our findings suggest that upon removal of ATP, the open channel closes to the C_2 state which likely has one ATP trapped in NBD1. Then, the C_2 to C_1 transition is coupled to the slow dissociation of this trapped ATP (Illustrated in Fig. 2-8A). However, as shown in Fig. 2-8B, once ATP is available to the closed channel in the C_1 state, theoretically, there could be a closed state (C_2*) with one ATP bound at NBD1 before the channel enters the open state. An immediate

FIGURE 2-8

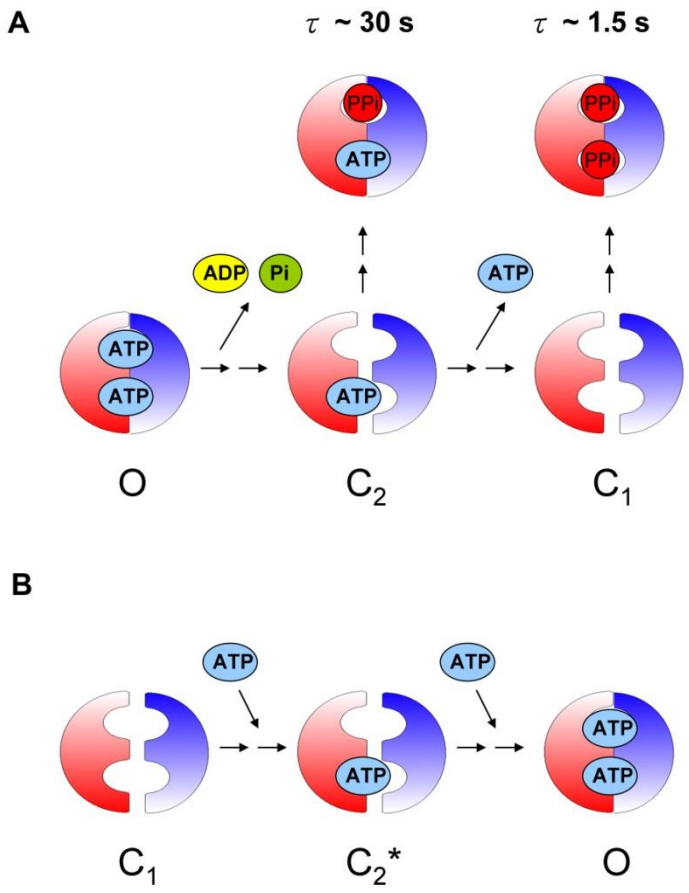

Figure 2-8. Multiple closed states of WT-CFTR. (A) Upon washout of ATP, the first closing step (O → C_2) involves ATP hydrolysis and dissociation of hydrolytic products from the NBD2 site. The second step (C_2 → C_1) is regulated by a slow dissociation of ATP from the NBD1 site. The two closed states respond to MgPPi differently. **(B)** Re-application of ATP brings the channel in the C_1 state to a hypothetical C_2^* state with one ATP bound in NBD1. Double arrows between each state reflect the likely existence of other unidentified closed states.

question arises: whether the two closed state (i.e., C_2 and C_2*) share the same property?

To address this question, we used Y1219G-CFTR to test whether MgPPi has the same effect on these two closed states. We reasoned that as this mutant has a >50-fold lower nucleotide binding affinity at NBD2 (Zhou et al., 2006), we can modify the distribution of channels in C_2 or C_2* states by using different concentrations of ATP. Treating the channels that have been closed for a long time (thus in the C_1 state) with a low concentration of ATP should favor an accumulation of the C_2* state as the transition rate from C_2* to O is significantly decreased by the Y1219G mutation, whereas a high concentration of ATP opens the channel more frequently and thus brings more channels to the C_2 state. If the two closed states respond to MgPPi in a similar manner, the subsequent addition of MgPPi to ATP solutions should result in a very similar response irrespective of the proportion of channels in the C_2 and C_2* state.

After PKA and ATP activation and a one minute washout, we first treated Y1219G channels with 500 μM ATP, which only elicited minimal current. Adding 2 mM MgPPi, as expected, greatly increased the channel activity. However, when the channels in the same patch were pretreated with 20 mM ATP, 2 mM of MgPPi plus 20 mM ATP locked open channels much faster (Fig. 2-9A). We compared the current increase 10 sec and 2 min after channels were exposed to 500 μM or 20 mM ATP plus MgPPi. In 6 patches, without exception, we found that more current was induced by MgPPi in the presence of 20 mM ATP (Fig. 2-9 B and C). These results

FIGURE 2-9

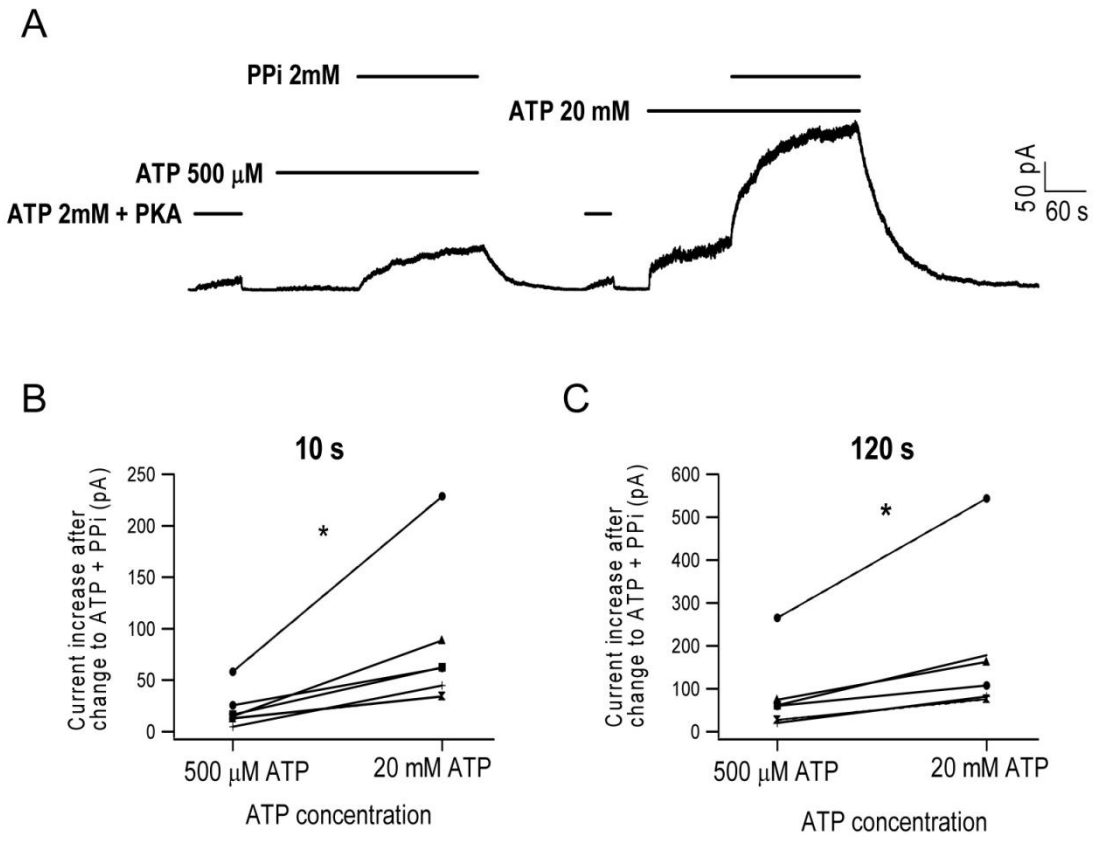

Figure 2-9. Effects of PPi are facilitated by channel opening. (A) A continuous current trace of Y1219G-CFTR. After the channels were activated by PKA and ATP, phosphorylated channels were first exposed to either 500 μM ATP or 20 mM ATP. Subsequent application of 2 mM MgPPi locked open the channels more efficiently when the channels were first opened by 20 mM ATP. **(B)** Comparison of the current increase 10 s after addition of MgPPi ($n = 6$, $P < 0.05$). Paired samples statistics: 21.7 ± 7.9 pA (500 μM ATP) and 73.8 ± 30.1 pA (20 mM ATP). **(C)** Comparison of the current increase 2 min after addition of MgPPi ($n = 6$, $P < 0.05$). Paired samples statistics: 84.5 ± 37.2 pA (500 μM ATP) and 190.1 ± 72.8 pA (20 mM ATP).

indicate that the C_2 and C_2* states are two distinct closed states. Furthermore, as 20 mM ATP shifts the channel distribution to the C_2 state, it is likely that the C_2 state has a stronger response to MgPPi than the C_2* state. The possible structural difference between the C_2 and C_2^* states will be discussed (see *Discussion*).

MgAMP-PNP Locks Open WT-CFTR with a Similar Mechanism as MgPPi

In the current study, we demonstrated that MgPPi binds to the ATP-primed C_2 state to induce lock-open events for CFTR channels. We wondered whether this mechanism could also explain the action of non-hydrolyzable ATP analogues that were reported to lock open the channel (Hwang et al., 1994). In Fig. 2-10A, we showed that the closed channels were relocked open after the ATP-containing solution was switched directly to one with 2 mM MgAMP-PNP (cf. Fig. 2-3A above). The slow current decay following MgAMP-PNP removal yields a time constant of 47.5 ± 7.3 s (n = 5). On the other hand, when the same concentration of MgAMP-PNP was applied 2 min after ATP washout, a very small current was elicited (cf. Fig. 2-1A). The ensemble macroscopic current relaxation could be fitted with a single exponential function with a time constant of 1.61s (n = 5). These results with MgAMP-PNP are qualitatively very similar to the effects of MgPPi.

Additionally, we showed that MgAMP-PNP and ATP compete for a common binding site (Fig. 2-10B and data not shown) and that ADP inhibits long open bursts induced by MgAMP-PNP once ATP was withdrawn (Fig. 2-10A). These effects have been demonstrated for MgPPi (cf. Figs. 2-5 and 2-6). Similar experiments as shown in Fig. 7 were carried out for MgAMP-PNP with W401G-CFTR and P-ATP, and

virtually identical results were obtained (data not shown). Interestingly however, we found that MgAMP-PNP, when applied minutes after removal of ATP (thus acting on the C_1 state), activates WT-CFTR with a maximally effective concentration of ~ 2 mM, which is significantly lower than that of MgPPi (see Fig. 2-2B). When MgAMP-PNP acts on the C_2 state, there is also very little difference between 2 mM and 10 mM MgAMP-PNP as the currents induced by these two concentrations of MgAMP-PNP immediately after ATP washout are 66.2 ± 3.9 % (n = 5) and 77.9 ± 4.1 % (n = 4) of the original ATP-induced current respectively. These results are consistent with those reported by Vergani et al., (2003), who showed that the effect of MgAMP-PNP, similar to ATP, is saturated at millimolar concentration. Therefore, the low efficacy of MgAMP-PNP in opening the channel by itself seems to reflect its intrinsic property as a poor ligand instead of a lower binding affinity than ATP.

If the ring-ring stacking interaction between the side chain of Y1219 and the adenine ring of ATP (or AMP-PNP) is indeed critical in determining the affinity of nucleotide binding at the NBD2 site, removing the side chain of Y1219 is expected to lower the binding affinity for ATP as well as MgAMP-PNP. As seen in Figs. 2-10B and 2-10C, when [ATP] = [MgAMP-PNP] = 2 mM, the fractional amplitudes of the slow component upon current relaxation are 73 ± 3% (n = 6) and 71 ± 4% (n = 6) for WT- and Y1219G-CFTR, respectively. Thus, although the Y1219G mutation alters the competition between ATP and MgPPi for the NBD2 site (Fig. 2-5), the same mutation does not affect the competition between ATP and MgAMP-PNP, suggesting that the Y1219G mutation decreases the binding affinity of ATP to a similar extent as it lowers the affinity for MgAMP-PNP.

FIGURE 2-10

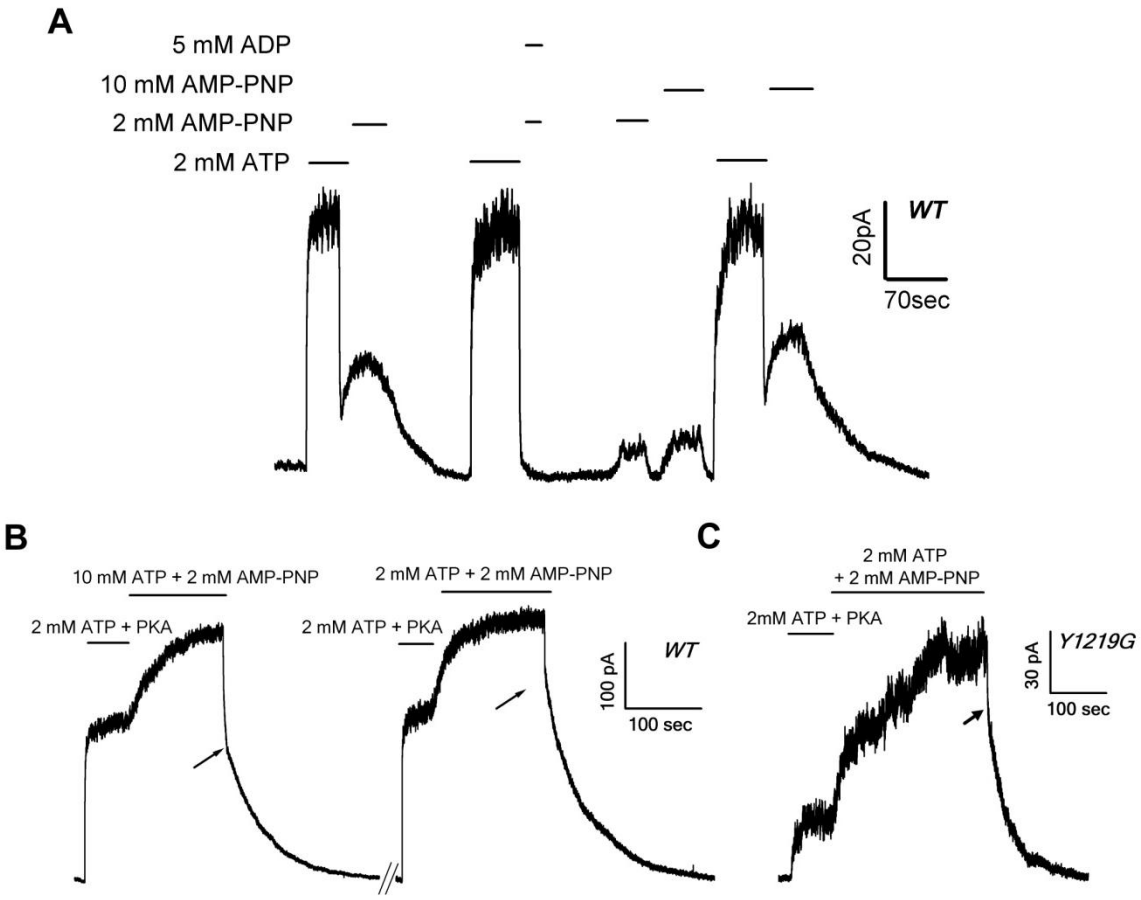
A
5 mM ADP
10 mM AMP-PNP
2 mM AMP-PNP
2 mM ATP
20pA
WT
70sec
B
10 mM ATP + 2 mM AMP-PNP
2 mM ATP + PKA
2 mM ATP + 2 mM AMP-PNP
2 mM ATP + PKA
100 pA
WT
100 sec
C
2 mM ATP
+ 2 mM AMP-PNP
2mM ATP + PKA
30 pA
Y1219G
100 sec

Figure 2-10. Modulation of CFTR gating by MgAMP-PNP. **(A)** A continuous recording shows that MgAMP-PNP locks open CFTR shortly after ATP removal (relaxation time constant τ = 47.5 ± 7.3s, n = 5). This effect was nearly completely abolished by mixing 2 mM MgAMP-PNP with 5 mM ADP. After a long nucleotide washout, 2 mM or 10 mM MgAMP-PNP induced short openings (ensemble current relaxation τ = 1.61s, n = 5). **(B)** WT-channels were exposed to 2 mM MgAMP-PNP plus 10 mM (left) or 2 mM ATP (right) after PKA activation. Parameters yielded by double exponential fit are F_{slow} = 51 ± 4.3%, τ_{fast} = 0.57 ± 0.17, τ_{slow} = 40.2 ± 4.9s, n = 5 (2 mM MgAMP-PNP + 10 mM ATP) and F_{slow} = 73 ± 3%, τ_{fast} = 0.45 ± 0.06, τ_{slow} = 45.7 ± 7.1s, n = 6 (2 mM MgAMP-PNP + 2 mM ATP). **(C)** Y1219G-channels opened by ATP + PKA were locked open by 2 mM MgAMP-PNP + 2 mM ATP. The bi-exponential current decay gives F_{slow} = 71 ± 4%, τ_{fast} = 0.45 ± 0.03, τ_{slow} = 36.7 ± 4.1s (n = 6). *Arrows* in (B) and (C) indicate the beginning of the slow component.

2-5. Discussion

In the current studies, using MgPPi as a probe, we identify three distinct closed states (C_1, C_2, and C_2^*) of the CFTR chloride channels and propose a multi-step channel closing scheme following ATP hydrolysis. Three novel findings are reported in the current report. First, MgPPi alone can open CFTR despite having a much lower apparent affinity than ATP. Second, MgPPi locks open ATP-primed channels that are already closed. Third, MgPPi affects CFTR gating in a state-dependent manner. The functional significance and potential structural implications of our results will be discussed.

MgPPi as a Ligand to Support CFTR Gating

Although it's generally agreed that ATP-dependent gating of WT-CFTR is predominantly controlled by ATP binding/hydrolysis events in NBD2 (Gadsby et al., 2006; Chen and Hwang, 2008), how ATP interacts with NBD2 to open the channel remains unclear. Nevertheless, a few clues for this question have already been provided by previous studies testing effects of different nucleotides on CFTR. First, it was reported that CFTR channels can be opened efficiently by a wide range of nucleoside triphosphates, including ATP, GTP, ITP, CTP, and UTP (Anderson et al. 1991). These results indicate that the base of the nucleoside triphosphate may not be critical in opening CFTR. In sharp contrast, the observation that ADP acts as a competitive inhibitor of ATP (Anderson et al., 1991; Anderson and Welsh, 1992; Gunderson and Kopito, 1994; Winter et al., 1994; Schultz et al., 1995; Bompadre et

al., 2005a) points to the crucial role of the phosphate group in triggering channel openings. That nucleotides with an altered bridging structure between β-γ phosphates, such as AMP-PNP, AMP-PCP and ATPγS, only induce minimal channel activity (Anderson et al., 1991; Nagel et al., 1992; Hwang et al., 1994; Aleksandrov et al., 2000; Vergani et al., 2003) also corroborates this idea.

The importance of the phosphate group of ATP in triggering CFTR channel opening is further supported by the current study where we demonstrated that pyrophosphate, which preserves the β-γ phosphate conformation (reviewed in Clark and Morley, 1976), elicits opening events in the complete absence of ATP (Fig. 1). To explain early failure in observing PPi's effect on CFTR, we found that PPi opens CFTR in a Mg^{2+} dependent manner (Fig. 2-2). This result probably is not surprising as the crystal structures of CFTR NBD1 (Lewis et al., 2004) have revealed that Mg^{2+} is coordinated by β-γ phosphates of ATP. The functional importance of this interaction between Mg^{2+} and β-γ phosphates is established by the observation that omission of Mg^{2+} can severely impair channel opening by ATP (Schultz et al., 1996; Aleksandrov et al., 2000; Ikuma and Welsh, 2000; Dousmanis et al., 2002).

More recent studies suggest a critical role of the evolutionarily conserved signature sequence (LSGGQ) in the signal transduction from ATP binding in NBDs to the gate of CFTR. First, several high-resolution crystal structures of ABC transporter proteins show that the oxygen atom in the γ phosphate of ATP forms hydrogen bonds with residues of the signature sequence once two NBDs establish a head-to-tail dimer (Hopfner et al., 2000; Smith et al., 2002; Chen et al., 2003; Zaitseva et al.,

2005). Second, the observation that the G551D mutation at the signature sequence completely abolishes ATP-dependent gating of CFTR (Bompadre et al., 2007 and 2008) point to the functional significance of this interaction. Third, while G551D-CFTR cannot be opened by ATP, this mutant channel can be gated by Cd^{2+}. Interestingly, when a cysteine residue, which is known to bind avidly to soft metals like Cd^{2+}, is engineered into the signature sequence of CFTR's NBD1, the mutant channels can also be gated by Cd^{2+} (Wang et al., 2009). This latest result suggests that the interaction between the ligand (ATP or Cd^{2+}) and the signature sequence is essential in transducing the molecular events in NBDs to the channel gate. If MgPPi is capable of binding to the same site occupied by the β-γ phosphates of ATP to interact with the signature sequence, it is not surprising that MgPPi by itself can gate CFTR.

The new result that MgPPi by itself can gate CFTR also offers clues for the role of the adenine ring of ATP in the gating process. Zhou et al. (2006) reported that Y1219G-CFTR, which presumably loses the π-electron stacking interaction between the aromatic side chain of the tyrosine residue and the adenine ring of ATP, has a far lower ATP binding affinity compared with WT-CFTR. In addition, P-ATP, an ATP analogue with an extra benzene ring attached to adenine (Zou et al. 2005, 2006), activates WT-CFTR at micromolar concentration. Taken together, these results suggest that the adenine ring, while not essential for ATP-dependent gating of CFTR, may help stabilizing binding of ATP molecules onto the NBD site. This idea predicts that a ligand without the base will have a lower binding affinity. Indeed, 15 mM MgPPi has yet to saturate the current response (Fig. 2-2B) whereas the maximal

current of WT-CFTR can be attained by 2.75 mM ATP (Zeltwanger et al., 1999). Although we cannot rule out the possibility that MgPPi has a low binding affinity simply because it doesn't bind to the Walker A domain as well as ATP, the observation that MgAMP-PNP elicits a maximal effect on CFTR at low millimolar concentration (Vergani et al., 2003; Fig. 2-10A) and that the binding affinity of MgAMP-PNP is weakened by Y1219G mutation (Fig. 2-10C) suggest that a lack of the ring-ring interaction may have a greater impact on the ligand binding affinity than a slight structural alteration of the phosphate group.

In addition to the difference in apparent affinity, another difference between ATP and MgPPi in channel gating is the burst duration. The current relaxation after MgPPi removal yields a time constant of ~ 1.5 sec while only ~ 400 ms after MgATP washout for WT-CFTR (Fig 2-1B). As PPi was reported to be hydrolyzed by many enzymes, including Glucose-6-phosphatase in rat liver (Nordlie et al., 1999), alkaline phosphates of *E.coli* (Anderson and Nordlie, 1967), pyrophosphate-dependent phosphofructokinase in plants (Carnal and Black, 1979), we first considered the possibility that MgPPi has a lower hydrolytic rate than ATP in the NBD2 composite site and thus the opening events are terminated more slowly. This hypothesis can be tested by comparing the gating kinetics of MgPPi in WT- and E1371S-CFTR, a mutant whose ATPase activity is abolished (Moody et al., 2002; Tombline et al., 2004; Vergani et al., 2005; Zhou et al., 2006; Stratford et al., 2007). We reasoned that if MgPPi elicits longer open bursts due to a slower hydrolysis rate, E1371S mutation should further prolong the burst duration induced by MgPPi. However, as can be seen in Fig. 2-S2, although the E1371S mutation dramatically increases the

relaxation time constant of the ATP-gated channels (τ = 126.1 ± 24.2 s, n = 5), the lifetime of MgPPi-induced openings for E1371S channels (1.65 s, ensemble current relaxation from 5 data) is very close to that of WT-CFTR (~ 1.5 s in Fig. 2-1B). This result suggests that both MgPPi-opened WT- and E1371S-CFTR channels close through a non-hydrolytic pathway. MgPPi elicits longer opening events in WT channels than ATP because ATP-induced openings are terminated by rapid ATP hydrolysis. Finally, the data also indicate that MgPPi is a poor ligand for CFTR channels because, unlike ATP, it fails to induce a stable open state with E1371S-CFTR.

MgPPi Locks Open CFTR Channels when an ATP is Bound in NBD1

The second novel finding presented in the current manuscript is that when the WT CFTR channels are first opened by ATP, MgPPi applied within seconds after ATP withdrawal locks open the channels (Fig. 2-3). The lifetime of this lock-open state (~ 30 s) is much longer than that opened by MgPPi alone after a three-minute ATP washout (~ 1.5 s) as described above. These results indicate the presence of two different closed states, C_1 and C_2, which respond to MgPPi differently. It should be noted that this conclusion is model independent. It is solely based on the experimental observation that MgPPi exerts different effects when applied at different times during which the channels are closed.

Because the longer the washout, the fewer the channels capable of entering the lock open state and the more the channels responding poorly to MgPPi, we postulate a dissipation of the C_2 state and an accumulation of the C_1 state over time during the

ATP washout phase. Since the C_2 to C_1 transition can be slowed down when the channel is first opened by a high-affinity ATP analogue, P-ATP (Fig. 2-7), we propose that there is at least one ATP molecule remained bound in the C_2 state. We envisage that the dissociation of this bound ATP in the C_2 state is associated with the transition from the C_2 state to the C_1 state. Thus a more tightly bound P-ATP can stabilize the C_2 state more strongly than ATP.

Two lines of evidence suggest that NBD1 is occupied by ATP during the C_2 state. First, biochemical studies showed that NBD2 is a site with a high nucleotide turnover rate due to rapid ATP hydrolysis, while NBD1 is a site of more stable nucleotide binding (Szabo et al., 1999; Aleksandrov et al., 2001, 2002, 2008; Basso et al., 2003). Second, W401G mutation, which likely reduces ATP binding affinity in NBD1 (Zhou et al. 2006), decreases the stability of the C_2 state. The fact that this mutational effect on the stability of the C_2 state can be at least partially overcome by P-ATP suggests that this mutational effect can be attributed to a lower binding affinity rather than some nonspecific allosteric effects.

If the NBD1 site of the C_2 state is occupied by ATP, the likely site for MgPPi's action is the presumably vacated NBD2 site following ATP hydrolysis and dissociation of the hydrolytic products. This idea is supported by the results that both ATP and ADP can compete with MgPPi for a common binding site (Figs. 2-5 and 2-6). Furthermore, the fact that MgPPi alone can open and lock open CFTR also corroborates this proposition because the NBD2 site plays a critical role in ligand-dependent opening of CFTR. Thus, the MgPPi-induced, lock-open configuration of

CFTR's two NBDs is composed of one MgPPi molecule in NBD2 and one ATP molecule in NBD1. Since essentially the same data were obtained for MgAMP-PNP-induced lock-open state, we propose a similar configuration of NBDs for the action of MgAMP-PNP (i.e. MgAMP-PNP in NBD2 and ATP in NBD1) (see *Results*; Fig. 2-10).

So far, we have discussed how MgPPi locks open CFTR in the absence of ATP, while in the literature, PPi is reported to exert this effect on CFTR when applied together with ATP. It is important to note that channels opened by MgPPi or ATP plus MgPPi have a similar relaxation time constant upon washout (Figs. 2-3A and 2-3B) suggesting a common lock-open state under these two conditions. However, when ATP and MgPPi are applied together, it becomes difficult to tell if MgPPi acts on the open state or the closed state. To differentiate these two scenarios, we measured the fractional amplitude of the slow component in the macroscopic current decay phase after washout of ATP plus MgPPi at different concentrations of ATP (see Fig. 2-5). A larger slow component indicates that the lock-open bursts occur more frequently. If MgPPi binds to the closed state to exert its effect, an increase of [ATP] should compete for binding and thus decreases the fraction of the slow component. In contrast, if MgPPi acts on the open state, the frequency of long-opening events should not be altered by varying [ATP] at the millimolar range. Our results showing that the frequency of lock-open bursts is inversely dependent on [ATP] suggest that MgPPi indeed binds to the closed state to exert its effects even when it is applied with ATP.

For channel closure from the MgPPi-induced locked open state, in theory, dissociation of either ATP in NBD1 or MgPPi in NBD2 may be associated with the closing step. In Fig. 2-S3, when the channels opened by ATP are constantly exposed to MgPPi after ATP removal, the macroscopic current can remain at a constant level for more than 2 min. The current decay upon subsequent MgPPi withdrawal yields a single time constant $\tau = 35.7 \pm 6.4$ s ($n = 3$) indicating that once the locked open channels close, they are readily locked open again by MgPPi. This result thus suggests that it is MgPPi dissociation from NBD2 but not ATP from NBD1 that is associated with channel closing from the locked open state. This idea again is consistent with the critical role of ligand binding/unbinding at NBD2 in CFTR gating.

Structural/Biochemical Implications of the Current Results

A puzzling question in the present study is why the C_1 and C_2 states respond to MgPPi so differently. As the fundamental difference between the two closed states is whether ATP remains bound at NBD1 or not, it appears that ATP binding in NBD1 can help stabilizing the open state induced by MgPPi. Echoing this observation, the lock-open duration of MgPPi is reduced by mutations that decrease the ATP binding affinity to NBD1, K464A and W401G, but can be partially restored by a high affinity ATP analogue, P-ATP (data not shown, cf. Powe et al., 2002; Zhou et al., 2006).

Since the open state of CFTR represents a dimerization of its two NBDs, we ask whether the dimer completely separates when ATP-opened channels close to the C_2 state. If there is a strict coupling between NBD dimerization and opening of the CFTR channel gate, the NBD dimer has to undergo some kind of dissociation upon

this O → C_2 transition. A complete separation of the NBD dimer for the closing step of WT-CFTR will leave one bound ATP at NBD1 well exposed to the bulk water as seen in the monomeric ATP-NBD1 crystal structure of CFTR (Lewis et al., 2004; Lewis et al., 2005). It seems difficult to envisage that this ATP can remain tightly bound for tens of seconds. Therefore, we speculate that the NBD dimer may only partially separate once the ligand (ADP and Pi after ATP hydrolysis, or MgPPi) dissociates from NBD2. Another ligand in NBD1 will remain trapped by the partial dimer until a complete separation of the two NBDs. Supporting this hypothesis, we demonstrated that the C_2 state dissipates much faster when residues at either NBD1 (W401G, Fig. 2-7B) or the signature sequence of NBD2 were mutated (S1347G, Fig. 2-S1).

One assumption behind the partial dimer hypothesis is that the ligand in NBD1 will undergo fast binding/unbinding if not trapped in the dimer interface. In the current study, using the Y1219G mutation to slow down the channel opening rate, we identify another closed state (C_2*) which exists before the channel is opened by ATP from the C_1 state (Figs. 2-8B and Fig. 2-9). This closed state either fails to respond to MgPPi or responds to MgPPi much more inefficiently than the C_2 state. We speculate that because the NBD dimer structure is not yet formed in the C_2* state as the channel is yet to open, the rather unstable binding of ATP in NBD1 results in a slower lock-open rate of MgPPi.

As described in the *Result* section, the configuration of the C_2 state proposed in the present study seems consistent with biochemical results demonstrating that

NBD1 is a site of stable nucleotide binding (Szabo et al., 1999; Aleksandrov et al., 2001, 2002; Basso et al., 2003). A careful re-examination, however, reveals two significant disagreements. First, it was shown that 8-azido-ATP can be occluded in NBD1 for tens of minutes (Basso et al., 2003). However, our results suggest that the ATP molecule retained in NBD1 after channel closure can almost completely dissociate within one minute (Fig. 2-4). More importantly, Aleksandrov and his colleagues (2008) recently reported that the occlusion of 8-azido-ATP occurs even when NBD2 is deleted. This latest result indicates that the intrinsic high binding affinity of NBD1 *per se* is sufficient to trap the nucleotide without a need of a partial dimer as we postulated above. Although one may attribute these discrepancies to very different materials and experimental procedures used in different laboratories, it's of great interest for us to understand how to reconcile functional and biochemical results in the near future.

2-6. Supplemental information

FIGURE 2-S1

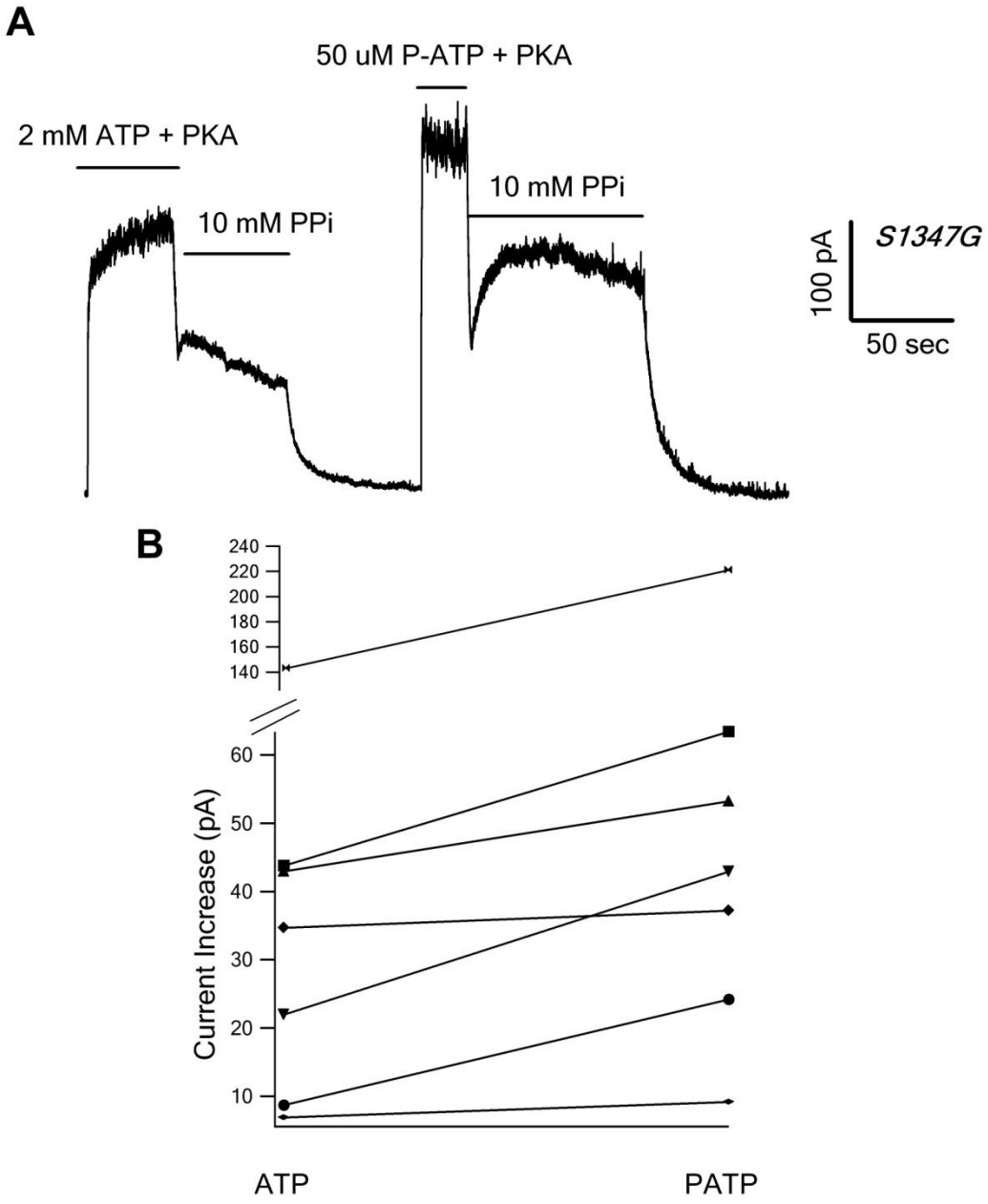

Figure 2-S1. Effects of MgPPi on S1347G-CFTR. (A) S1347G channels were activated with either 2 mM ATP or 50 μM P-ATP plus PKA. Subsequent solution switch to 10 mM MgPPi led to reopening of channels. Note that MgPPi not only induced a smaller amount of current (56 ± 3.2 % of ATP current, n = 7) compared with WT-CFTR (125 ± 7 % of ATP current, n = 5) ($P < 0.01$), but the current dropped rapidly over time even MgPPi was continuously applied (compared with Fig. S3). Pretreatment of P-ATP partially restored the decreased response of S1347G-CFTR to MgPPi. In addition, a continuous application of MgPPi can better sustain the macroscopic current than channels opened by ATP. **(B)** A comparison between MgPPi-induced maximal current after channels were opened by ATP or PATP. Data from 7 patches were presented here (paired t-test, $P < 0.05$).

FIGURE 2-S2

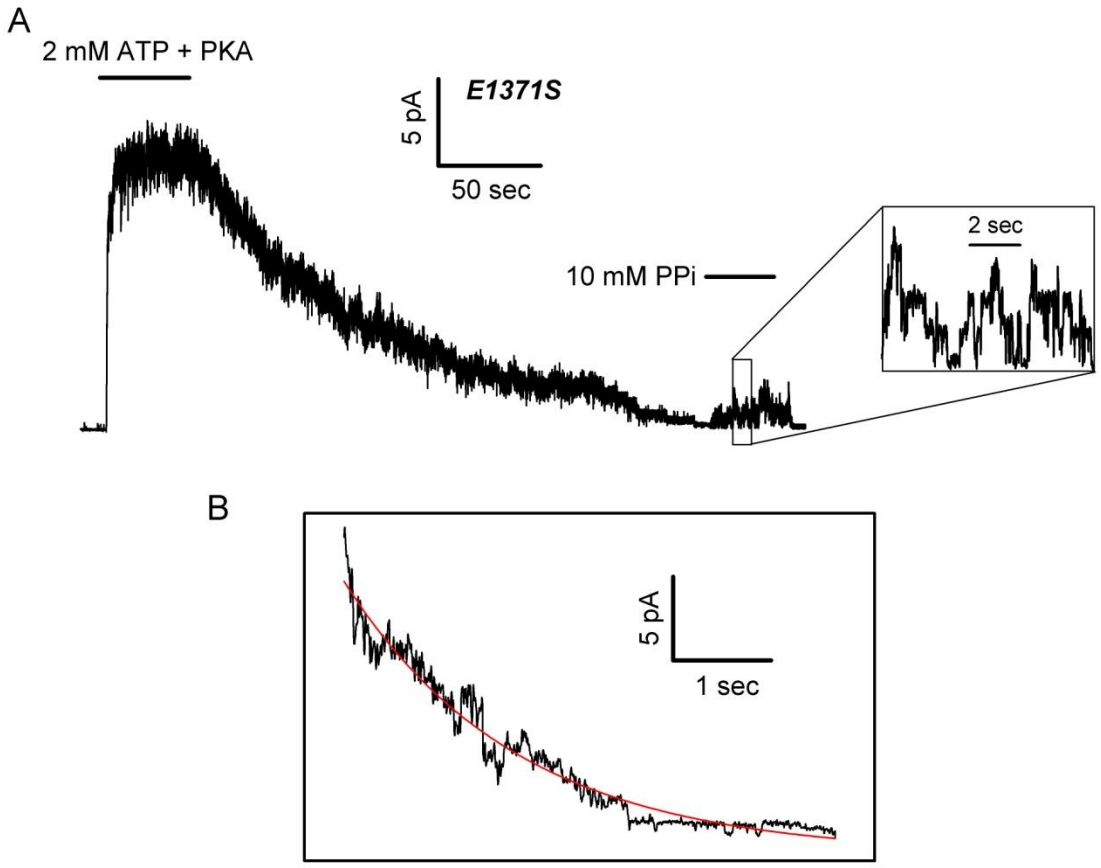

Figure 2-S2. Effects of MgPPi on E1371S-CFTR. (A) E1371S channels were first activated with 2 mM ATP + PKA. The slow current relaxation upon washout gave a time constant τ = 126.1 ± 24.2 s (n = 5). After all channels closed, application of 10 mM MgPPi alone induced short openings (inset). **(B)** Current relaxations upon MgPPi washout from 5 patches were summed. A single exponential fit of the ensemble current results in τ = 1.65 s.

FIGURE 2-S3

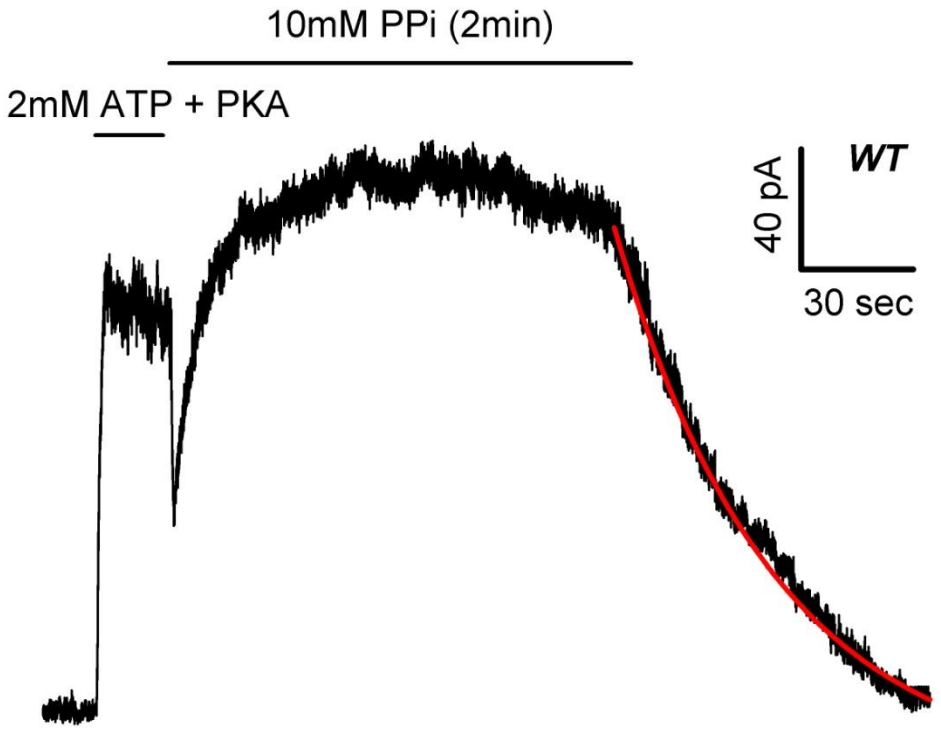

Figure 2-S3. A continuous current trace shows that macroscopic WT-CFTR current from locked open channels can be maintained for more than 2 minutes when continuously treated with 10 mM MgPPi. The current relaxation after MgPPi withdrawal gave a time constant $\tau = 35.7 \pm 6.4$ s (n = 3).

2-7. References

Aleksandrov,A.A., X.Chang, L.Aleksandrov, and J.R.Riordan. 2000. The non-hydrolytic pathway of cystic fibrosis transmembrane conductance regulator ion channel gating. *J. Physiol* 528 Pt 2:259-265.

Aleksandrov,L., A.Aleksandrov, and J.R.Riordan. 2008. Mg2+ -dependent ATP occlusion at the first nucleotide-binding domain (NBD1) of CFTR does not require the second (NBD2). *Biochem. J.* 416:129-136.

Aleksandrov,L., A.A.Aleksandrov, X.B.Chang, and J.R.Riordan. 2002. The First Nucleotide Binding Domain of Cystic Fibrosis Transmembrane Conductance Regulator Is a Site of Stable Nucleotide Interaction, whereas the Second Is a Site of Rapid Turnover. *J. Biol. Chem.* 277:15419-15425.

Aleksandrov,L., A.Mengos, X.Chang, A.Aleksandrov, and J.R.Riordan. 2001. Differential interactions of nucleotides at the two nucleotide binding domains of the cystic fibrosis transmembrane conductance regulator. *J. Biol. Chem.* 276:12918-12923.

Anderson,M.P., H.A.Berger, D.P.Rich, R.J.Gregory, A.E.Smith, and M.J.Welsh. 1991. Nucleoside triphosphates are required to open the CFTR chloride channel. *Cell* 67:775-784.

Anderson,M.P. and M.J.Welsh. 1992. Regulation by ATP and ADP of CFTR chloride channels that contain mutant nucleotide-binding domains. *Science* 257:1701-1704.

Anderson,W.B. and R.C.Nordlie. 1967. Inorganic pyrophosphate-glucose phosphotransferase activity associated with alkaline phosphatase of Escherichia coli. *J. Biol. Chem.* 242:114-119.

Basso,C., P.Vergani, A.C.Nairn, and D.C.Gadsby. 2003. Prolonged nonhydrolytic interaction of nucleotide with CFTR's NH2-terminal nucleotide binding domain and its role in channel gating. *J. Gen. Physiol* 122:333-348.

Baukrowitz,T., T.C.Hwang, A.C.Nairn, and D.C.Gadsby. 1994. Coupling of CFTR Cl- channel gating to an ATP hydrolysis cycle. *Neuron* 12:473-482.

Berger,A.L., M.Ikuma, J.F.Hunt, P.J.Thomas, and M.J.Welsh. 2002. Mutations that change the position of the putative gamma-phosphate linker in the nucleotide binding domains of CFTR alter channel gating. *J. Biol. Chem.* 277:2125-2131.

Bompadre,S.G., T.Ai, J.H.Cho, X.Wang, Y.Sohma, M.Li, and T.C.Hwang. 2005a. CFTR gating I: Characterization of the ATP-dependent gating of a phosphorylation-independent CFTR channel (DeltaR-CFTR). *J. Gen. Physiol* 125:361-375.

Bompadre,S.G., J.H.Cho, X.Wang, X.Zou, Y.Sohma, M.Li, and T.C.Hwang. 2005b. CFTR gating II: Effects of nucleotide binding on the stability of open states. *J. Gen. Physiol* 125:377-394.

Bompadre,S.G., M.Li, and T.C.Hwang. 2008. Mechanism of G551D-CFTR (cystic fibrosis transmembrane conductance regulator) potentiation by a high affinity ATP analog. *J. Biol. Chem.* 283:5364-5369.

Bompadre,S.G., Y.Sohma, M.Li, and T.C.Hwang. 2007. G551D and G1349D, two CF-associated mutations in the signature sequences of CFTR, exhibit distinct gating defects. *J. Gen. Physiol* 129:285-298.

Cai,Z., A.Taddei, and D.N.Sheppard. 2006. Differential sensitivity of the cystic fibrosis (CF)-associated mutants G551D and G1349D to potentiators of the cystic fibrosis transmembrane conductance regulator (CFTR) Cl- channel. *J. Biol. Chem.* 281:1970-1977.

Carnal,N.W. and C.C.Black. 1979. Pyrophosphate-dependent 6-phosphofructokinase, a new glycolytic enzyme in pineapple leaves. *Biochem. Biophys. Res. Commun.* 86:20-26.

Carson,M.R., M.C.Winter, S.M.Travis, and M.J.Welsh. 1995. Pyrophosphate stimulates wild-type and mutant cystic fibrosis transmembrane conductance regulator Cl-channels. *J. Biol. Chem.* 270:20466-20472.

Chen,J., G.Lu, J.Lin, A.L.Davidson, and F.A.Quiocho. 2003. A tweezers-like motion of the ATP-binding cassette dimer in an ABC transport cycle. *Mol. Cell* 12:651-661.

Chen,T.Y. and T.C.Hwang. 2008. CLC-0 and CFTR: chloride channels evolved from transporters. *Physiol Rev.* 88:351-387.

Clark,G.M. and R.Morley. 1976. Inorganic pyro-compounds $M_a[(X_2O_7)_b]$. *Chem. Soc. Rev.* 5:269-295

Cortic, T., P. Zhang, N. Todorovic, and C.M. Canessa. 2003. The extracellular domain determines the kinetics of desensitization in acid-sensitive ion channel 1. *J. Biol. Chem*. 278: 45240-45247.

Cotten,J.F., L.S.Ostedgaard, M.R.Carson, and M.J.Welsh. 1996. Effect of cystic fibrosis-associated mutations in the fourth intracellular loop of cystic fibrosis transmembrane conductance regulator. *J. Biol. Chem.* 271:21279-21284.

Csanady,L., K.W.Chan, A.C.Nairn, and D.C.Gadsby. 2005. Functional roles of nonconserved structural segments in CFTR's NH2-terminal nucleotide binding domain. *J. Gen. Physiol* 125:43-55.

Csanady,L., K.W.Chan, D.Seto-Young, D.C.Kopsco, A.C.Nairn, and D.C.Gadsby. 2000. Severed channels probe regulation of gating of cystic fibrosis transmembrane conductance regulator by its cytoplasmic domains. *J. Gen. Physiol* 116:477-500.

Dousmanis,A.G., A.C.Nairn, and D.C.Gadsby. 2002. Distinct Mg(2+)-dependent steps rate limit opening and closing of a single CFTR Cl(-) channel. *J. Gen. Physiol* 119:545-559.

Gadsby,D.C., P.Vergani, and L.Csanady. 2006. The ABC protein turned chloride channel whose failure causes cystic fibrosis. *Nature* 440:477-483.

Gunderson,K.L. and R.R.Kopito. 1994. Effects of pyrophosphate and nucleotide analogs suggest a role for ATP hydrolysis in cystic fibrosis transmembrane regulator channel gating. *J. Biol. Chem.* 269:19349-19353.

Gunderson,K.L. and R.R.Kopito. 1995. Conformational states of CFTR associated with channel gating: the role ATP binding and hydrolysis. *Cell* 82:231-239.

Higgins,C.F. and K.J.Linton. 2004. The ATP switch model for ABC transporters. *Nat. Struct. Mol. Biol.* 11:918-926.

Hopfner,K.P., A.Karcher, D.S.Shin, L.Craig, L.M.Arthur, J.P.Carney, and J.A.Tainer. 2000. Structural biology of Rad50 ATPase: ATP-driven conformational control in DNA double-strand break repair and the ABC-ATPase superfamily. *Cell* 101:789-800.

Hwang,T.C., G.Nagel, A.C.Nairn, and D.C.Gadsby. 1994. Regulation of the gating of cystic fibrosis transmembrane conductance regulator C1 channels by phosphorylation and ATP hydrolysis. *Proc. Natl. Acad. Sci. U. S. A* 91:4698-4702.

Ikuma,M. and M.J.Welsh. 2000. Regulation of CFTR Cl- channel gating by ATP binding and hydrolysis. *Proc. Natl. Acad. Sci. U. S. A* 97:8675-8680.

Lansdell,K.A., J.F.Kidd, S.J.Delaney, B.J.Wainwright, and D.N.Sheppard. 1998. Regulation of murine cystic fibrosis transmembrane conductance regulator Cl- channels expressed in Chinese hamster ovary cells. *J. Physiol* 512 (Pt 3):751-764.

Lewis,H.A., S.G.Buchanan, S.K.Burley, K.Conners, M.Dickey, M.Dorwart, R.Fowler, X.Gao, W.B.Guggino, W.A.Hendrickson, J.F.Hunt, M.C.Kearins, D.Lorimer, P.C.Maloney, K.W.Post, K.R.Rajashankar, M.E.Rutter, J.M.Sauder, S.Shriver, P.H.Thibodeau, P.J.Thomas, M.Zhang, X.Zhao, and S.Emtage. 2004. Structure of nucleotide-binding domain 1 of the cystic fibrosis transmembrane conductance regulator. *EMBO J.* 23:282-293.

Lewis,H.A., X.Zhao, C.Wang, J.M.Sauder, I.Rooney, B.W.Noland, D.Lorimer, M.C.Kearins, K.Conners, B.Condon, P.C.Maloney, W.B.Guggino, J.F.Hunt, and S.Emtage. 2005. Impact of the deltaF508 mutation in first nucleotide-binding domain of human cystic fibrosis transmembrane conductance regulator on domain folding and structure. *J. Biol. Chem.* 280:1346-1353.

Mense,M., P.Vergani, D.M.White, G.Altberg, A.C.Nairn, and D.C.Gadsby. 2006. In vivo phosphorylation of CFTR promotes formation of a nucleotide-binding domain heterodimer. *EMBO J.* 25:4728-4739.

Moody,J.E., L.Millen, D.Binns, J.F.Hunt, and P.J.Thomas. 2002. Cooperative, ATP-dependent association of the nucleotide binding cassettes during the catalytic cycle of ATP-binding cassette transporters. *J. Biol. Chem.* 277:21111-21114.

Nagel,G., T.C.Hwang, K.L.Nastiuk, A.C.Nairn, and D.C.Gadsby. 1992. The protein kinase A-regulated cardiac Cl- channel resembles the cystic fibrosis transmembrane conductance regulator. *Nature* 360:81-84.

Nordlie,R.C., J.D.Foster, and A.J.Lange. 1999. Regulation of glucose production by the liver. *Annu. Rev. Nutr.* 19:379-406.

Powe,A.C., Jr., L.Al-Nakkash, M.Li, and T.C.Hwang. 2002. Mutation of Walker-A lysine 464 in cystic fibrosis transmembrane conductance regulator reveals functional interaction between its nucleotide-binding domains. *J. Physiol* 539:333-346.

Ramjeesingh,M., C.Li, E.Garami, L.J.Huan, K.Galley, Y.Wang, and C.E.Bear. 1999. Walker mutations reveal loose relationship between catalytic and channel-gating activities of purified CFTR (cystic fibrosis transmembrane conductance regulator). *Biochemistry* 38:1463-1468.

Riordan,J.R., J.M.Rommens, B.Kerem, N.Alon, R.Rozmahel, Z.Grzelczak, J.Zielenski, S.Lok, N.Plavsic, J.L.Chou, and . 1989. Identification of the cystic fibrosis gene: cloning and characterization of complementary DNA. *Science* 245:1066-1073.

Schultz,B.D., R.J.Bridges, and R.A.Frizzell. 1996. Lack of conventional ATPase properties in CFTR chloride channel gating. *J. Membr. Biol.* 151:63-75.

Schultz,B.D., C.J.Venglarik, R.J.Bridges, and R.A.Frizzell. 1995. Regulation of CFTR Cl- channel gating by ADP and ATP analogues. *J. Gen. Physiol* 105:329-361.

Scott-Ward,T.S., Z.Cai, E.S.Dawson, A.Doherty, A.C.Da Paula, H.Davidson, D.J.Porteous, B.J.Wainwright, M.D.Amaral, D.N.Sheppard, and A.C.Boyd. 2007. Chimeric constructs endow the human CFTR Cl- channel with the gating behavior of murine CFTR. *Proc. Natl. Acad. Sci. U. S. A* 104:16365-16370.

Smith,P.C., N.Karpowich, L.Millen, J.E.Moody, J.Rosen, P.J.Thomas, and J.F.Hunt. 2002a. ATP binding to the motor domain from an ABC transporter drives formation of a nucleotide sandwich dimer. *Mol. Cell* 10:139-149.

Smith,P.C., N.Karpowich, L.Millen, J.E.Moody, J.Rosen, P.J.Thomas, and J.F.Hunt. 2002b. ATP binding to the motor domain from an ABC transporter drives formation of a nucleotide sandwich dimer. *Mol. Cell* 10:139-149.

Stratford,F.L., M.Ramjeesingh, J.C.Cheung, L.J.Huan, and C.E.Bear. 2007. The Walker B motif of the second nucleotide-binding domain (NBD2) of CFTR plays a key role in ATPase activity by the NBD1-NBD2 heterodimer. *Biochem. J.* 401:581-586.

Szabo,K., G.Szakacs, T.Hegeds, and B.Sarkadi. 1999. Nucleotide occlusion in the human cystic fibrosis transmembrane conductance regulator. Different patterns in the two nucleotide binding domains. *J. Biol. Chem.* 274:12209-12212.

Tombline,G., L.Bartholomew, K.Gimi, G.A.Tyndall, and A.E.Senior. 2004. Synergy between conserved ABC signature Ser residues in P-glycoprotein catalysis. *J. Biol. Chem.* 279:5363-5373.

Thibodeau,P.H., C.A.Brautiqam, M.Machius, and P.J.Thomas. 2005. Side chain and backbone contributions of Phe508 to CFTR folding. *Nat. Struct. Mol. Biol.* 12:10-16.

Vergani,P., S.W.Lockless, A.C.Nairn, and D.C.Gadsby. 2005. CFTR channel opening by ATP-driven tight dimerization of its nucleotide-binding domains. *Nature* 433:876-880.

Vergani,P., A.C.Nairn, and D.C.Gadsby. 2003. On the mechanism of MgATP-dependent gating of CFTR Cl- channels. *J. Gen. Physiol* 121:17-36.

Walker,J.E., M.Saraste, M.J.Runswick, and N.J.Gay. 1982. Distantly related sequences in the alpha- and beta-subunits of ATP synthase, myosin, kinases and other ATP-requiring enzymes and a common nucleotide binding fold. *EMBO J.* 1:945-951.

Wang,X., S.G.Bompadre, M.Li, and T.C.Hwang. 2009. Mutations at the signature sequence of CFTR create a Cd^{2+}-gated chloride channel. *J. Gen. Physiol* 133:69-77.

Winter,M.C., D.N.Sheppard, M.R.Carson, and M.J.Welsh. 1994. Effect of ATP concentration on CFTR Cl- channels: a kinetic analysis of channel regulation. *Biophys. J.* 66:1398-1403.

Zaitseva,J., S.Jenewein, T.Jumpertz, I.B.Holland, and L.Schmitt. 2005. H662 is the linchpin of ATP hydrolysis in the nucleotide-binding domain of the ABC transporter HlyB. *EMBO J.* 24:1901-1910.

Zeltwanger,S., F.Wang, G.T.Wang, K.D.Gillis, and T.C.Hwang. 1999. Gating of cystic fibrosis transmembrane conductance regulator chloride channels by adenosine triphosphate hydrolysis. Quantitative analysis of a cyclic gating scheme. *J. Gen. Physiol* 113:541-554.

Zhou,Z., S.Hu, and T.C.Hwang. 2001. Voltage-dependent flickery block of an open cystic fibrosis transmembrane conductance regulator (CFTR) channel pore. *J. Physiol* 532:435-448.

Zhou,Z., X.Wang, M.Li, Y.Sohma, X.Zou, and T.C.Hwang. 2005. High affinity ATP/ADP analogues as new tools for studying CFTR gating. *J. Physiol* 569:447-457.

CHAPTER 3

STABLE ATP BINDING MEDIATED BY A PARTIAL NBD DIMER OF THE CFTR CHLORIDE CHANNEL

3-1. Abstract

Cystic fibrosis transmembrane conductance regulator (CFTR), a member of the ATP binding cassette (ABC) superfamily, is an ATP-gated chloride channel. Like other ABC proteins, CFTR, encompass two nucleotide binding domains (NBD1 and NBD2), each accommodating an ATP binding site. It is generally accepted that CFTR's opening-closing cycles, each completed within 1 second, are driven by rapid ATP binding and hydrolysis events in NBD2. Here, by recording CFTR currents in real-time with a ligand exchange protocol, we demonstrated that during many of these gating cycles, NBD1 is constantly occupied by a stably bound ATP or 8-N_3-ATP molecule for tens of seconds. We provided evidence that this tightly bound ATP or 8-N_3-ATP also interacts with residues in the signature sequence of NBD2, a telltale sign for an event occurring at the NBD1-NBD2 interface. The open state of CFTR has been shown to represent a two-ATP bound NBD dimer. Our results indicate that upon ATP hydrolysis in NBD2, the channel closes into a "partial NBD dimer" state where the NBD interface remains partially closed preventing ATP dissociation from NBD1 but allowing the release of hydrolytic products and binding of the next ATP to

occur in NBD2. Opening and closing of CFTR can then be coupled to the formation and "partial" separation of the NBD dimer. The tightly bound ATP molecule in NBD1 can occasionally dissociate from the partial dimer state resulting in a nucleotide-free monomeric state of NBDs. Our data together with other structural/functional studies of CFTR's NBDs suggest that this process is poorly reversible, implying that the channel in the partial dimer state or monomeric state enters the open state through different pathways. We therefore proposed a gating model for CFTR with two distinct cycles. Structural and functional significance of our results to other ABC proteins is discussed.

3-2. Introduction

The cystic fibrosis transmembrane conductance regulator (CFTR), whose dysfunction results in the lethal genetic disease cystic fibrosis, is a unique member in the ATP-binding cassette (ABC) transporter superfamiliy (Riordan et al., 1989) in that it functions as a chloride ion channel (Bear et al., 1992). ABC proteins possess two nucleotide binding domains (NBD1 and NBD2) and two transmembrane domains (TMDs). The TMDs are structurally diversified in order to fulfill their distinct roles in accommodating different substrates for transport. However, NBDs, the energy-harvest machine, are highly conserved among members in this family. All NBDs share the same basic architecture (Reviewed in Davidson and Chen, 2004; Oswald et al., 2006) with a larger core subdomain (head) comprising an ATP binding site that binds and hydrolyzes ATP and a smaller helical subdomain (tail)

containing the ABC signature sequence (LSGGQ), so called because it's the hallmark of ABC proteins. High-resolution crystal structures (for example, smith et al., 2002; Chen et al., 2003; Zaitseva et al., 2005) have demonstrated that NBD1 and NBD2 rest monomerically without nucleotide while in the presence of ATP, they coalesce into a head-to-tail dimer with two ATPs buried at interfacial ATP binding pockets, where each ATP bound in the head subdomain of one NBD also interacts with the tail subdomain of the partner NBD.

CFTR can be classified into a group of "asymmetric" ABC proteins, which typically exist in eukaryotes and, less frequently, in bacteria (reviewed in Procko et al., 2009). This asymmetry is so defined because of the finding that in some ATP-interacting motifs, including those critical for catalyzing ATP hydrolysis, CFTR's NBD2 retains all conserved residues, but its NBD1 presents several non-consensus substitutions. An expected functional consequence of this structural asymmetry is that the NBD1 of CFTR displays a much lower catalytic ability than NBD2. This prediction appears to be supported by two lines of experimental approaches. First, photolabelling experiments demonstrated that 8-N_3ATP is occluded in NBD1 for tens of minutes even with extensive washing but is turned over quickly in NBD2 (Aleksandrov et al., 2002; Basso et al., 2003). Second, our previous study (Tsai et al., 2009) using electrophysiological recordings has shown that rapid ATP hydrolysis in NBD2 closes wild-type (WT) CFTR into an intermediate state with a lifetime of many seconds, during which an ATP molecule remains bound in NBD1. This single-ATP-bound, intermediate state is distinguishable from the nucleotide-free state because of its exceptionally robust response to pyrophosphate (PPi).

A careful examination of these biochemical and functional results, however, reveals several potential problems. It can be seen from monomeric structures of CFTR's NBD1 (Lewis et al., 2004; Lewis et al., 2005) that the ATP binding site is well exposed to the aqueous environment. Therefore, even though NBD1 may have a reduced ATPase activity, it seems inconceivable that ATP can stay bound for seconds (Tsai et al., 2009) or even minutes (Basso et al., 2003). This puzzle might be explained by a simple hypothesis that the stably bound ATP molecule is "trapped" by the NBD1 head and the NBD2 tail at the dimer interface. Nonetheless, it was reported that a mutant CFTR with the whole NBD2 truncated (ΔNBD2-CFTR) still occludes 8-N_3ATP for minutes (Aleksandrov et al., 2008). Moreover, phosphorylation of CFTR, known to facilitate cross-linking of CFTR's two NBDs into a head-to-tail dimer configuration (Mense et al., 2006) and play a critical role in opening of the CFTR channel through ATP-dependent dimerization of NBDs (reviewed in Gadsby et al., 2006; Chen and Hwang 2008), bears little influence on the occlusion of 8-N_3ATP by WT-CFTR (Basso et al., 2003).

While the aforementioned photolabelling experiments provide results that contradict the idea of a dimer-mediated ATP trapping, our functional studies (Tsai et al., 2009) do implicate a role played by both the head of NBD1 and the tail of NBD2 in regulating the stability of the single-ATP-bound state. Regardless of this mechanistic difference, it's also unclear why the ATP dwell times in NBD1 measured by these two sets of approaches differ by > 50-fold. These conflicting ideas as well as results prompt us to design a real-time ligand exchange experiment to further investigate the structural and kinetic mechanisms by which stable ATP binding in

NBD1 is attained. Our results suggest that a tight binding of ATP and 8-N_3ATP in the head of NBD1 requires interactions of the nucleotide with the tail of NBD2.

These findings lead to the establishment of a molecular model where the dominant opening-closing cycle of CFTR is coupled to the interconversion of NBDs between a full dimer state and a "partial dimer" state, where the two NBDs are partially connected by the stably bound ATP molecule in NBD1 allowing nucleotide exchange to occur only in NBD2. Based on further experimental results, we were able to demonstrate a second gating cycle of CFTR involving a rare complete disengagement of the two NBDs. The structural/functional implications of this new molecular model for other ABC proteins will be discussed.

3-3. Material and methods

Cell Culture and Transient Expression System

All membrane patches used in the current study were from Chinese hamster ovary (CHO) cells, which were grown at 37 ˚C in Dulbecco's Modified Eagle's Medium supplemented with 10% fetal bovine serum. The cDNA constructs of CFTR were cotransfected with pEGFP-C3 (CLONTECH Laboratories, Mountain View, CA), encoding the green fluorescence protein, using PolyFect transfection reagent (QIAGEN, Valencia, CA). The transfected CHO cells were plated on sterile glass chips in 35 mm tissue dishes. Electrophysiological experiments were performed 2-4 days after transfection.

Electrophysiological Recordings

Patch-clamp pipettes were prepared from borosilicate capillary glass using a Flaming/Brown type micropipette puller, P97 (Sutter Instrument, Novato, CA). The pipette tips were then fire-polished with a homemade microforge to ~1 μm external diameter, resulting in a pipette resistance of 2 ~ 4 MΩ in the bath solution in a continuously perfused recording chamber located on the stage of an inverted microscope (Olympus, Japan). Glass chips containing transfected CHO cells were transferred to the chamber before recordings. After inside-out patches with seal resistance of more than 40 GΩ were obtained, CFTR channel currents were recorded at room temperature with an EPC-10 patch-clamp amplifier, filtered at 100 Hz with an eight-pole Bessel filter (Warner Instrument, Hamden, CT) and captured onto a hard disk at a sampling frequency of 500 Hz. The membrane potential was held at -60 mV and the inward current in all figures was inverted for clearer data presentation.

All experiments were done with a fast solution exchange device, SF-77B (Warner Instrument, Hamden, CT). To test the dead time of our solution exchange, we perfused two solutions with different concentrations of NaCl to the patch pipette. Exponential fit of the resulting current changes yielded a dead time ~30 ms (Tsai et al., 2009).

Chemicals and Composition of Solutions

The pipette solution contained (in mM): 140 N-methyl-D-glucamine chloride (NMDG-Cl), 2 $MgCl_2$, 5 $CaCl_2$, and 10 HEPES (pH 7.4 with NMDG). Cells were perfused with a bath solution containing (in mM): 145 NaCl, 5 KCl, 2 $MgCl_2$, 1 $CaCl_2$, 5 glucose, 5 HEPES and 20 sucrose (pH 7.4 with NaOH). After the establishment of an inside-out configuration, the patch was perfused with a standard perfusion solution (i.e. intracellular solution) containing (in mM): 150 NMDG-Cl, 2 $MgCl_2$, 10 EGTA and 8 Tris (pH 7.4 with NMDG).

MgATP and PKA were purchased from Sigma-Aldrich (St Louis, MO). 8-N_3-ATP was obtained from MP Biomedicals (Solon, OH). N^6-(2-phenyltehyl)-ATP (PATP) was from Biolog Life Science Institute (Bremen, Germany). MgATP and 8-N_3-ATP were stored respectively in 250 mM and in 10 mM stock solutions at -20 ˚C. PATP stock solution was 10 mM and was stored at -60 ˚C. All nucleotides were dissolved in perfusion solution for the experiments and the pH was adjusted to 7.4 with NMDG.

Data Analysis and Statistics

Recordings from patches containing one CFTR channel were selected for single-channel kinetic analysis. These data were further filtered at 50 Hz and analyzed using software written by Dr. Csanády (Csanády, 2000). A three-state kinetic model, C↔O↔B, was adopted to extract ATP-dependent kinetic parameters as described previously (Bompadre et al., 2005). Macroscopic current recordings were analyzed

using Igor Pro program (version 4.07, Wavemetrics, Lake Oswego, OR). Current relaxations were fitted with single or double exponential function using a Levenberg-Marquardt based algorithm within the Igor Pro program. All results are presented as means ± SEM.; n represents the number of independent experiments. Student's *t*-test was performed with Sigmaplot (version 8.0, SPSS Science, Chicago, IL). $P < 0.01$ was considered significant.

To convert the time constants presented in Fig. 3-10E to the percentage of channels with ligand exchange occurred in NBD1 (Y-axis of Fig. 3-10F), we solved the following equations:

$$y + a = 100\%$$

$$72.4y + 30.5a = b$$

where

y is the percentage of CFTR with PATP bound in NBD1 (Y value in Fig. 3-10F);

a is the percentage of CFTR with ATP bund in NBD1;

30.5 s is the current decay time constant measured when CFTR is only exposed to ATP + PPi; **72.4** s is the current decay time constant measured when CFTR is only exposed to PATP + PPi;

b is the current decay time constant measured when CFTR originally opened by ATP + PPi was subsequently treated with different durations of PATP + PPi (Y value in Fig. 3-10E).

3-4. Results

Ligand Exchange Experiments Reveal Stable ATP Binding in NBD1 during CFTR Gating

As an opening-closing cycle of CFTR lasts for ~1 s (Zeltwanger et al., 1999; Vergani et al., 2003), biochemical demonstrations of the occlusion of 8-N_3ATP in NBD1 for tens of minutes described in the *Introduction* section lead to the proposition that an ATP molecule can remain bound in CFTR's NBD1 for many gating cycles without dissociation (Basso et al., 2003; Gadsby et al., 2006). This contention however needs more direct experimental evidence for the following reasons. First, tight ATP binding in NBD1 is so far only observed under conditions when CFTR is kept in a closed state in membrane patches (Tsai et al., 2009) or when CFTR proteins are in biochemical buffers, where their functional state is unknown (Aleksandrov et al., 2002; Basso et al., 2003). Thus, it has not been demonstrated directly that an ATP molecule stays tightly bound in NBD1 for repeated gating cycles. Second, even if those functional and biochemical data can be used to support this idea, the dramatic difference in the measured dwell time for the trapped ATP between these two assays would have to come to a very different conclusion regarding exactly how many gating cycles proceed before this tightly bound ATP dissociates.

Here, we designed a real-time ligand-exchange experiment to monitor the ATP binding status in NBD1 and NBD2 during CFTR gating. For a representative

experiment (Fig. 3-1A, similar results were seen in 9 other patches containing a single channel), a highly-phosphorylated wild-type (WT) CFTR channel in an excised inside-out patch was initially opened by 2.75 mM ATP (first black trace). Then, the ligand was suddenly changed (hence the name ligand-exchange experiment) to 50 μM N_6-2-phenylethyl-ATP (PATP), a high-affinity hydrolyzable ATP analogue (Zhou et al., 2005). It can be seen that after switching the ligand from ATP to PATP, the open probability (Po) of the channel increased in two distinct steps; the channel closed time was shortened immediately (first red trace), but following a ~30 s delay, longer open-time became apparent (second red trace). Fig. 3-1B plots this two-step change in channel kinetics and shows that ligand switches from PATP back to ATP also cause an immediately changed closed time and a delayed alteration of the open-time.

Because single-channel data are stochastic in nature and a lengthy recording window is needed for meaningful kinetic analysis, it is difficult to accurately quantify the time course of current changes upon switching the ligand. This limitation of single-channel recordings however can be overcome by carrying out similar experiments in patches yielding macroscopic currents. We acquired macroscopic recordings from patches containing hundreds of WT channels. Here, changing the ligand from ATP to PATP resulted in a bi-phasic increase of the macroscopic current (Fig. 3-2A), fit well with a double-exponential time course (red line) with a rapid (τ = 0.34 ± 0.03 s, n = 20) and a much slower (τ = 51 ± 5 s, n=19) phases. We removed PATP and fit the subsequent current relaxations with a single exponential function at the end of the rapid (τ = 0.45 ± 0.05 s, n=10, green line) and the slow phases (τ = 0.79 ± 0.04 s, n = 19, blue line). Comparing the time constants

FIGURE 3-1

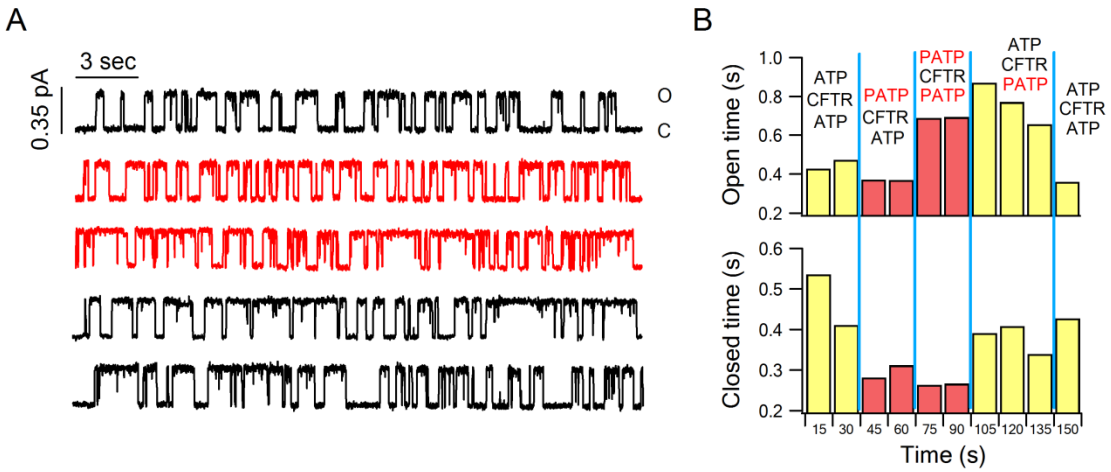

Figure 3-1. Changes of WT-CFTR gating kinetics upon ATP/PATP exchange. **(A)** A continuous single-channel current trace (a representative trace from 10 single channel recordings) showing effects of ligand exchanges between ATP (black traces) and PATP (red traces). **(B)** A history plot of the recording shown in (A). Kinetic parameters were extracted with a 15-second time window. The hypothesized nucleotide binding status of CFTR at different time windows is marked.

of these two current decay traces with that after the withdrawal of ATP (Fig. 3-2B, τ = 0.46 ± 0.02 s, n = 25), we found that PATP induces longer channel open-time only after the appearance of the second phase. Therefore, as seen in single-channel results (Fig. 3-1), the application of PATP instantaneously decreases the closed time of CFTR (i.e., fast current increase) but elicits longer openings with a delay (i.e., slow current increase). It is notable that these macroscopic experiments not only confirm single-channel results shown in Fig. 3-1, but also provide the distinct advantage that the time course of current changes can be quantified and compared accurately.

The simplest interpretation for the results described above (see *Discussion* for details) is that the two NBDs have different nucleotide dwell times: ~350 ms in one NBD and ~50 s in the other NBD, based on values derived from macroscopic experiments. After changing the ligand from ATP to PATP, one NBD is immediately (in ~350 ms) vacated allowing PATP to bind and exert its first effect rapidly (shortened closed time). The other NBD however remains occupied by an ATP molecule for ~50 s and therefore PATP's second effect (prolonged open-time) takes place with a delay of tens of seconds (Fig. 3-1B). Thus, an ATP molecule won't dissociate from CFTR for ~50 s even when many gating cycles catalyzed by PATP in the NBD site with a fast nucleotide turnover have occurred.

The hypothesis that NBD1 is the site where ATP can bind for ~50 s during gating of CFTR appears to be more in line with what has been reported previously including the observation that NBD1 and NBD2 assume very different catalytic ability for ATP hydrolysis (see *Introduction)*. This hypothesis can be tested by

FIGURE 3-2

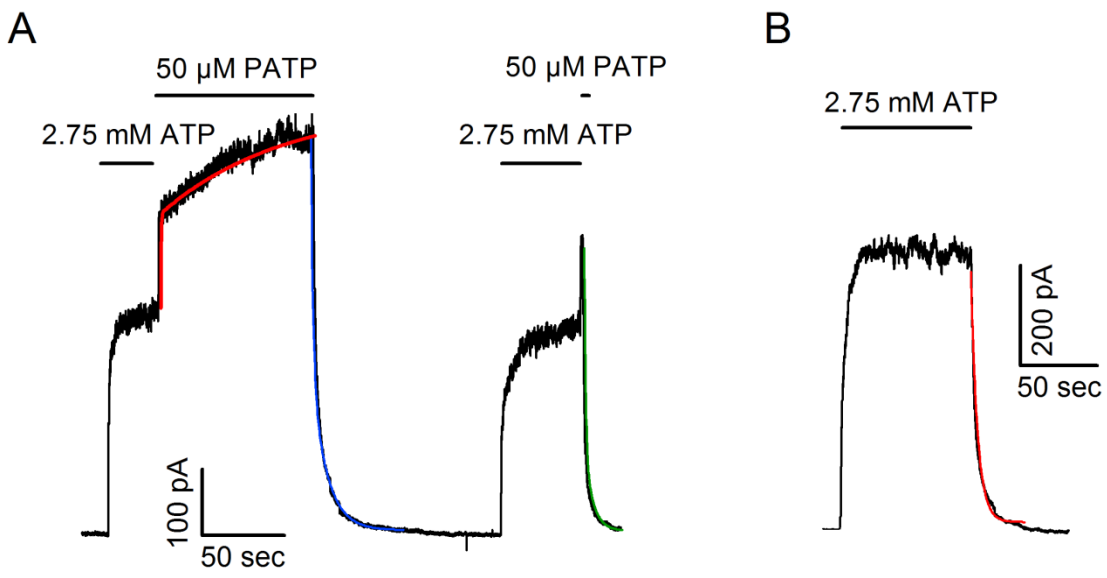

Figure 3-2. Changes of macroscopic WT-CFTR currents upon ATP/PATP exchange. (**A**) Macroscopic experiments showing a two-step current increase induced by a sudden ATP/PATP switch. PATP was removed at the end of each step. (**B**) Current relaxation of WT-CFTR upon removal of ATP. The current decay upon washout of ATP was fitted with a single exponential function (red line).

carrying out experiments with mutations that likely perturb ATP-NBD1 interactions (e.g., Zhou et al., 2006; Tsai et al., 2009). The tryptophan residue at position 401 (W401) was chosen because the crystal structure of human NBD1 shows that the side-chain indole ring of W401 stacks against the adenine moiety of ATP (Lewis et al., 2005). When the ligand exchange experiment was carried out with a single W401G channel (Fig. 3-3A, similar results were seen in 5 other single channel recordings), PATP (red trace) induced longer openings without an obvious delay observed with WT channels (compare Fig. 3-3B with Fig. 3-1B). This result was recapitulated by PATP-elicited two-step current increase (Fig. 3-3C, red line) in macroscopic experiments: the first phase has a time constant of 0.32 ± 0.03 s (Fig. 3-3D, n = 11) not different from that for WT-CFTR, but the second phase (caused by longer open-time) has a time constant of 2.58 ± 0.37 s (Fig. 3-3E, n = 11), ~20 times shorter than that observed with WT-CFTR. We interpreted these results as that the W401G mutation in NBD1 significantly decreases the resident time of the stably-bound ATP molecule (from ~50 s for WT- to ~2.5 s for W401G-CFTR) so that PATP can replace it more rapidly and exert its second effect: increasing channel open-time. Similar macroscopic experiments were conducted with W401I and W401Y mutations. The shorter time constant was not significantly affected by either of the mutations (Fig. 3-3D), whereas the second time constant (Fig. 3-3E) was shortened by non-aromatic substitutions of W401 (W401I) but increased by the conservative W401Y mutation. These results strongly support the idea that the catalysis-incapable NBD1 is the site for stable ATP binding (~50 s). It follows that rapid ATP

FIGURE 3-3

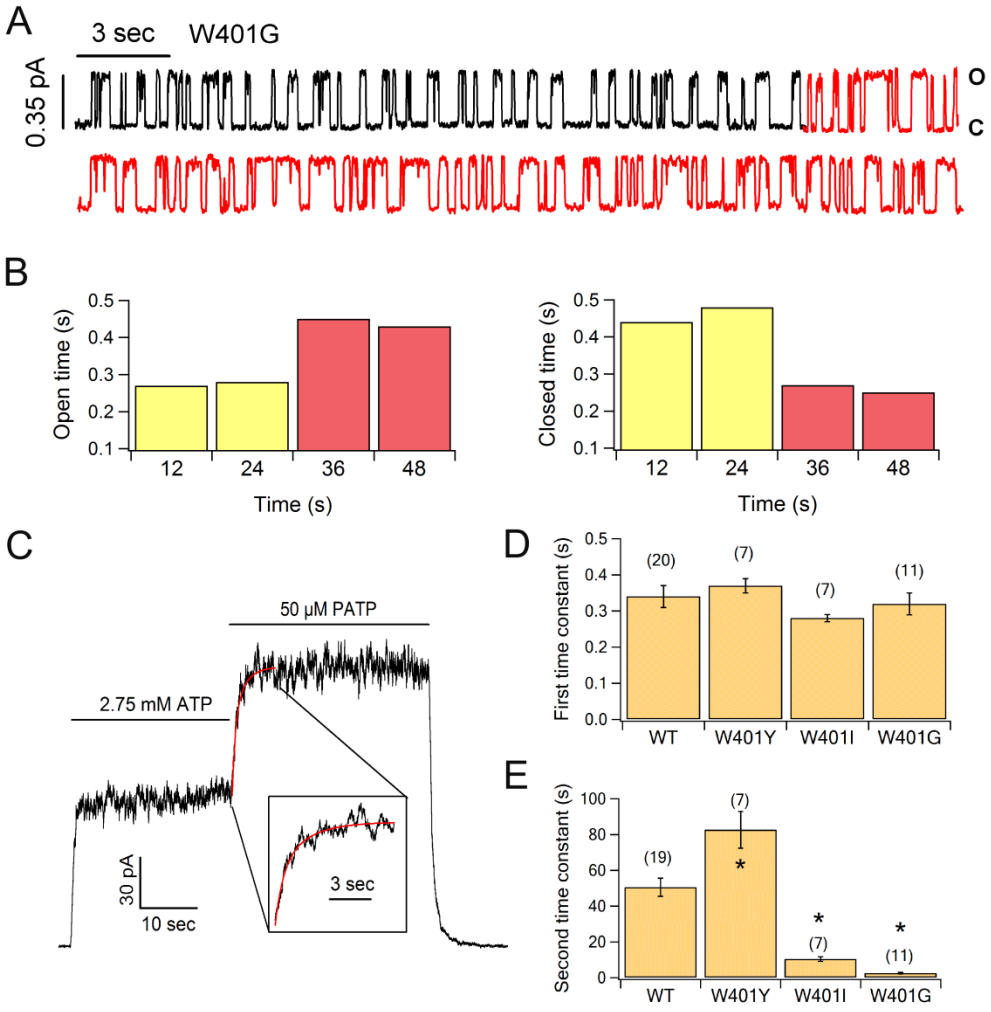
A
3 sec
W401G
0.35 pA
o
c
B
Open time (s)
0.5
0.4
0.3
0.2
0.1
12
24
36
48
Time (s)
Closed time (s)
0.5
0.4
0.3
0.2
0.1
12
24
36
48
Time (s)
C
50 μM PATP
2.75 mM ATP
30 pA
10 sec
3 sec
D
First time constant (s)
0.5
0.4
0.3
0.2
0.1
0.0
(20)
(7)
(7)
(11)
WT
W401Y
W401I
W401G
E
Second time constant (s)
100
80
60
40
20
0
(19)
(7)
*
*
(7)
*
(11)
WT
W401Y
W401I
W401G

Figure 3-3. Effects of W401 mutations on ligand exchange. **(A)** The response of a single ATP-gated W401G channel to a sudden exposure of PATP (red trace). The prolongation of the open-time occurred instantly upon ligand switch. Similar observation was seen in 5 other patches containing a single W401G-CFTR channel. **(B)** Single channel kinetics was extracted every 12 s from (A) **(C)** Macroscopic currents recorded from hundreds of W401G channels. The current rising phase elicited by PATP was fitted with a double-exponential function (inlet), yielding two time constants. **(D)** The fast time constants and **(E)** the slow time constants for WT-CFTR and different W401 mutations. Asterisk: $P < 0.01$ when compared to WT-CFTR.

turn-over (mean nucleotide dwell time ~350 ms) should occur in NBD2, which retains key residues for catalyzing ATP hydrolysis.

The Role of NBD Signature Sequence in Mediating Stable ATP Binding in NBD1

It was reported that the occlusion of 8-N_3 ATP in NBD1 occurs in a CFTR construct without NBD2 (Aleksandrov et al., 2008). This observation implies that it is the monomeric NBD1 that can bind ATP tightly. In contrast, functional studies (Tsai et al., 2009) do suggest that stable binding of ATP occurs at the dimer interface. We now address this conflict by carrying out ligand exchange experiments with mutant channels that contain substitutions in the signature sequence of NBD2's tail subdomain, where an extensive hydrogen bond network between ATP and the signature motif is seen in structures of many ABC proteins (Fig. 3-4A; also see Smith et al., 2002; Zaitseva et al., 2005). Ser 1347 (S1347) is the first candidate as its side chain (arrow in Fig. 3-4A) and the γ-phosphate of ATP are close enough to form a hydrogen bond. Indeed, single S1347G channels, like W401G-CFTR (Fig. 3-3A), opened into long bursts without a delay after changing the ligand from ATP to PATP (red trace in Fig. 3-4B, channel kinetics summarized in Fig. 3-4C), suggesting that the S1347G mutation in NBD2 dramatically shortens the dwell time of ATP in NBD1. (Similar recordings were seen in 6 other patches containing a single channel.) At the macroscopic level, PATP also increased the current in two phases in several S1347 mutants (two representative traces are shown in Figs. 3-4D, 3-S1-S2). The time constants of the first phase for all S1347 mutants were similar to that of WT-CFTR (Fig. 3-5A). However, the time constants of the second phase became much shorter

FIGURE 3-4

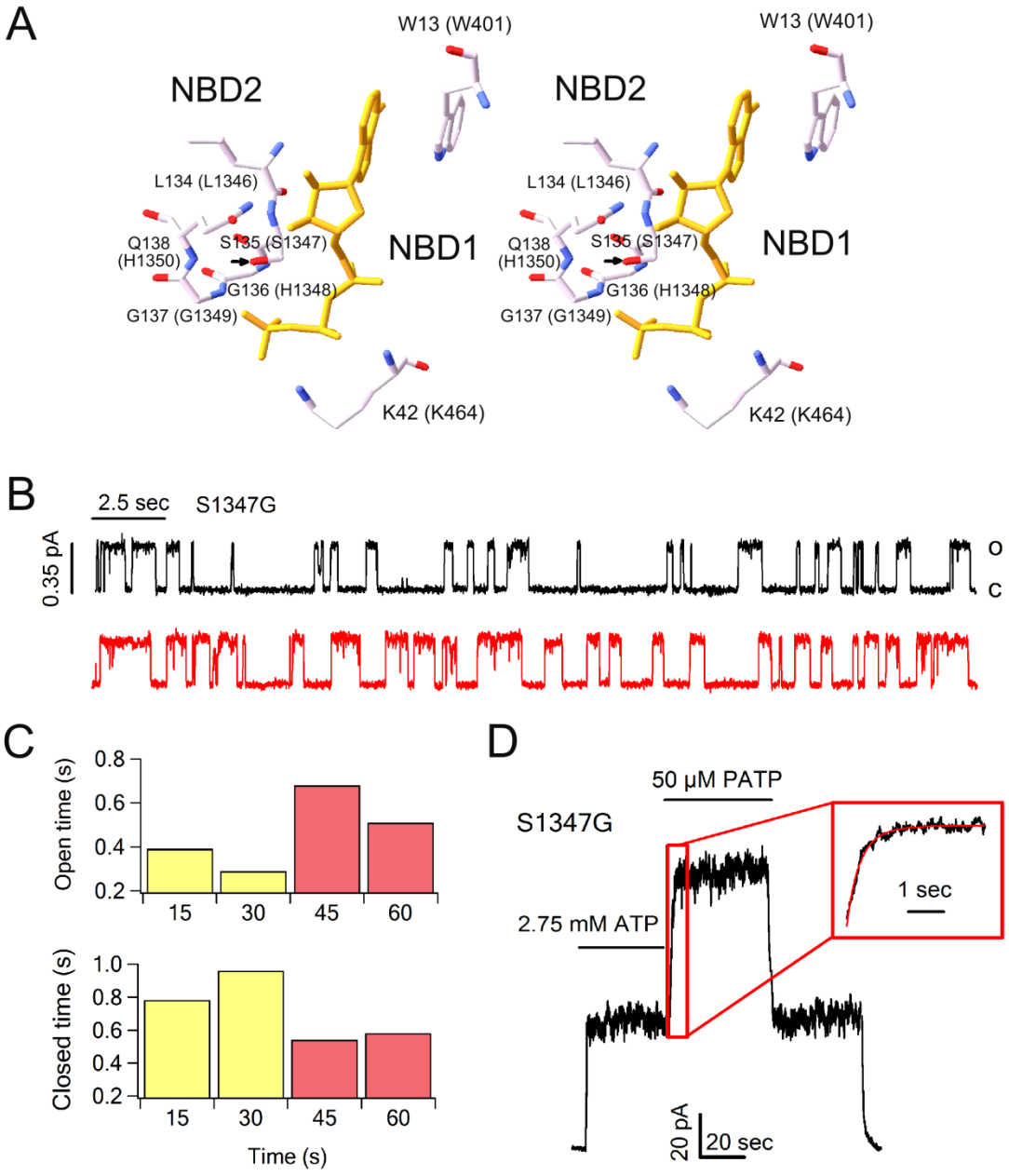
A
W13 (W401)
NBD2
L134 (L1346)
Q138 (H1350)
S135 (S1347)
NBD1
G136 (H1348)
G137 (G1349)
K42 (K464)
W13 (W401)
NBD2
L134 (L1346)
Q138 (H1350)
S135 (S1347)
NBD1
G136 (H1348)
G137 (G1349)
K42 (K464)
B
2.5 sec
S1347G
0.35 pA
o
c
C
Open time (s)
0.8
0.6
0.4
0.2
15
30
45
60
Closed time (s)
1.0
0.8
0.6
0.4
0.2
15
30
45
60
Time (s)
D
50 μM PATP
S1347G
2.75 mM ATP
1 sec
20 pA
20 sec

Figure 3-4. Effects of the S1347G mutation on ligand exchange. (A) Stereoview of interactions of ATP with key residues at the NBD dimer interface. The crystal structure of *E. coli* MalK NBD dimer (Protein Data Bank 1Q12) was used to illustrate these interactions. The residue numbers in the parentheses represent the equivalent amino acids in CFTR. Arrow: the side chain of S1347. **(B)** A representative single S1347G-CFTR channel trace from 7 similar recordings. **(C)** The channel entered longer openings without an obvious delay after ATP/PATP change. **(D)** Macroscopic currents from S1347G channels. PATP-induced current increase can be fitted well with a double exponential function (inlet).

as S1347 were altered to valine or glycine, which are incapable of forming hydrogen bonds (Fig. 3-5B).

It is important to note a correlation between the degree of changes in the second time constant and the chemical nature of the mutations. As in the case for mutations at W401 (Fig. 3-3E), more drastic mutations at S1347, e.g., S1347V and S1347G, shorten this time constant to a greater extent than the more conservative mutation such as S1347T (Fig. 3-5B). This correlation makes it less likely that the results are due to nonspecific effects of the mutations.

We then extended our mutations to other residues in the signature sequence of the NBD2 tail. PATP induced biphasic current increase in these mutants (Figs. S1-S2) and the time constants of the first phase were again similar to that of WT-CFTR (Fig. 3-5A). The second time constant, however, was decreased by most of the mutations (Fig. 3-5B). Of particular note is the H1348G mutation, which increased the time constant of the second phase (Fig. 3-5B), suggesting that this mutation actually prolongs the ATP dwell time in NBD1. This result echoes typical dimeric structures of NBDs (Smith et al., 2002; Chen et al., 2003; Zaitseva et al., 2005), where the equivalent residue of H1348 is often a glycine that can interact with ATP through its backbone amide group (Fig. 3-4A); thus the presence of an imidazole ring at this position likely destabilizes ATP binding due to steric hindrance. Consistent with this idea, for the ABC protein TAP2 whose corresponding residue of H1348 is valine, a steric clash is predicted to occur as reported in a crystallographic study (Procko et al., 2006). Taken together, we conclude that both the NBD1 head

FIGURE 3-5

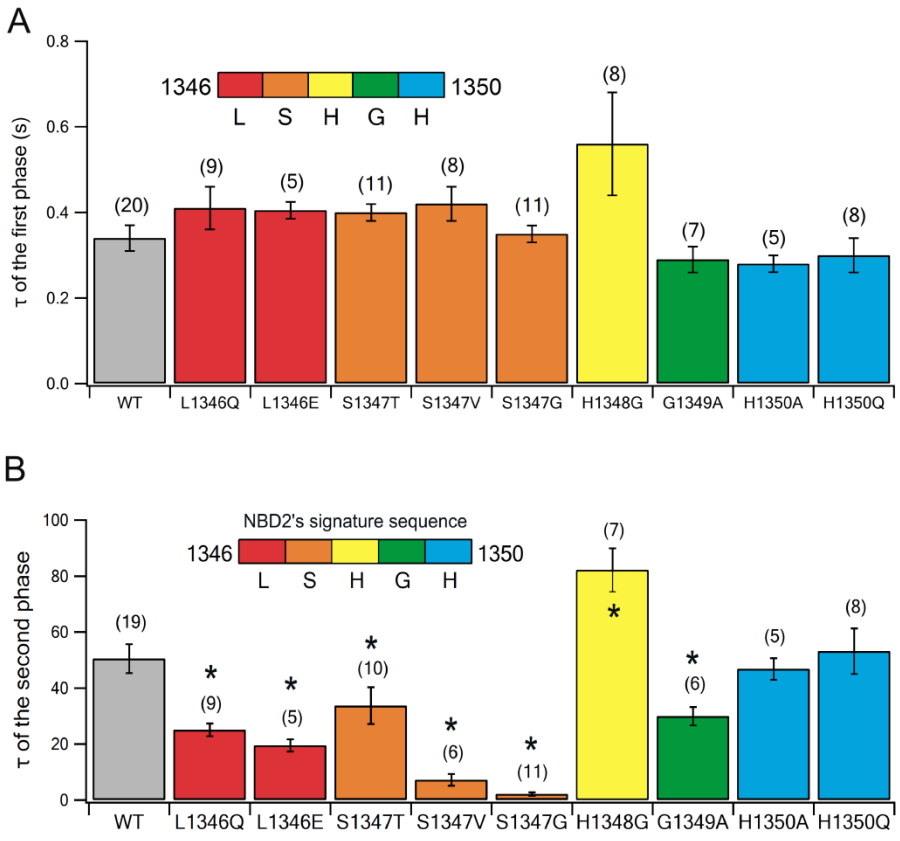

Figure 3-5. Time constants of the first phase **(A)** and the second phase **(B)** of the PATP-induced current increase for WT CFTR channels and mutations in NBD2's signature sequence. Although the time constants of the first phase for all mutants tested are similar to that of WT-CFTR, the time constants for the second phase vary greatly among different mutant channels. For some mutants, the data numbers for the first and the second time constants are different. This is due to loss of the patch during recordings of the second phase. Asterisk: $P < 0.01$ when compared to WT-CFTR.

and the NBD2 tail are necessary for the tight ATP binding observed in the current study.

Since different nucleotides were used in our experiments (ATP and PATP) and the photolabelling experiments (8-N_3-ATP), we wondered whether this could be the reason that biochemical occlusion can be observed even when the whole NBD2 is severed. In other words, we considered the possibility that the intrinsic high affinity of 8-N_3-ATP might be sufficient to support a tight binding of this nucleotide in NBD1 for tens of minutes independently of NBD2. To examine this possibility, we first characterized the effect of 8-N_3-ATP on WT-CFTR gating and the results were presented in Fig. 3-S3. In brief, compared with 2.75 mM ATP, 8-N_3-ATP at a saturating concentration (~100 μM) catalyzes opening of WT-CFTR at a 2~3-fold slower rate but induces openings ~4-fold longer, resulting in a maximal Po for channels gated by 8-N_3-ATP 40% higher than that gated by ATP. These results are very similar to those reported by Basso et al. (2003).

We then asked which binding site, NBD1 or NBD2, is responsible for these differences in gating kinetics between ATP and 8-N_3-ATP. In Fig. 3-6A, it can be seen that, upon a sudden solution change from 100 μM 8-N_3-ATP to 2.75 mM ATP, the macroscopic current of WT-CFTR channels decreased immediately and reached a steady state within seconds. After a continuous exposure of the channels to ATP for 60 seconds, ATP was removed and the time course of the current decay was fitted with a single-exponential function. The resulting time constant (red line, $\tau = 0.42 \pm 0.03$ s, n = 4) was not significantly different from that with only a 10-second

FIGURE 3-6

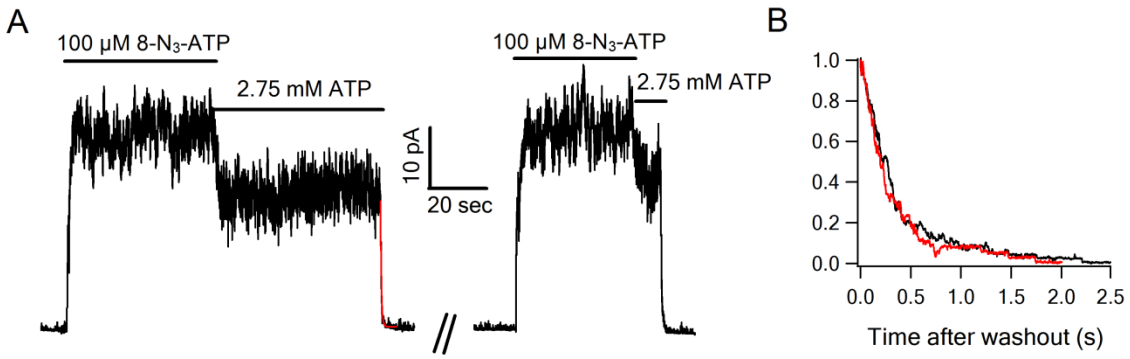

Figure 3-6. Changes of WT-CFTR currents upon 8-N_3-ATP/ATP exchange. **(A)** Macroscopic currents immediately dropped to a steady state when the solutions were switched from 8-N_3-ATP to ATP. ATP was removed either 60 s or 10 s after solution changes. **(B)** The subsequent current relaxations were compared. Red trace: 60-s exposure to ATP. Black trace: 10-s exposure to ATP.

exposure to ATP (τ = 0.37 ± 0.03 s, n = 4) as shown in Fig. 3-6B or that when channels were only opened by ATP without 8-N_3-ATP (τ = 0.34 ± 0.03 s, n = 20) as presented in Fig. 3-2B. Thus, although channels gated by 8-N_3-ATP, like those by PATP, exhibit a longer open time, this effect of 8-N_3-ATP, unlike that of PATP, can be eliminated without a delay by switching the ligand to ATP. We interpret these results as that ATP changes the open-time and the opening rate of 8-N_3-ATP-gated channels by replacing the ligand at the fast turn-over site (i.e., NBD2). In other words, the differences of 8-N_3-ATP and ATP on CFTR gating are caused solely by their different effects on NBD2. It also suggests that 8-N_3-ATP and ATP exert similar effects on gating kinetics when binding to NBD1. Indeed, as shown and explained in more detail in Fig. 3-S4, the lock-open time with 8-N_3-ATP plus PPi is nearly identical as that with ATP plus PPi; in addition, just like ATP, 8-N_3-ATP fails to increase the activity of G551D-CFTR by binding to NBD1.

If NBD1 indeed does not differentiate 8-N_3-ATP from ATP binding, we anticipate that solution changes from 8-N_3-ATP to PATP should result in a biphasic change of macroscopic currents like those observed upon ATP/PATP exchange (Fig. 3-2A), because the replacement of 8-N_3-ATP by PATP in NBD1 will similarly lead to an increased channel open-time. This prediction is indeed valid as shown in Fig. 3-7A. The current rising phase upon solution changes from 8-N_3-ATP to PATP was fitted with a double exponential function yielding two time constants (τ_1 = 0.81 ± 0.17 s, n = 4 and τ_2 = 46 ± 6 s, n = 5). The τ_1, which reflects ligand exchange in NBD2, is slightly longer than that observed in ATP/PATP exchange experiment. This observation is expected since the turnover of 8-N_3-ATP in NBD2 is slower than that

FIGURE 3-7

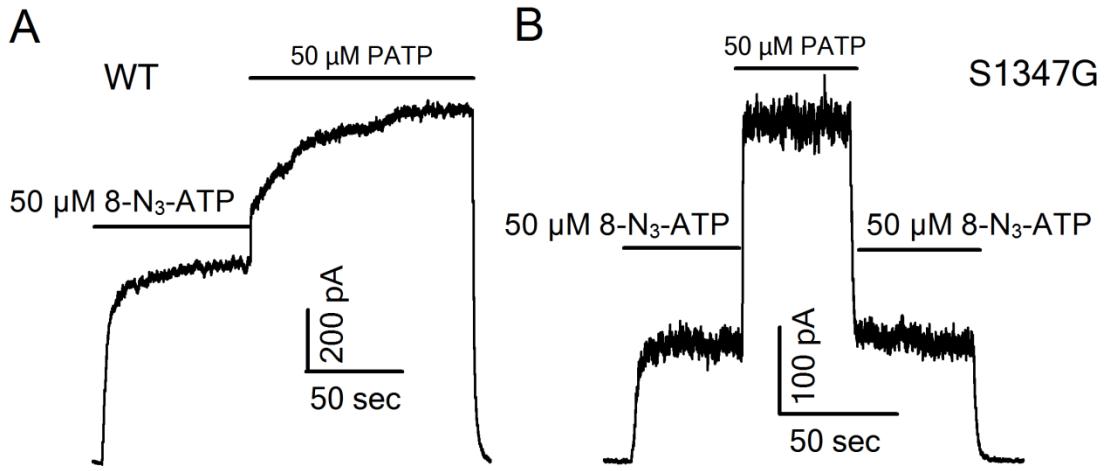

Figure 3-7. Changes of WT- and S1347G-CFTR currents upon 8-N_3-ATP/PATP exchange. (A) Macroscopic currents recorded from WT-CFTR channels showed a biphasic increase when 8-N_3-ATP was changed to PATP. **(B)** The second-phase current increase seen in (A) was essentially abolished by the S1347G mutation.

of ATP as reflected by the longer open-time seen with 8-N_3-ATP-gated channels (Fig. 3-S3). The observation that τ_2, which represents ligand exchange in NBD1, is similar to that for ATP/PATP exchange shown in Fig. 3-2A corroborates the idea that 8-N_3-ATP is trapped in NBD1 for about the same time as ATP. Furthermore, unlike the "nucleotide occlusion" phenomenon demonstrated biochemically (Aleksandrov et al., 2008), the trapping of 8-N_3-ATP in the current study is also dependent on the tail of NBD2 since the S1347G mutation essentially abolished the second phase of current increase elicited by PATP upon switching the ligand from 8-N_3-ATP to PATP (Fig. 3-7B).

Opening and Closing of CFTR are Coupled to the Formation and Partial Separation of the NBD Dimer

The findings described above can be interpreted in the context of the structural mechanism of CFTR gating. It is evident from the crystal structures of ABC transporters (Smith et al., 2002; Chen et al., 2003; Zaitseva, et al., 2005) that the NBDs form a dimer in a two-ATP bound state. In CFTR, this dimeric state has been shown to represent the open state (Vergani et al., 2005; Mense et al., 2006). What remain unknown are the conformational changes of NBDs after the channel is closed by ATP hydrolysis in NBD2 (Gadsby et al., 2006; Chen and Hwang, 2008). That an ATP molecule is trapped by the NBD1 head and the NBD2 tail for ~50 s indicates that during a long period of repeated CFTR opening and closing, the NBD1 head and the NBD2 tail are kept connected by the stably bound ATP molecule. Thus, we propose that ATP hydrolysis in NBD2 brings CFTR into a "partial dimer" state,

FIGURE 3-8

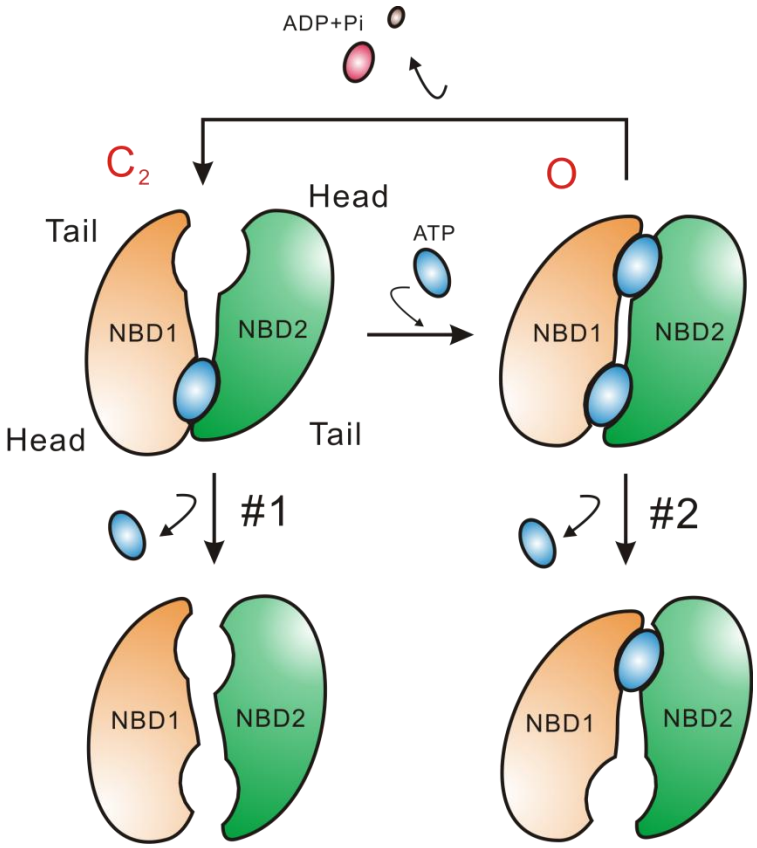

Figure 3-8. Diagram showing the dominant gating cycle of CFTR ($C_2 \leftrightarrow O$) and two possible pathways for the stably bound ATP molecule to dissociate.

where the dimer interface remains partially closed to trap ATP in NBD1, allowing NBD2 to be vacated for the next ATP molecule to bind. As a result, the opening and closing of CFTR are coupled to the interconversion between a full NBD dimer (open state) and a partial NBD dimer (closed state), driven by ATP binding and hydrolysis at NBD2 ($C_2 \leftrightarrow O$ in Fig. 3-8).

The Partial Dimer State of NBDs Occasionally Falls into a Monomeric State

Crystal structures of ABC proteins also reveal that the two NBDs rest monomerically in a nucleotide-free state (Smith et al., 2002; Chen et al., 2003; Lu et al., 2005; Zaitseva, et al., 2005). This monomeric NBD state is most likely a closed state for CFTR since CFTR rarely open in the absence of ATP. We then ask how this state can be incorporated into the gating model proposed above. It is noted that during the slow current rising phase in Fig. 3-2A, the stably bound ATP molecule in NBD1 was eventually replaced by PATP and thus during CFTR gating, the NBD1 head and the NBD2 tail must occasionally disengage to allow ATP/PATP exchange. In theory, this separation can occur either in C_2 (#1 in Fig. 3-8) or O (#2 in Fig. 3-8) states. To distinguish these two possibilities, we carried out similar ligand exchange experiments (as Fig. 3-2A) but with ATP being replaced by a lower concentration of PATP. Thus, ligand exchange in NBD1 will take place under a condition where proportionally more WT-channels are in the closed (C_2) state. Fig. 3-9A shows such an experiment. Upon switching ATP to 2 μM PATP, the macroscopic current changed in two phases; there was an immediate current drop followed by a slow current increase to a steady state with a time constant of 31 ± 2 s (n = 7), which is

FIGURE 3-9

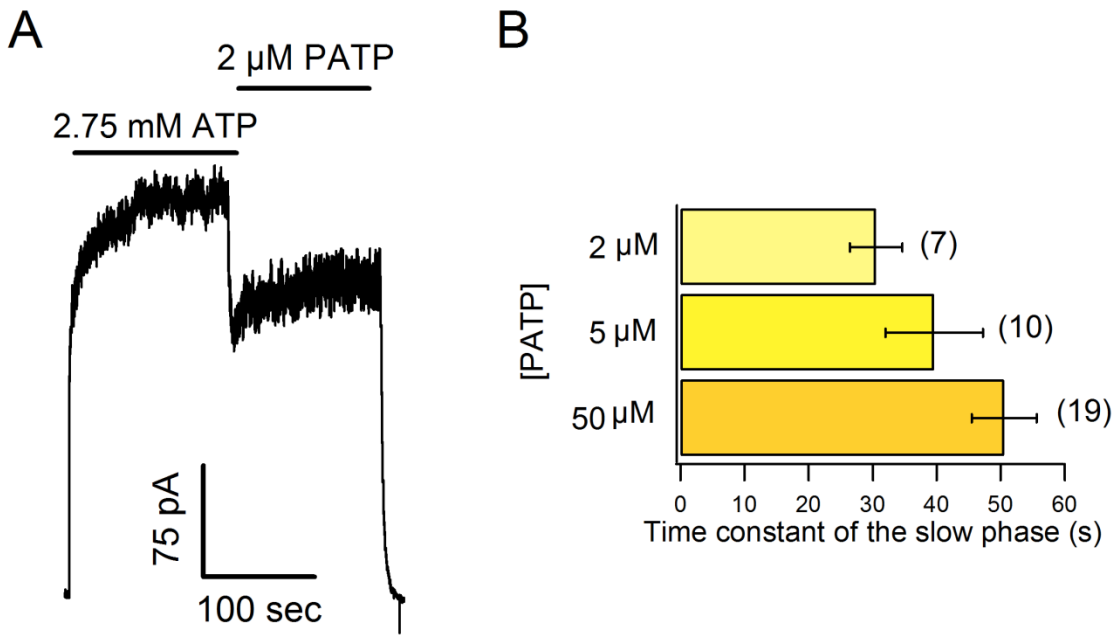

Figure 3-9. State dependence of ATP/PATP exchange. (A) Ligand exchange experiments with solution switches from ATP to 2 μM PATP. The macroscopic current dropped first and then slowly increased to a steady state. **(B)** A bar chart comparing the time constants of the slow current increase phase when 2 μM, 5 μM, or 50 μM PATP were used for ligand exchange experiments.

significantly shorter ($P < 0.01$) than that observed when 50 μM of PATP was used (Fig. 3-2A). Similar biphasic changes of the macroscopic current were also observed when ATP was switched to 5 μM PATP and the time constant of the current increase phase fell between those measured with 2 μM and 50 μM PATP (Fig. 3-9B). These results support the notion that ATP/PATP exchange in NBD1 occurs more rapidly during the closed state (C_2). If this is indeed the case, one would predict that ATP/PATP exchange in NBD1 will take place more slowly in the open state.

Our previous studies (Tsai et al., 2009) have established that WT-CFTR can be locked open by ATP and MgPPi for ~30 sec in a configuration where MgPPi binds in NBD2 while ATP occupies the NBD1 site (Fig. 3-10A). Since most channels will stay in the open state when exposed to ATP and MgPPi, the subsequent solution change to PATP plus MgPPi will allow us to test whether ligand exchange in NBD1 occurs from the open state. If ATP/PATP exchange does occur in the open state (Fig. 3-10B), PATP will further prolong the lock-open time since it's known that the lock-open state with MgPPi bound in NBD2 and PATP in NBD1 is more stable than that with ATP in NBD1 (Tsai et al., 2009). A sample experiment is shown in Fig. 3-10C. It can be seen in Fig. 3-10D that 50 μM PATP + 2 mM MgPPi (green trace) induced a more stable open state than 2.75 mM ATP + 2 mM MgPPi (red trace) did. However, when the channels were first locked open by ATP and MgPPi, changing the solution to one containing PATP and MgPPi for even 120 s did not change the lock-open time significantly (blue trace in Fig. 3-10D). In fact, a 300-s exposure to PATP and MgPPi yield a lock-open time that is still shorter than that induced by PATP and MgPPi alone (Fig. 3-10E). Fig. 3-10F plots the percentage of channels with ATP/PATP

FIGURE 3-10

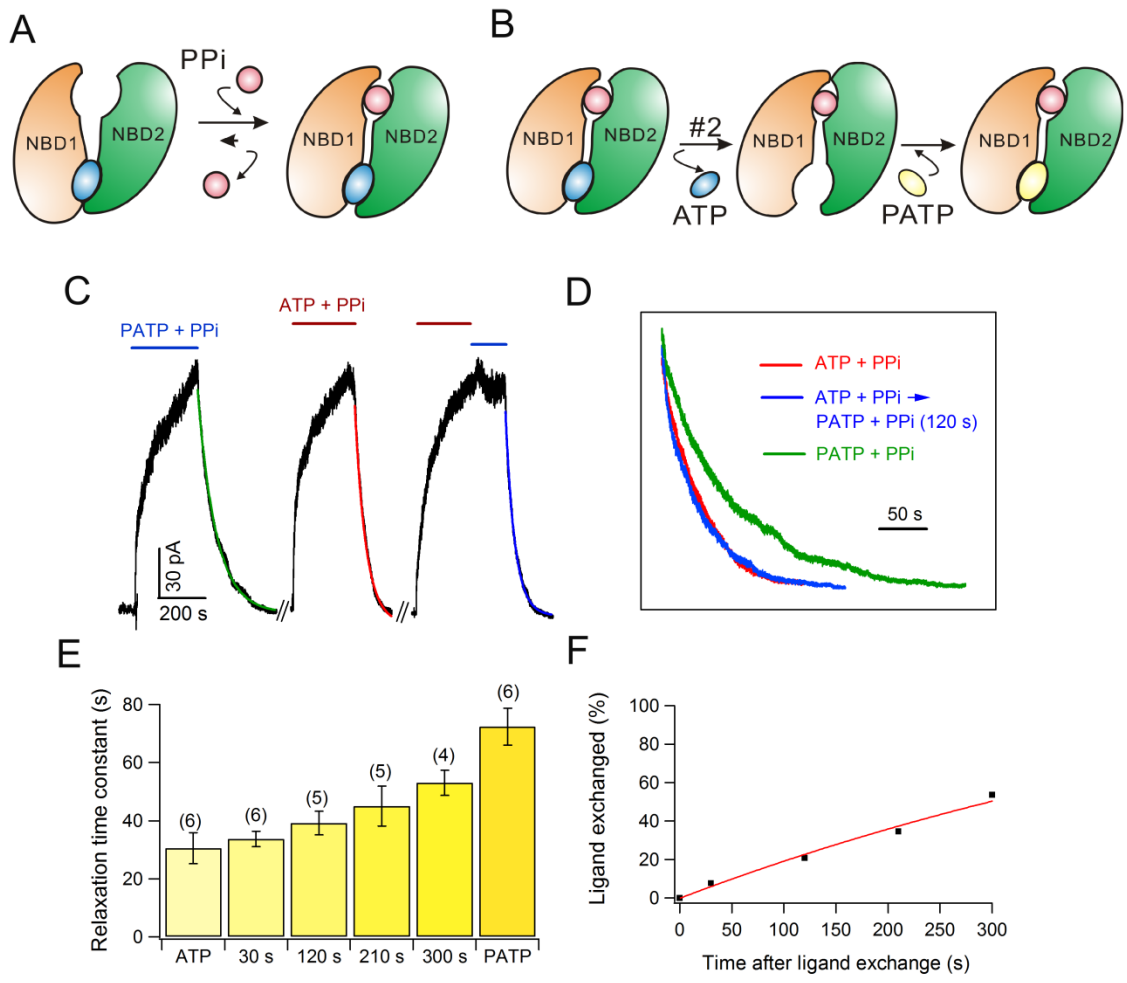
A
PPi
NBD1
NBD2
NBD1
NBD2
B
NBD1
NBD2
#2
ATP
NBD1
NBD2
PATP
NBD1
NBD2
C
PATP + PPi
ATP + PPi
30 pA
200 s
D
ATP + PPi
ATP + PPi
PATP + PPi (120 s)
PATP + PPi
50 s
E
Relaxation time constant (s)
0
20
40
60
80
(6)
(6)
(5)
(5)
(4)
(6)
ATP
30 s
120 s
210 s
300 s
PATP
F
Ligand exchanged (%)
0
20
40
60
80
100
0
50
100
150
200
250
300
Time after ligand exchange (s)

Figure 3-10. ATP/PATP exchange for WT-CFTR channels locked open by ATP/PATP plus PPi. (A) Cartoon illustrating the configurations of two NBDs of CFTR for the effect of PPi. The lock-open state of CFTR induced by ATP and PPi is in a configuration where ATP occupies NBD1 but PPi binds in NBD2. **(B)** Cartoon showing a possible ligand exchange for WT-CFTR in the lock-open state. If ATP/PATP exchange in NBD1 can occur when CFTR is locked open, the channel will enter into a more stable lock-open state where NBD1 binds a PATP molecule. **(C)** Current traces showing WT-CFTR channels locked into open states by ATP + PPi, PATP + PPi, or ATP + PPi followed by PATP + PPi. The currents decayed slowly after washout. **(D)** A comparison for current decay traces shown in (C). **(E)** After the application of ATP + PPi, the longer the subsequent exposure of WT-CFTR channels to PATP + PPi, the slower the current relaxation upon washout. **(F)** The current decay time constants measured under different exposure times of PATP + PPi were converted to the proportion of channels whose ATP in NBD1 has been replaced by PATP (see *Materials and Methods*). Data points were fitted with a single exponential function (red curve). It's noted that since significant closed durations are expected over an experimental time span of hundreds of seconds, the resulting time constant (522 s) likely underestimates the ATP dwell time in NBD1 when CFTR is in the lock-open state. Thus the rate of ATP/PATP exchange, ~0.002 s^{-1} (or 1/522 s), can only be considered as an upper limit for the rate of exchange for the open state.

exchange already occurred in NBD1 over different durations of channels' exposure to PATP and PPi, based on the assumption that the increased portion of the lock-open time (Fig. 3-10E) reflects an increased percentage of channels whose NBD1 have already undergone ligand exchange (see *Material and Methods*). Fitting the data points with a single exponential function (red curve in Fig. 3-10F) gave a time constant of 522 s, indicating that the ATP dwell time is >10-fold longer than that measured when CFTR is not locked in the open state (Figs 3-2 & 3-9). Thus, we conclude that during the open state (full NBD dimer state), ligand exchange in NBD1 takes place extremely slowly. These results together with that shown in Fig. 3-9 lead us to propose that in the partial dimer state (C_2), NBD1 and NBD2 can occasionally fall apart into the monomeric resting state (i.e., $C_2 \rightarrow C_1$ in Fig. 3-12A), enabling nucleotide exchange to occur in NBD1.

A Second Gating Cycle of CFTR

We next asked after the complete disengagement of CFTR's two NBDs, if the resting state can sojourn directly to the stable partial dimer state ($C_1 \rightarrow C_2$ in Fig. 3-12A) before the channel opens. Alternatively, the channel must first open before a closed, ATP-trapped state can form ($C_1 \rightarrow C_2' \rightarrow O \rightarrow C_2$ in Fig. 3-12A). G551D, a mutation in the signature sequence of the NBD1 tail offers an opportunity to differentiate these two possibilities. Since this mutation eliminates ATP-dependent openings of CFTR with rare spontaneous openings left (Bompadre et al., 2007), the stable partial dimer state will not exist for G551D-CFTR if its formation requires prior ATP-induced openings ($C_1 \rightarrow C_2' \rightarrow O \rightarrow C_2$ in Fig. 3-12A). Our previous studies

FIGURE 3-11

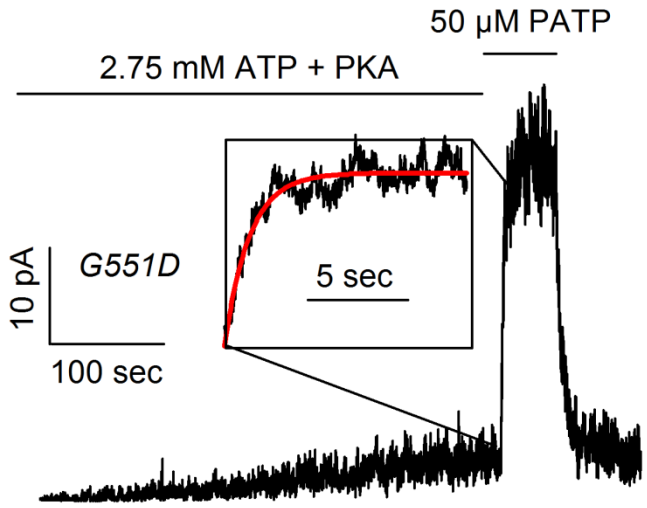

Figure 3-11. Ligand exchange experiments conducted with G551-CFTR. The G551D mutant channels were activated by PKA and ATP to a steady state before the solution was changed to one containing PATP. The macroscopic current increased monotonically (inlet) by PATP, although G551D-CFTR did not respond to ATP.

FIGURE 3-12

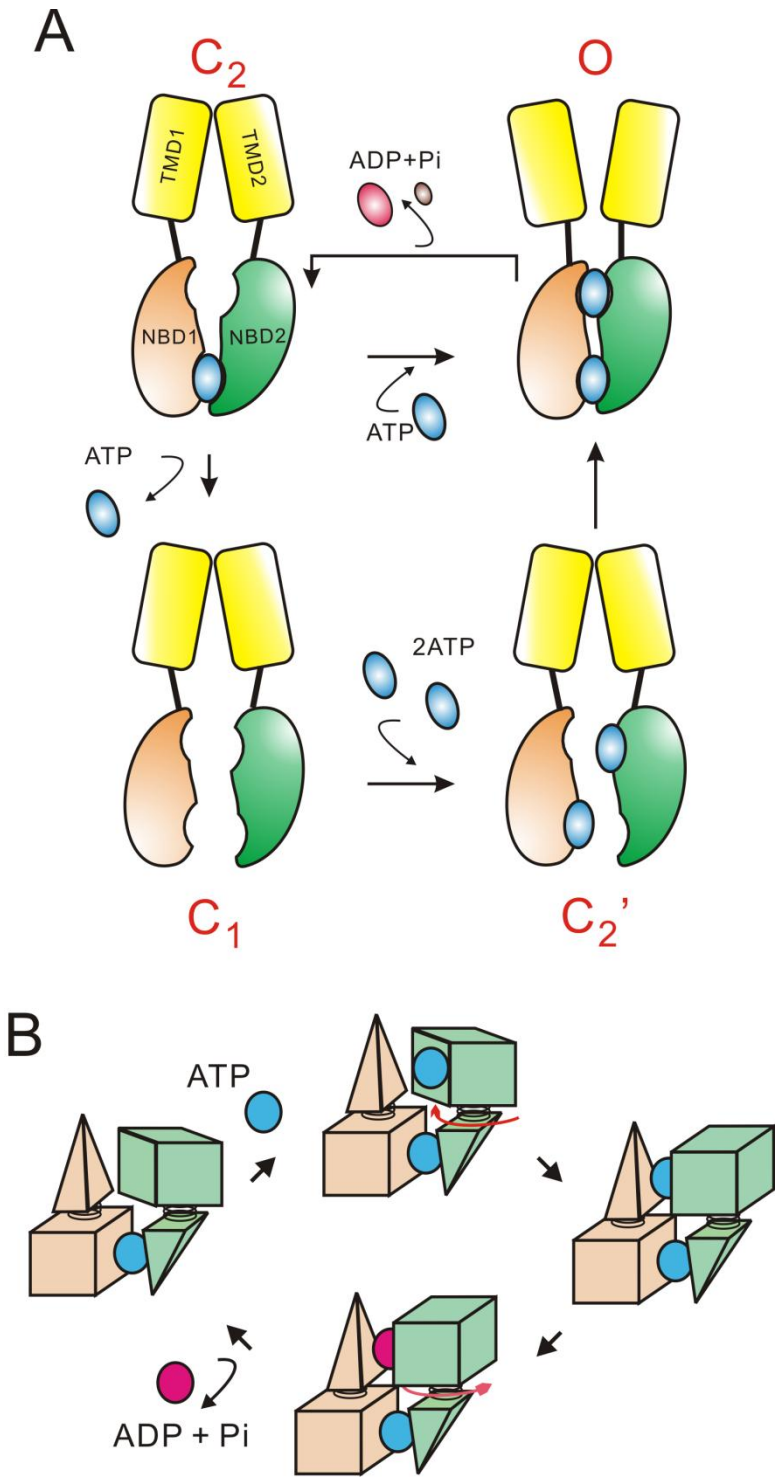

Figure 3-12. Molecular model of CFTR gating. **(A)** A simplified diagram illustrating dominant gating transitions ($C_2 \leftrightarrow O$) and a second gating cycle ($C_1 \rightarrow C_2' \rightarrow O \rightarrow C_2 \rightarrow C_1$) involving complete disengagement of the two NBDs. **(B)** A proposed mechanism for partial separation and re-formation of the NBD dimer. Cubes: head subdomains of NBDs; pyramids: tail subdomains of NBDs.

have demonstrated that PATP increases the Po of G551D channels by binding to NBD1 while exerts no effects when binding to NBD2 (Bompadre et al., 2008). Thus, the time course of current rise upon ATP/PATP switch will reflect the dissociation rate of ATP from NBD1 of G551D-CFTR. In the current trace shown in Fig. 3-11, after ligand changes from ATP to PATP, the rapid monophasic (τ = 2.1 ± 0.3 s, n = 11) increase of G551D currents indicates that unlike WT channels, ATP is not stably trapped in NBD1 of G551D-CFTR. In other words, binding of ATP in G551D-CFTR's NBD1 does not lead to a stable partial dimer state. We thus propose that the disassembly of the partial NBD dimer ($C_2 \rightarrow C_1$ in Fig. 3-12A) is a poorly reversible process. The implication for this proposition is that the channel in the resting state has to open first before a closed, ATP-trapped partial dimer state can form ($C_1 \rightarrow C_2$' $\rightarrow O \rightarrow C_2$ in Fig. 3-12A). That is, the channel in the monomeric state enters into the open state through a second gating cycle, distinct from the dominant gating cycle discussed above ($C_2 \leftrightarrow O$ in Fig. 3-12A).

We noticed that an alternative interpretation of the results shown in Fig. 3-11 is that ATP binding to NBD1 can bring the channel into the partial dimer state (i.e. the step C_1 to C_2 is readily reversible) but the partial dimer state is so severely destabilized that the NBD1 site can be loaded by PATP rapidly after ligand exchange. In this scenario, the G551D mutation in the helical subdomain of NBD1 has to allosterically affect tight nucleotide binding observed in NBD1's core subdomain in spite of >10 Å distance in between (Lewis et al., 2004; Lewis et al., 2005). One possibility to envision such allosteric communication is that the negatively charged

D551 side chain could somehow clash with the ATP or PATP molecule bound in the head of NBD2, pushing the two NBDs away from each other. In Figs. 3-S5 & 3-S6, we however show that this is unlikely the case since introducing the Y1219G mutation, which greatly disrupts ATP or PATP binding in NBD2 (Fig. 3-S5), into the G551D background does not significantly (P = 0.78) alter the time constant of current increase upon ATP/PATP switch (Fig. 3-S6). We acknowledge that we cannot test and rule out all possible allosteric mechanisms, but our proposition of the irreversibility for the $C_2 \rightarrow C_1$ step is at least consistent with two lines of structural/functional observations as detailed in the *Discussion* section.

3-5. Discussion

In the current study, we designed a novel ligand exchange protocol to investigate the ATP binding status in CFTR's two NBDs. The results led us to propose that an ATP molecule stays in NBD1 for tens of seconds spanning many gating cycles of CFTR, and that this stably bound ATP molecule is trapped by the NBD1 head and the NBD2 tail at the dimer interface. Based on findings in the current studies as well as those in the literature, we can establish a molecular mechanism for CFTR gating by its two NBDs. We posit that the dominant gating cycle of CFTR represents a repeated interconversion between the full NBD dimer and the partial dimer state ($C_2 \leftrightarrow O$ in Fig. 3-12A). We also present evidence for a second gating cycle, which involves a poorly reversible process of partial dimer separation into the rarely existed monomeric NBD state ($O \rightarrow C_2 \rightarrow C_1 \rightarrow C_2' \rightarrow O$ in Fig. 3-12A).

Stable Nucleotide Binding in NBD1 and the Underlying Structural Mechanism

Our ATP/PATP exchange experiments to investigate ATP binding status in CFTR's NBDs led to several conclusions generally consistent with our previous work (Tsai et al., 2009) that employed an independent experimental strategy. On the other hand, our conclusions are qualitatively and quantitatively different from those of photolabelling experiments (Basso et al., 2003; Aleksandrov et al., 2008) because the stable ATP binding in NBD1 demonstrated here was ~50-fold less stable than the biochemically observed 8-N_3-ATP occlusion and because in our study the signature sequence of NBD2 plays a key role for ATP to bind tightly in NBD1.

Before we discuss possible explanations for these discrepancies, however, we first acknowledge that the limitation of our functional approach is that, unlike photolabelling experiments, it does not allow us to "see" directly the bound ATP molecules in CFTR. Instead, our direct experimental observations were that upon ATP/PATP exchange, one of the gating properties with ATP (shorter open-time than that induced by PATP) can last for ~50 s, as if the channel can remember its history of being gated by ATP even after the ligand has been replaced by PATP for ~50 s. This long-lasting "memory" can be explained by a simple idea that an ATP molecule can physically bind in the CFTR protein for tens of seconds without dissociation so that the shorter open-time of ATP-gated CFTR can be maintained. We did realize that there are alternative explanations for this long-lasting effect of ATP. For example, one can argue that ATP may dissociate immediately once the ATP-containing solution is changed but the ATP-induced conformational changes can

persist for tens of seconds. In other words, it is not the ATP binding per se, but the relaxation of the conformational changes that takes a long time to complete. However, our observation that non-conservative mutations at W401, a residue that interacts with ATP in the crystal structure of CFTR's NBD1 (Lewis et al., 2005), greatly accelerated the dissipation of ATP's long-lasting effects on channel open-time after ATP/PATP exchange (Fig. 3-3), strongly suggests that this long-lasting remembrance of the gating history is due to a physically bound ATP molecule that stays in the CFTR protein for tens of seconds.

The results that mutations in either the W401 residue or in the signature sequence of NBD2 modulate how long ATP's effect on CFTR open-time can last (or how long the delay is for PATP to catalyze long openings) suggests that the stable ATP binding occurs at the interface between the NBD1 head and the NBD2 tail. It should be noted that these mutational effects are relatively specific because we observed a correlation between the chemical nature of the mutations and the degree of perturbations (Figs. 3-3-5) and also because all these mutations mostly affect the second kinetic change (i.e. changes in the open-time) after ligand switches, while bear little influence on the first step (i.e. changes in the closed time) (Fig. 3-5). The proposition that a tightly bound ATP molecule in NBD1 prevents PATP from inducing long CFTR openings also corroborates previous reports that PATP affects the open state stability by its interactions with NBD1 (Zhou et al., 2005; Zhou et al., 2006; Tsai et al., 2009).

The exact reason for the aforementioned discrepancy between our functional data and biochemical studies (Basso et al., 2003; Aleksandrov et al., 2008) is unclear. We can, however, at least argue that the difference in the ligand used in these two sets of experiments is unlikely the culprit since our data suggest that 8-N_3-ATP is trapped at the dimer interface for nearly identical time as ATP. One may simply speculate that in the membrane preparation used for photolabelling experiments and in excised inside-out membrane patches, CFTR proteins adopt different tertiary structures and thus have distinct structural mechanisms for retaining nucleotides in NBD1. We reasoned that a more likely scenario to explain the discrepancy lies in the fact that not all CFTR proteins in the cell are mature and functional. Since only functional channels yield currents in electrophysiological recordings, our approach inevitablely targets only functional CFTR proteins residing in the plasma membrane.

Two Gating Cycles of CFTR Channels

In the *Result* section, we proposed that the primary mode of CFTR's opening-closing cycle represents a repeated switch between a full NBD dimer (open state, Vergani et al., 2005) and a partial NBD dimer (closed state) ($C_2 \leftrightarrow O$ in Fig. 3-12A). During these gating cycles, the NBD1 head and the NBD2 tail are connected so as to retain an ATP molecule at the NBD interface for tens of seconds. A model with a similar molecular picture has been proposed before (Gadsby et al., 2006), based on the assumption that biochemically demonstrated nucleotide occlusion in NBD1 occurs at the NBD dimer interface. The validity of this assumption has however been

undermined by a similar occlusion phenomenon observed with ΔNBD2-CFTR (Aleksandrov et al., 2008).

Crystallographic studies of the ABC proteins have provided a clue for how partial separation of an NBD dimer could be achieved. It has been demonstrated that compared with the ATP-free form, the ATP-bound monomeric NBD shows a rigid-body rotation of the helical subdomain relative to the core subdomain for over 10 degree (Karpowich et al., 2001; Yuan et al., 2001; Smith et al., 2002; Chen et al., 2003; Zaitseva et al., 2005), moving the NBDs into a dimerization-favoring orientation, where the helical subdomain from one NBD now faces the ATP binding site in the core subdomain of the partner NBD. It was also thought that upon ATP hydrolysis, a reverse rotation happens to expose the ATP binding site to facilitate nucleotide exchange (Karpowich et al., 2001). We propose that similar rotational movements of CFTR's NBD2, induced by ATP binding and hydrolysis, may also open and close the interface between CFTR's NBD2 head and the NBD1 tail (Fig. 3-12B). These "limited" molecular motions may constitute the fundamental mechanism by which NBDs control the CFTR gate.

For the other binding site where ATP is not hydrolyzed but trapped at the dimer interface, dissociation of the tightly bound ATP molecule likely requires some degree of separation of the NBD1 head and the NBD2 tail. Interestingly, our data (Figs. 3-8-10) suggest that this occurs more readily when CFTR is in the partial dimer state than in the full dimer state. Thus, it appears that the closing of the dimer interface between the head of NBD2 and the tail of NBD1 can somehow stabilize the

other interface formed by the head of NBD1 and the tail of NBD2, indicating an allosteric communication mechanism. This communication is likely bi-directional since it has also been demonstrated that a tighter binding of nucleotides at the dimer interface between the head of NBD1 and the tail of NBD2 slows down channel closure (Zhou et al., 2005), which represents the separation of the interface between the NBD2 head and the NBD1 tail. It's noted that our observation of allosteric interactions between the two interfaces again contradicts results from photolabelling experiments where nucleotide occlusion in NBD1 was not affected by mutations of the conserved lysine (K1250) residue in NBD2, and ATP binding at NBD2 was also unaffected by mutations of the equivalent residue (K464) in NBD1 (Aleksandrov et al., 2002).

The finding that G551D-CFTR, unlike WT channels, does not trap ATP in NBD1 (Fig. 3-11) was interpreted as that the disassembly of the stable partial NBD dimer ($C_2 \rightarrow C_1$ in Fig. 3-12A) is a poorly reversible process. That is, ATP binding in NBD1 is insufficient to induce a stable partial NBD dimer (see also the *Result* section). We realized that even we have conducted some control experiments (Figs. 3-S5-S6), it remains virtually impossible for us to exclude the possibility that this observation is due to a non-specific mutational effect on the stability of the C_2 state as elaborated in the *Result* section. However, we should point out that our proposition is at least consistent with some structural data in the literature. First, the crystal structure of mouse CFTR's NBD1 shows little conformational difference between nucleotide-free, ADP-, or ATP-bound forms (Lewis et al., 2004), as opposed to the NBDs of many other ABC proteins (Karpowich et al., 2001; Yuan et al., 2001; Smith et al., 2002;

Chen et al., 2003; Zaitseva et al., 2005). Thus, ATP binding in NBD1 may not induce necessary conformational changes thought to favor NBD dimerization. Second, an evolutionarily conserved hydrogen bond pair critical for NBD dimerization (Vergani et al., 2005) was only found in the NBD2 head (R555) and the NBD1 tail (T1246). The corresponding residues in the NBD1 head and the NBD2 tail cannot form a hydrogen bond. Therefore, in the resting state, the energy barrier to form a stable partial dimer state ($C_1 \rightarrow C_2$) may be much higher than that for the resting state to enter the open state ($C_1 \rightarrow C_2' \rightarrow O$) where the transition state may be stabilized by the hydrogen bond (R555-T1246) at the dimer interface.

If the aforementioned argument made for the G551D-CFTR is also valid for WT-CFTR, when WT channels occasionally exit from the primary gating cycle ($C_2 \leftrightarrow O$) through a rare separation of the partial dimer ($C_2 \rightarrow C_1$), the channel, now in the monomeric NBD state, will re-enter the open state via a distinct opening pathway, during which ATP binding in NBD1 is relatively unstable. This process represents a second gating cycle for CFTR ($O \rightarrow C_2 \rightarrow C_1 \rightarrow C_2' \rightarrow O$). The dynamic interaction between two NBDs during the transition from the monomeric state to the dimeric state ($C_1 \rightarrow C_2' \rightarrow O$) is unclear and is awaiting more thorough investigations. We speculate that ATP binding to the head of monomeric NBD2 may recruit the NBD1 tail, initiating a closure of the dimer interface. We envision that this molecular motion then proceeds to completion by including the ATP molecule in NBD1 and thus leads to a stabilized ATP binding there.

The Structural/Functional Implications for Other ABC Proteins

The molecular model (Fig. 3-12) we proposed in the current study also poses several structural and functional implications for other ABC proteins. First, although the separation of the NBD dimer from the two-ATP bound state to the nucleotide-free state is evident from crystal structures of ABC transporters, it's unclear whether hydrolysis of one ATP molecule is sufficient to open an NBD dimer (discussed in van der Does and Tampé, 2004; Oswald et al., 2006; Sauna et al., 2007; Davidson et al., 2008; Procko et al., 2009). To directly address this issue, it is necessary to characterize a single-ATP bound state of NBDs. However, isolating such an intermediate state has proven difficult for experimental approaches to date. Molecular dynamic (MD) simulations may provide helps to understand its structural properties but results from different groups are contradictory (Wen and Tajkhorshid, 2008; Jones and George, 2009). In the current study, we demonstrated that after hydrolysis of one ATP molecule, the NBD dimer, at least for CFTR, can remain partially connected by the remaining ATP molecule (i.e. partial dimer state). Although the detailed 3D structure of the partial dimer state is unknown, we believe that crystallization of NBDs in this state can be attained by mutating catalytic residues in only one of an ABC protein's two NBDs, mimicking the asymmetric catalytic ability of CFTR's NBDs.

How the function of ABC proteins is supported by ATP binding and hydrolysis events occurred in NBDs has received great attention in the ABC protein field. Recent advances in solving the structures of full-length ABC transporters have

revealed that the TMDs of these proteins adopt inward- and outward-facing conformations respectively when the NBDs are in the ATP-free monomeric and two-ATP bound dimeric forms (for example, Ward et al., 2007; Aller et al., 2009; Khare et al., 2009). Thus, the opening and closing of the NBD dimer interface appears to drive the "alternating access" (Jardetzky, 1966) of the substance binding site located in the TMDs so that the cargo can bind from one side of the membrane and be released from the other side, fulfilling the structural requirement of an active transporter. A structure-based model has therefore emerged with the function of ABC proteins being coupled to the "large-scale" movements of repeated formation and separation of the NBD dimer (Reviewed in Hollenstein et al., 2007; Oldham et al., 2008; Rees et al., 2009). This model however overlooks the single-ATP bound state discussed above.

Since the NBDs seldom disengage completely for many CFTR gating cycles, we propose that, unlike the structure-based model, "limited motions" of NBDs (i.e. partial separation and reformation) are sufficient to complete a cycle of conformational changes in TMDs for CFTR. For many asymmetric ABC proteins such as human multiple drug resistant protein 1 (MRP1) or sulfonylurea receptor (SUR1), their NBD1, similar to CFTR, also has substitutions in key catalytic residues and thus display a stable ATP binding phenomenon (Matsuo et al., 1999; Ueda et al., 1999; Gao et al., 2000; Hou et al., 2000; Matsuo et al., 2000; Nagata et al., 2000). If the duration of their functional cycle is substantially shorter than the ATP dwell time in NBD1, and if the tight ATP binding is also mediated by a partial dimer state, one has

to conclude that limited movements of NBDs can also be sufficient to support the function of these asymmetric ABC proteins.

For ABC proteins with two catalysis-competent sites, the stoichiometry of ATP hydrolysis per functional cycle has been under intense debates. The "sequential hydrolysis" or "processive clamp" model suggests that hydrolysis of two ATP molecules is necessary for a single functional cycle (Janas et al., 2003), thus inferring that a functional cycle involves a complete separation of the NBD dimer. This mechanism appears to gain supports from crystallographic studies as no structure so far is solved in a single-ATP bound form. On the other hand, an "alternating catalytic sites" model was proposed for human P-glycoproteins (Urbatsch et al., 1995; Tombline et al., 2004) and *E. coli* maltose transporters ($MalFGK_2$) (Sharma et al., 2000) suggesting that only one ATP molecule is hydrolyzed in a transport cycle. Our proposition of limited NBD motions between a full NBD dimer and a single-ATP bound partial dimer provides support for this latter model. In fact, based on the crystal structure of Sav1866, a bacterial ABC protein with both NBDs capable of catalyzing ATP hydrolysis, it was argued that the motion of NBDs is restrained by TMDs and thus probably cannot carry out large movements as suggested by the aforementioned structure-based model (Schuldiner, 2006).

Potential Applications of Ligand Exchange Experiments

In addition to tracing ATP binding in CFTR's NBDs, the ligand exchange experiments developed here can also be a powerful tool to investigate how different nucleotide ligands affect CFTR's function. Upon solution switches from ATP to a

second ligand, since one ATP can stay bound in NBD1 for ~50 s, an immediate change of CFTR's gating kinetics is caused by the binding of the second ligand to NBD2. It follows that if the ligand can exert some effects on CFTR's function by binding to NBD1, this effect will occur only after a ~50 s delay. Using this method, we have found that 8-N_3-ATP induces a slower opening rate but a longer open-time than ATP simply because of its different interactions with CFTR's NBD2 (Figs. 3-6-7 and Figs. 3-S3-4). On the other hand, PATP catalyzes fast channel openings by binding to NBD2 but long open bursts by interacting with NBD1. CFTR can be opened by a wide range of nucleotide triphosphates other than ATP, including GTP, UTP, ITP, CTP, AMP-CPP, etc (Anderson et al., 1991). Comparing the mechanism of these ligands' influence on CFTR gating may represent an opportunity for a better understanding of ligand-NBD interactions in the future.

3-6. Supplemental information

FIGURE 3-S1

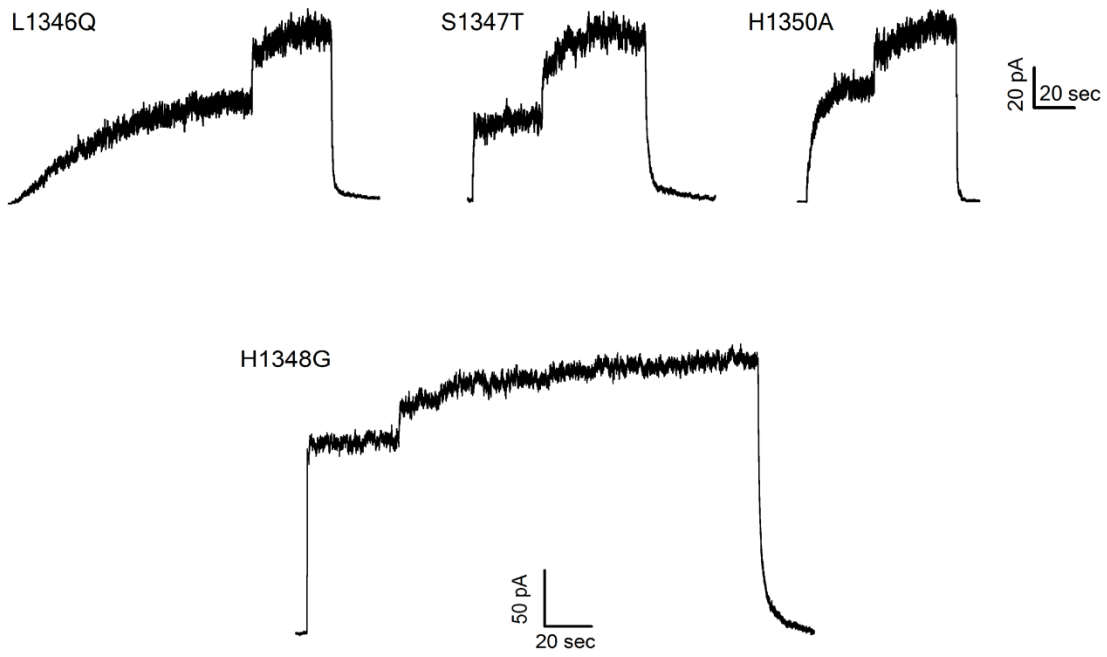

Figure 3-S1. Ligand exchange experiments conducted with macroscopic current recordings for mutations in the signature sequence of NBD2. The mutant channels were first opened by 2.75 mM ATP. Solution was then changed to 50 μM PATP until the current reached a steady state. PKA was present in all solutions to maintain a maximal phosphorylation level. Current traces for L1346Q-, S1347T-, and H1350A-CFTR share the same time and amplitude scales.

FIGURE 3-S2

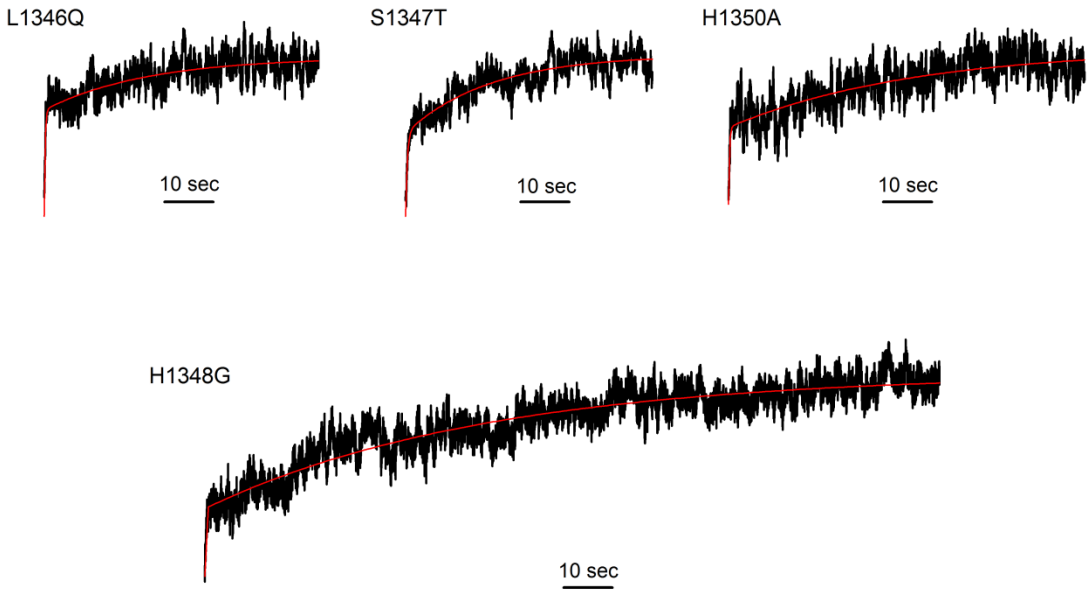

Figure 3-S2. The time courses of PATP-induced two-step current rise from Fig. 3-S1. All traces were fitted with a double exponential function (red lines).

FIGURE 3-S3

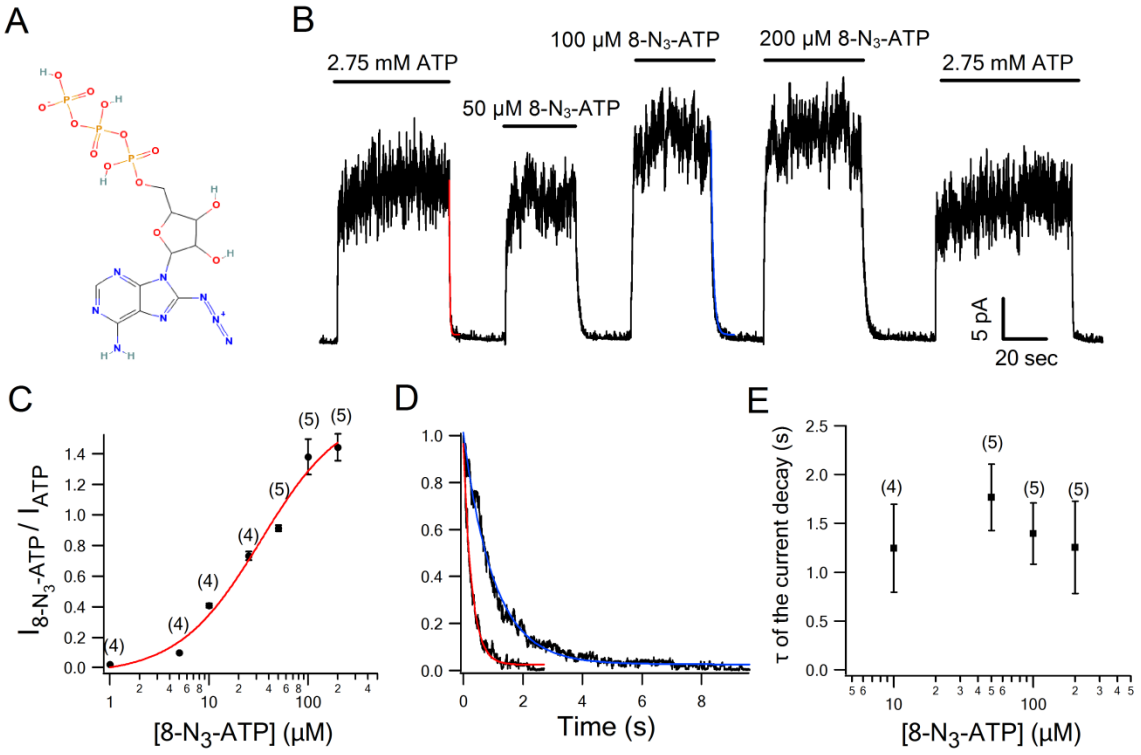
A
B
2.75 mM ATP
50 μM 8-N3-ATP
100 μM 8-N3-ATP
200 μM 8-N3-ATP
2.75 mM ATP
5 pA
20 sec
C
I8-N3-ATP / IATP
[8-N3-ATP] (μM)
D
Time (s)
E
τ of the current decay (s)
[8-N3-ATP] (μM)

Figure 3-S3. Gating of WT-CFTR by 8-N_3-ATP. (A) The structural formula of 8-N_3-ATP downloaded from NCBI. **(B)** WT-CFTR channels were exposed to different concentrations of 8-N_3-ATP. 100 μM seemed to be close to the maximally effective concentration. The Po induced by 100 μM 8-N_3-ATP is ~1.4-fold higher than that induced by 2.75 mM ATP. **(C)** The dose response relationship of 8-N_3-ATP on WT-CFTR. The amplitude of macroscopic current induced by 8-N_3-ATP was normalized to that by 2.75 mM ATP in the same patch. The data was then fitted with the Hill equation (red curve) with a $K_{1/2}$ of 33.44 ± 13.4 μM and the Hill coefficient of 1.04 ± 0.39. **(D)** The current decay trace (from B) after washing out of 2.75 mM ATP or 100 μM 8-N_3-ATP. The red and blue curves represent single exponential fits. 8-N_3-ATP apparently elicited longer openings than ATP. **(E)** The relaxation time constant after the removal of 8-N_3-ATP at different concentrations was approximately constant and was ~4-fold longer than that of ATP. Since the mean macroscopic current in the presence of a maximal concentration of 8-N_3-ATP was only 1.4 fold higher than that with 2.75 mM ATP, the opening rate of 8-N_3-ATP-gated WT-CFTR was estimated to be 2~3-fold lower than that of 2.75 mM ATP.

FIGURE 3-S4

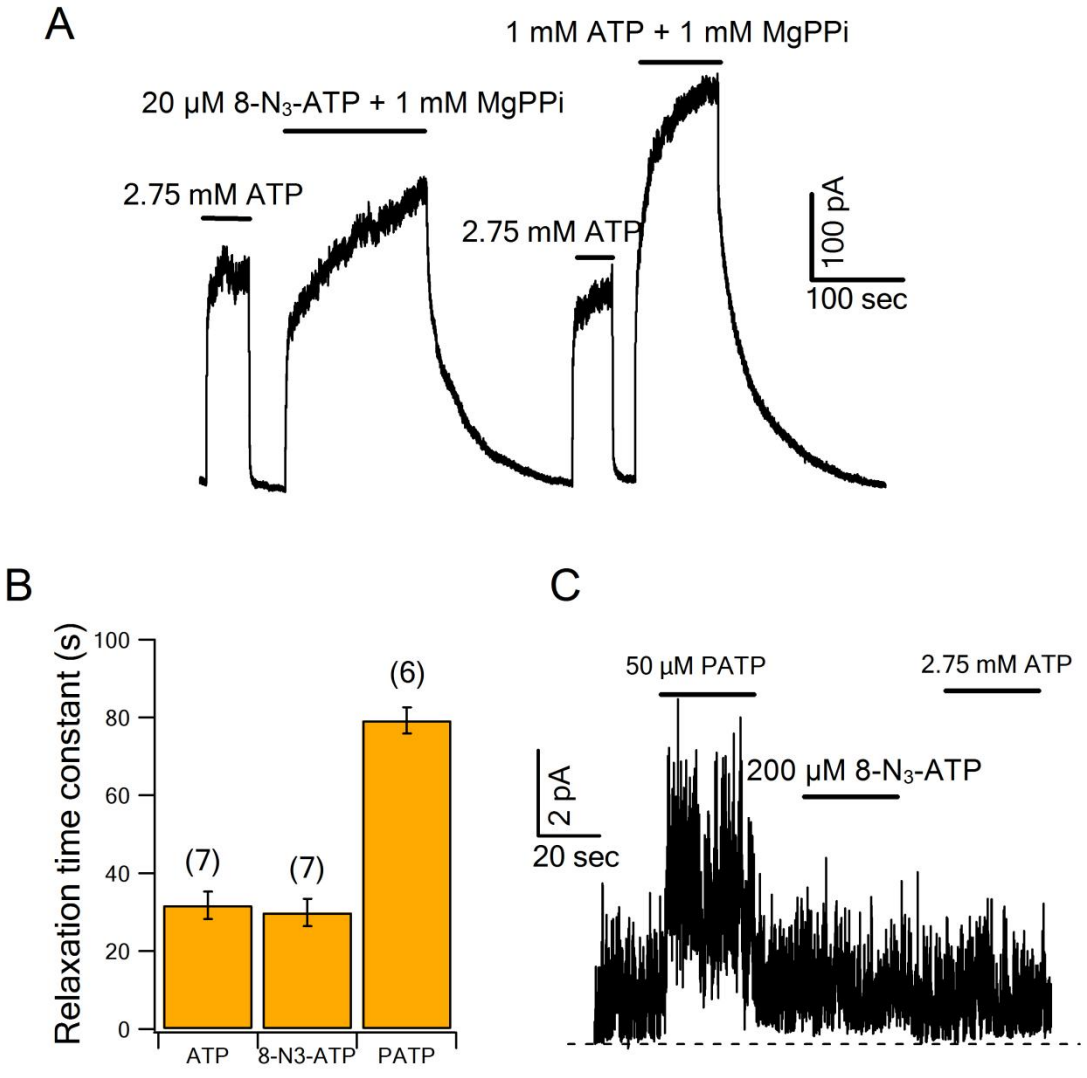
A
1 mM ATP + 1 mM MgPPi
20 µM 8-N3-ATP + 1 mM MgPPi
2.75 mM ATP
2.75 mM ATP
100 pA
100 sec
B
Relaxation time constant (s)
100
80
60
40
20
0
(7)
(7)
(6)
ATP
8-N3-ATP
PATP
C
50 µM PATP
2.75 mM ATP
200 µM 8-N3-ATP
2 pA
20 sec

Figure 3-S4. The idea that 8-N_3-ATP and ATP exert similar effects on CFTR gating kinetics when binding to NBD1 predicts two functional consequences. First, the burst duration for channels locked open by ATP plus MgPPi should be similar to that with 8-N_3-ATP plus MgPPi since in the lock-open state, NBD2 is occupied by MgPPi while the nucleotide (ATP or 8-N_3-ATP) is bound in NBD1. This was indeed the case as shown in (A) and (B). In contrast, PATP, which prolongs channel open time by binding to NBD1, greatly enhance the stability of the lock-open state (B). Second, 8-N^3-ATP, like ATP, should pose little effect on G551D-CFTR as the G551D mutation eliminates nucleotide's effects on NBD2. This prediction is again valid. G551D-CFTR channels responded to neither ATP nor 8-N^3-ATP (**e**, n = 3). PATP, on the other hand, potentiated G551D channels (C).

FIGURE 3-S5

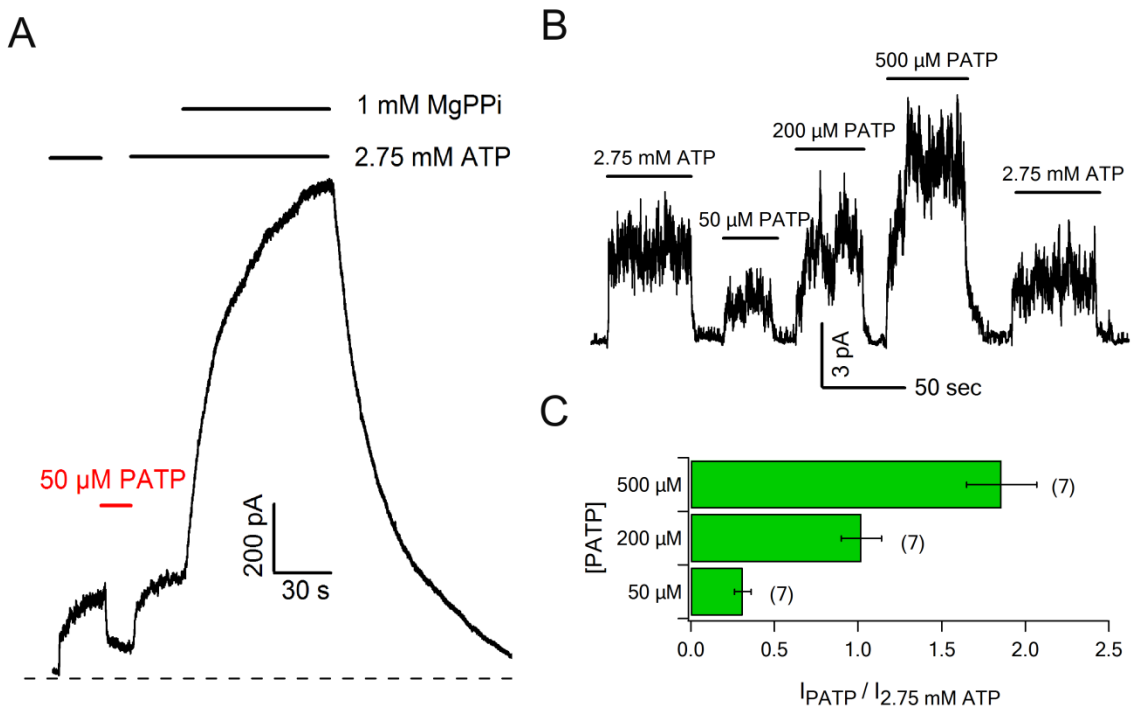

Figure 3-S5. **Effect of the Y1219G mutation on the apparent affinity for ATP**. **(A)** In this macroscopic current trace (similar result was seen in 3 other patches), 50 µM PATP only opened a very small portion (< 10%) of the Y1219G channels as revealed by a much larger current elicited by subsequent addition of ATP + MgPPi. Thus, the Po induced by 50 µM PATP in Y1219G-CFTR channels is lower than that observed for WT-CFTR as shown in Fig. 1A. **(B)(C)** The effects of Y1219G mutation can be overcome by higher concentrations (200 and 500 µM) of PATP, supporting the idea that this mutation does reduce the apparent affinity for PATP in NBD2.

FIGURE 3-S6

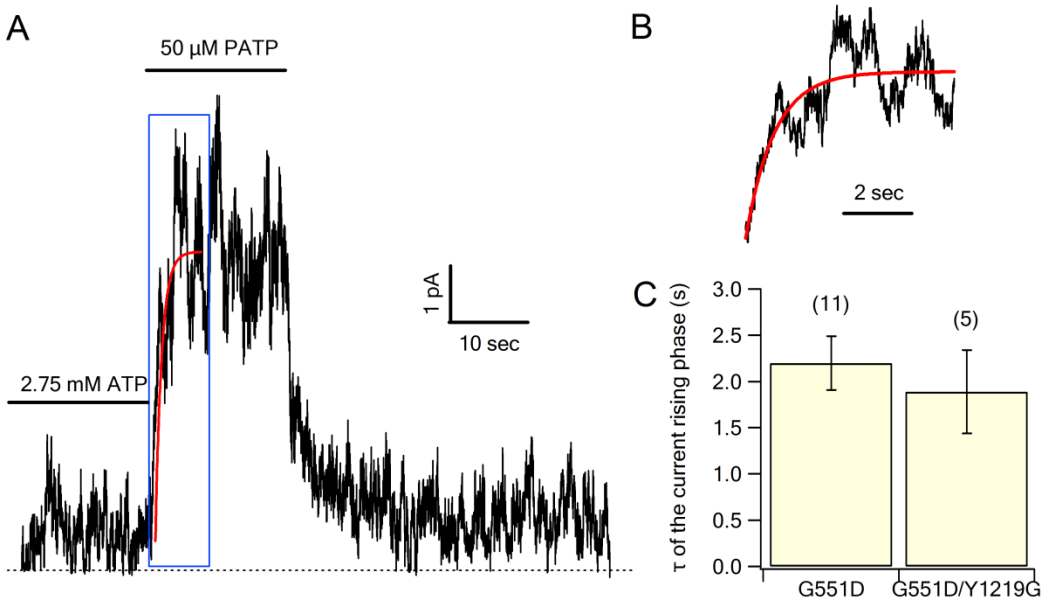

Figure 3-S6. **Ligand exchange experiments carried out with G551D/Y1219G-CFTR channels. (A)** Macroscopic current recordings from G551D/Y1219G double mutant channels. PATP induced rapid current increase upon solution changes. **(B)** The time course of current increase can be reasonably fitted with a single exponential function (red line). **(C)**, Time constants of the current rise upon ATP/PATP exchange as shown in (A). There is little difference (P = 0.78) between the time constant for G551D and that for G551D/Y1219G channels. These results suggest that G551D channels fail to trap ATP in NBD1 not because of the electrostatic repulsion between the aspartate site chain at the position 551 and the ATP or PATP molecule bound in the NBD2 site.

3-7. References

Aleksandrov, L., A. Aleksandrov, and J.R. Riordan. 2008. Mg2+ -dependent ATP occlusion at the first nucleotide-binding domain (NBD1) of CFTR does not require the second (NBD2). *Biochem J*. 416:129-136.

Aleksandrov, L., A.A. Aleksandrov, X.B. Chang, and J.R. Riordan. 2002. The First Nucleotide Binding Domain of Cystic Fibrosis Transmembrane Conductance Regulator Is a Site of Stable Nucleotide Interaction, whereas the Second Is a Site of Rapid Turnover. *J Biol Chem*. 277:15419-15425.

Aller, S.G., J. Yu, A. Ward, Y. Weng, S. Chittaboina, R. Zhuo, P.M. Harrell, Y.T. Trinh, Q. Zhang, I.L. Urbatsch, and G. Chang. 2009. Structure of P-glycoprotein reveals a molecular basis for poly-specific drug binding. *Science*. 323:1718-1722.

Anderson, M.P., H.A. Berger, D.P. Rich, R.J. Gregory, A.E. Smith, and M.J. Welsh. 1991. Nucleoside triphosphates are required to open the CFTR chloride channel. *Cell*. 67:775-784.

Basso, C., P. Vergani, A.C. Nairn, and D.C. Gadsby. 2003. Prolonged nonhydrolytic interaction of nucleotide with CFTR's NH2-terminal nucleotide binding domain and its role in channel gating. *J Gen Physiol*. 122:333-348.

Bear, C.E., C.H. Li, N. Kartner, R.J. Bridges, T.J. Jensen, M. Ramjeesingh, and J.R. Riordan. 1992. Purification and functional reconstitution of the cystic fibrosis transmembrane conductance regulator (CFTR). *Cell*. 68:809-818.

Bompadre, S.G., T. Ai, J.H. Cho, X. Wang, Y. Sohma, M. Li, and T.C. Hwang. 2005. CFTR gating I: Characterization of the ATP-dependent gating of a phosphorylation-independent CFTR channel (DeltaR-CFTR). *J Gen Physiol*. 125:361-375.

Bompadre, S.G., M. Li, and T.C. Hwang. 2008. Mechanism of G551D-CFTR (cystic fibrosis transmembrane conductance regulator) potentiation by a high affinity ATP analog. *J Biol Chem*. 283:5364-5369.

Bompadre, S.G., Y. Sohma, M. Li, and T.C. Hwang. 2007. G551D and G1349D, two CF-associated mutations in the signature sequences of CFTR, exhibit distinct gating defects. *J Gen Physiol*. 129:285-298.

Chen, J., G. Lu, J. Lin, A.L. Davidson, and F.A. Quiocho. 2003. A tweezers-like motion of the ATP-binding cassette dimer in an ABC transport cycle. *Mol Cell*. 12:651-661.

Chen, T.Y., and T.C. Hwang. 2008. CLC-0 and CFTR: chloride channels evolved from transporters. *Physiol Rev*. 88:351-387.

Csanady, L. 2000. Rapid kinetic analysis of multichannel records by a simultaneous fit to all dwell-time histograms. *Biophys J*. 78:785-799.

Davidson, A.L., and J. Chen. 2004. ATP-binding cassette transporters in bacteria. *Annu Rev Biochem*. 73:241-268.

Davidson, A.L., E. Dassa, C. Orelle, and J. Chen. 2008. Structure, function, and evolution of bacterial ATP-binding cassette systems. *Microbiol Mol Biol Rev*. 72:317-364, table of contents.

Gadsby, D.C., P. Vergani, and L. Csanady. 2006. The ABC protein turned chloride channel whose failure causes cystic fibrosis. *Nature*. 440:477-483.

Gao, M., H.R. Cui, D.W. Loe, C.E. Grant, K.C. Almquist, S.P. Cole, and R.G. Deeley. 2000. Comparison of the functional characteristics of the nucleotide binding domains of multidrug resistance protein 1. *J Biol Chem*. 275:13098-13108.

Hollenstein, K., R.J. Dawson, and K.P. Locher. 2007. Structure and mechanism of ABC transporter proteins. *Curr Opin Struct Biol*. 17:412-418.

Hou, Y., L. Cui, J.R. Riordan, and X. Chang. 2000. Allosteric interactions between the two non-equivalent nucleotide binding domains of multidrug resistance protein MRP1. *J Biol Chem*. 275:20280-20287.

Janas, E., M. Hofacker, M. Chen, S. Gompf, C. van der Does, and R. Tampe. 2003. The ATP hydrolysis cycle of the nucleotide-binding domain of the mitochondrial ATP-binding cassette transporter Mdl1p. *J Biol Chem*. 278:26862-26869.

Jardetzky, O. 1966. Simple allosteric model for membrane pumps. *Nature*. 211:969-970.

Jones, P.M., and A.M. George. 2009. Opening of the ADP-bound active site in the ABC transporter ATPase dimer: evidence for a constant contact, alternating sites model for the catalytic cycle. *Proteins*. 75:387-396.

Karpowich, N., O. Martsinkevich, L. Millen, Y.R. Yuan, P.L. Dai, K. MacVey, P.J. Thomas, and J.F. Hunt. 2001. Crystal structures of the MJ1267 ATP binding

cassette reveal an induced-fit effect at the ATPase active site of an ABC transporter. *Structure*. 9:571-586.

Khare, D., M.L. Oldham, C. Orelle, A.L. Davidson, and J. Chen. 2009. Alternating access in maltose transporter mediated by rigid-body rotations. *Mol Cell*. 33:528-536.

Lewis, H.A., S.G. Buchanan, S.K. Burley, K. Conners, M. Dickey, M. Dorwart, R. Fowler, X. Gao, W.B. Guggino, W.A. Hendrickson, J.F. Hunt, M.C. Kearins, D. Lorimer, P.C. Maloney, K.W. Post, K.R. Rajashankar, M.E. Rutter, J.M. Sauder, S. Shriver, P.H. Thibodeau, P.J. Thomas, M. Zhang, X. Zhao, and S. Emtage. 2004. Structure of nucleotide-binding domain 1 of the cystic fibrosis transmembrane conductance regulator. *EMBO J*. 23:282-293.

Lewis, H.A., X. Zhao, C. Wang, J.M. Sauder, I. Rooney, B.W. Noland, D. Lorimer, M.C. Kearins, K. Conners, B. Condon, P.C. Maloney, W.B. Guggino, J.F. Hunt, and S. Emtage. 2005. Impact of the deltaF508 mutation in first nucleotide-binding domain of human cystic fibrosis transmembrane conductance regulator on domain folding and structure. *J Biol Chem*. 280:1346-1353.

Lu, G., J.M. Westbrooks, A.L. Davidson, and J. Chen. 2005. ATP hydrolysis is required to reset the ATP-binding cassette dimer into the resting-state conformation. *Proc Natl Acad Sci U S A*. 102:17969-17974.

Matsuo, M., N. Kioka, T. Amachi, and K. Ueda. 1999. ATP binding properties of the nucleotide-binding folds of SUR1. *J Biol Chem*. 274:37479-37482.

Matsuo, M., K. Tanabe, N. Kioka, T. Amachi, and K. Ueda. 2000. Different binding properties and affinities for ATP and ADP among sulfonylurea receptor subtypes, SUR1, SUR2A, and SUR2B. *J Biol Chem*. 275:28757-28763.

Mense, M., P. Vergani, D.M. White, G. Altberg, A.C. Nairn, and D.C. Gadsby. 2006. In vivo phosphorylation of CFTR promotes formation of a nucleotide-binding domain heterodimer. *EMBO J*. 25:4728-4739.

Nagata, K., M. Nishitani, M. Matsuo, N. Kioka, T. Amachi, and K. Ueda. 2000. Nonequivalent nucleotide trapping in the two nucleotide binding folds of the human multidrug resistance protein MRP1. *J Biol Chem*. 275:17626-17630.

Oldham, M.L., A.L. Davidson, and J. Chen. 2008. Structural insights into ABC transporter mechanism. *Curr Opin Struct Biol*. 18:726-733.

Oswald, C., I.B. Holland, and L. Schmitt. 2006. The motor domains of ABC-transporters. What can structures tell us? *Naunyn Schmiedebergs Arch Pharmacol*. 372:385-399.

Procko, E., I. Ferrin-O'Connell, S.L. Ng, and R. Gaudet. 2006. Distinct structural and functional properties of the ATPase sites in an asymmetric ABC transporter. *Mol Cell*. 24:51-62.

Procko, E., M.L. O'Mara, W.F. Bennett, D.P. Tieleman, and R. Gaudet. 2009. The mechanism of ABC transporters: general lessons from structural and functional studies of an antigenic peptide transporter. *FASEB J*. 23:1287-1302.

Rees, D.C., E. Johnson, and O. Lewinson. 2009. ABC transporters: the power to change. *Nat Rev Mol Cell Biol*. 10:218-227.

Riordan, J.R., J.M. Rommens, B. Kerem, N. Alon, R. Rozmahel, Z. Grzelczak, J. Zielenski, S. Lok, N. Plavsic, J.L. Chou, and et al. 1989. Identification of the cystic fibrosis gene: cloning and characterization of complementary DNA. *Science*. 245:1066-1073.

Sauna, Z.E., I.W. Kim, and S.V. Ambudkar. 2007. Genomics and the mechanism of P-glycoprotein (ABCB1). *J Bioenerg Biomembr*. 39:481-487.

Schuldiner, S. 2006. Structural biology: the ins and outs of drug transport. *Nature*. 443:156-157.

Sharma, S., and A.L. Davidson. 2000. Vanadate-induced trapping of nucleotides by purified maltose transport complex requires ATP hydrolysis. *J Bacteriol*. 182:6570-6576.

Smith, P.C., N. Karpowich, L. Millen, J.E. Moody, J. Rosen, P.J. Thomas, and J.F. Hunt. 2002. ATP binding to the motor domain from an ABC transporter drives formation of a nucleotide sandwich dimer. *Mol Cell*. 10:139-149.

Tombline, G., L.A. Bartholomew, I.L. Urbatsch, and A.E. Senior. 2004. Combined mutation of catalytic glutamate residues in the two nucleotide binding domains of P-glycoprotein generates a conformation that binds ATP and ADP tightly. *J Biol Chem*. 279:31212-31220.

Tsai, M.F., H. Shimizu, Y. Sohma, M. Li, and T.C. Hwang. 2009. State-dependent modulation of CFTR gating by pyrophosphate. *J Gen Physiol*. 133:405-419.

Ueda, K., J. Komine, M. Matsuo, S. Seino, and T. Amachi. 1999. Cooperative binding of ATP and MgADP in the sulfonylurea receptor is modulated by glibenclamide. *Proc Natl Acad Sci U S A*. 96:1268-1272.

Urbatsch, I.L., B. Sankaran, J. Weber, and A.E. Senior. 1995. P-glycoprotein is stably inhibited by vanadate-induced trapping of nucleotide at a single catalytic site. *J Biol Chem*. 270:19383-19390.

van der Does, C., and R. Tampe. 2004. How do ABC transporters drive transport? *Biol Chem*. 385:927-933.

Vergani, P., S.W. Lockless, A.C. Nairn, and D.C. Gadsby. 2005. CFTR channel opening by ATP-driven tight dimerization of its nucleotide-binding domains. *Nature*. 433:876-880.

Vergani, P., A.C. Nairn, and D.C. Gadsby. 2003. On the mechanism of MgATP-dependent gating of CFTR Cl- channels. *J Gen Physiol*. 121:17-36.

Ward, A., C.L. Reyes, J. Yu, C.B. Roth, and G. Chang. 2007. Flexibility in the ABC transporter MsbA: Alternating access with a twist. *Proc Natl Acad Sci U S A*. 104:19005-19010.

Wen, P.C., and E. Tajkhorshid. 2008. Dimer opening of the nucleotide binding domains of ABC transporters after ATP hydrolysis. *Biophys J*. 95:5100-5110.

Yuan, Y.R., S. Blecker, O. Martsinkevich, L. Millen, P.J. Thomas, and J.F. Hunt. 2001. The crystal structure of the MJ0796 ATP-binding cassette. Implications for the structural consequences of ATP hydrolysis in the active site of an ABC transporter. *J Biol Chem*. 276:32313-32321.

Zaitseva, J., S. Jenewein, T. Jumpertz, I.B. Holland, and L. Schmitt. 2005. H662 is the linchpin of ATP hydrolysis in the nucleotide-binding domain of the ABC transporter HlyB. *EMBO J*. 24:1901-1910.

Zeltwanger, S., F. Wang, G.T. Wang, K.D. Gillis, and T.C. Hwang. 1999. Gating of cystic fibrosis transmembrane conductance regulator chloride channels by adenosine triphosphate hydrolysis. Quantitative analysis of a cyclic gating scheme. *J Gen Physiol*. 113:541-554.

Zhou, Z., X. Wang, M. Li, Y. Sohma, X. Zou, and T.C. Hwang. 2005. High affinity ATP/ADP analogues as new tools for studying CFTR gating. *J Physiol*. 569:447-457.

Zhou, Z., X. Wang, H.Y. Liu, X. Zou, M. Li, and T.C. Hwang. 2006. The two ATP binding sites of cystic fibrosis transmembrane conductance regulator (CFTR) play distinct roles in gating kinetics and energetics. *J Gen Physiol*. 128:413-422.

CHAPTER 4

OPTIMIZATION OF THE COMPOSITE SITE 1 RECTIFIES THE FUNCTIONAL DEFECTS OF CYSTIC FIBROSIS RELATED MUTANT CFTR CHANNELS

4-1. Abstract

CFTR chloride channel is the ABC protein whose defects cause the lethal genetic disease cystic fibrosis (CF). Opening of wild type (WT)-CFTR is initiated when two ATP molecules connect the nucleotide binding domains (NBD1 and NBD2) into a head-to-tail dimer, where each ATP at interfacial composite sites (site 1 and site 2) contacts the Walker motifs from one NBD and the signature motif from the other NBD. The CF-associated mutation G551D, by introducing a negative charge to NBD1's signature motif, a constituent of site 2, completely abolishes ATP-dependent opening of CFTR presumably by hindering closure of the NBD interface. Guided by crystal structures of ABC proteins, we identified site 1 mutations W401Y/F and H1348G that conferred ATP response for G551D channels resulting in a ~25-fold increase of channel activity. Our data suggest that these mutations optimize ATP-site 1 interactions so that ATP can link the two NBD components of site 1 for many seconds even site 2 may remain vacant. During this period, optimized G551D channels exhibited a distinct gating behavior characterized by a slower opening rate but a prolonged open time compared with normal WT-CFTR gating. This strategy of

improving channel function is not limited to G551D-CFTR as the W401F/H1348G mutation doubled the open probability of WT-CFTR and increased the activity of ΔF508-CFTR by ~7-fold. That CFTR's innate site 1 is not optimized for ATP binding grants a unique opportunity to develop pharmaceutical reagents that better fit into this site for the treatment of patients with CF.

4-2. Introduction

ATP binding cassette (ABC) proteins share a basic architecture comprising two transmembrane domains (TMDs) and two cytoplasmic nucleotide binding domains (NBD1 & NBD2). Crystallographic studies have revealed that each NBD can be divided into a larger core (head) subdomain and a smaller helical (tail) subdomain; the former contains the conserved Walker motifs for binding and hydrolyzing ATP, while the latter comprises the signature motif (LSGGQ) unique to ABC proteins (Davidson and Chen, 2004; Oswald et al., 2006). The two monomeric NBDs are so arranged that the head subdomain from one NBD faces the tail subdomain from the other NBD. Upon ATP binding, the NBDs assemble into a head-to-tail dimer connected by two ATP molecules at interfacial composite sites (site 1 and site 2). This NBD dimer is subsequently destabilized when the enclosed ATP molecules are hydrolyzed.

CFTR belongs to a subgroup of asymmetric ABC proteins (Riordan et al., 1989; Procko et al., 2009) as the constituents of its site 2 (i.e. NBD2's Walker motifs and NBD1's LSGGQ motif) retain all conserved residues, while those of its site 1 (i.e.

NBD1's Walker motifs and NBD2's signature motif: LSHGH) present several non-consensus substitutions. This structural asymmetry is accompanied by the functional asymmetry that gating of the CFTR pore located in TMDs is mainly controlled by ATP binding and hydrolysis events in the catalysis-competent site 2 (Gadsby et al., 2006; Chen and Hwang, 2008). This "site 2-controlled gating" of WT-CFTR can be impaired by CF-related mutations. For example, the G551D mutation completely eliminates ATP-catalyzed openings of CFTR (Bompadre et al., 2007). This phenomenon is not surprising as in the dimeric structures of NBDs for other ABC proteins (Smith et al., 2002; Chen et al., 2003), the G551 residue of NBD1's signature motif (site 2) interacts with ATP's γ-phosphate and thus a negatively charged Asp side-chain is expected to hinder the formation of the NBD dimer. ΔF508, the most common CF-associated mutation, also exhibits defective gating (Ostedgaard et al., 2007; Serohijos et al., 2008; Miki et al., 2010). In this case, the exact structural mechanism underlying the abnormal channel function remains unsettled (Ostedgaard et al., 2007; Serohijos et al., 2008; Kanelis et al., 2010; Miki et al., 2010).

It has been shown that for many ABC proteins with two catalysis-competent composite sites, mutating conserved residues in one site does not abolish protein functions entirely (Davidson et al., 2008). We thus reasoned that re-building the degenerated site 1 of CFTR might allow G551D channels to maintain a certain level of function even its site 2 is disabled. This idea gains supports from our previous observation that a hydrolyzable ATP analogue N_6-2-phenylethyl-ATP (PATP) potentiates G551D-CFTR by binding to NBD1's head subdomain (Bompadre et al.,

2008), a component of site 1! In the current study, guided by accumulated structural and functional understanding of NBDs, we were able to "optimize" site 1 of G551D-CFTR by introducing additional mutations. These mutations rendered the mutant channel ATP-responsive. We demonstrated that the same maneuver could amend the functional defects of ΔF508 channels. Structural and pharmacological implications of our results will be discussed.

4-3. Material and methods

Expression system and electrophysiological recordings

The experimental protocol has been described in detail in a previous report (Tsai et al., 2009). In brief, inside-out patches were obtained from Chinese hamster ovary (CHO) cells expressing WT or mutant CFTR channels. The pipette solution contained (in mM) 140 N-methyl-D-glucamine chloride (NMDG-Cl), 2 $MgCl_2$, 5 $CaCl_2$, and 10 HEPES (pH 7.4). The bath solution contained 150 NMDG-Cl, 2 $MgCl_2$, 10 EGTA and 8 Tris (pH 7.4). CFTR channels were first activated by 2.75 mM MgATP and 50 U / ml PKA until the current reached a steady state. All test solutions contained 10 U / ml PKA to maintain phosphorylation level. The concentration for ATP, PATP, and PPi were 2.75 mM, 50 μM, and 2 mM, respectively for all experiments. Membrane potential was held at -60 mV and the inward chloride current was inverted for clearer data presentation. Perfusion solutions were exchanged using a fast perfusion change device SF-77B (Warner Instrument Cop.) with a dead time of ~30 ms.

Data analysis and statistics

Measurements of steady state macroscopic current amplitude and fitting of current relaxations were done using the Igor Pro program (v 4.07, Wavemetrics). Recordings with less than 4 simultaneous opening steps were selected for single-channel kinetic analysis. These data were filtered at 50 Hz and analyzed using software kindly provided by Dr. Csanády (Csanady, 2000). A three-state kinetic model, C↔O↔B, was adopted to extract kinetic parameters. The fold-increase of opening rate presented in Fig. 4F were estimated by the equation $Rco\text{-}_{ATP}/Rco\text{-}_{basal} = I_{ATP}/I_{basal} * \tau_{o\text{-}basal}/\tau_{o\text{-}ATP}$, where I_{ATP}/I_{basal} is the ratio of current amplitude in the presence or absence of ATP in macroscopic current recordings (Figs. 4-2B & 4-3E) and $\tau_{o\text{-}basal}/\tau_{o\text{-}ATP}$ is the ratio of mean channel open time measured in the bath or the ATP-containing solutions (Fig. 4-4E). Results were presented as means ± SEM.; n represents the number of independent experiments (marked above the bars in all figures). Student's *t*-test was performed with Sigmaplot (v 8.0, SPSS Science) with $P < 0.01$ considered significant.

4-4. Results

Fig. 4-1A shows a representative current recording of G551D channels in an inside-out patch. It can be seen that the channels failed to respond to ATP and exhibited only spontaneous openings. This "ATP independent gating" is also observed with WT-CFTR in the absence of ATP and has an open probability (Po)

FIGURE 4-1

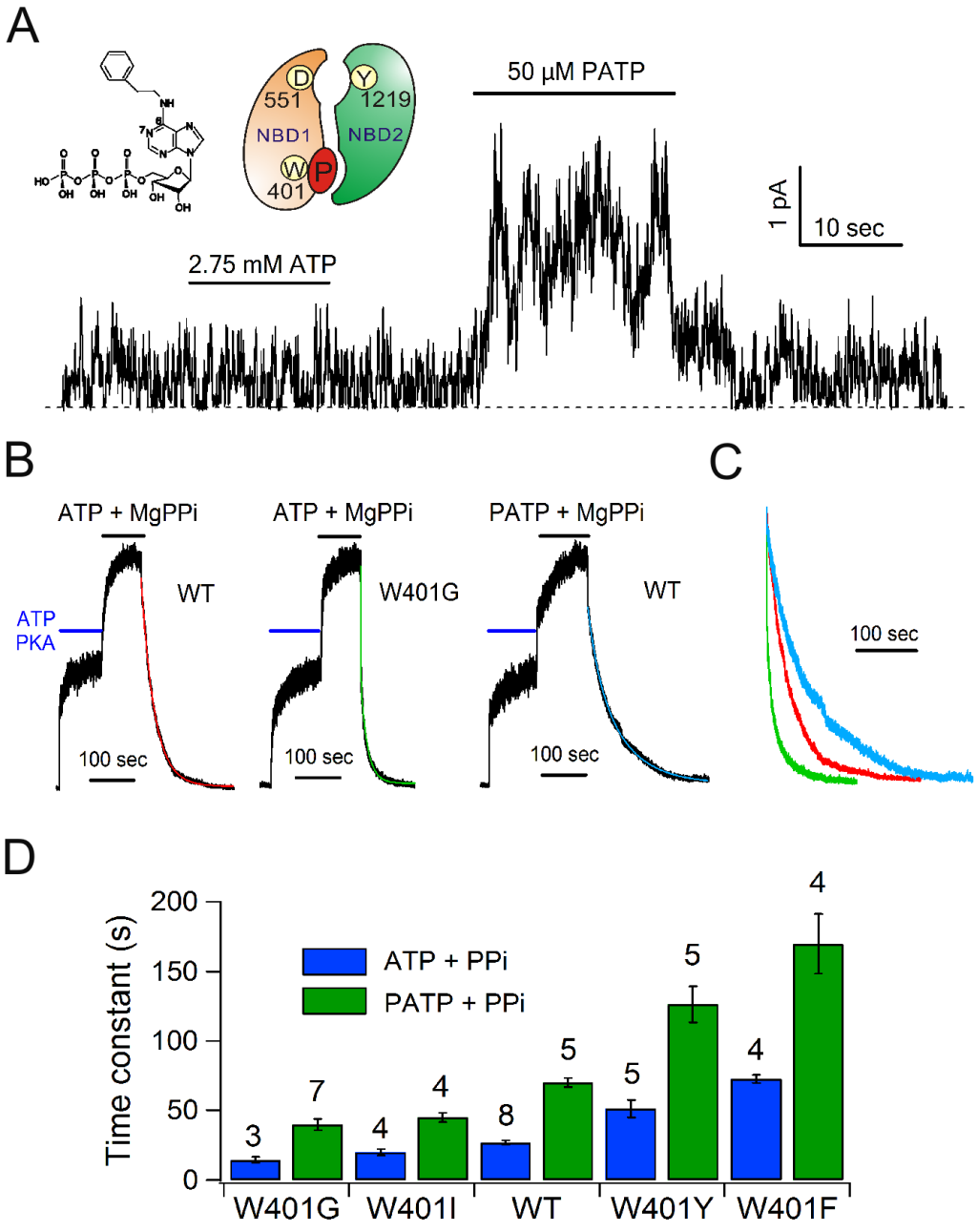
A
D
551
NBD1
Y
1219
NBD2
W
401
P
50 μM PATP
1 pA
10 sec
2.75 mM ATP
B
ATP + MgPPi
ATP + MgPPi
PATP + MgPPi
WT
W401G
WT
ATP
PKA
100 sec
100 sec
100 sec
C
100 sec
D
Time constant (s)
200
150
100
50
0
ATP + PPi
PATP + PPi
3
7
4
4
8
5
5
5
4
4
W401G
W401I
WT
W401Y
W401F

Figure 4-1. An assay to evaluate the effect of W401 mutations on the tightness of NBD1-ATP interactions. (A) A macroscopic current recording of G551D channels, treated with ATP, PATP, or bath solution. Top left, the structural formula of PATP and a cartoon showing that NBD1's core subdomain is the site of PATP's action. **(B)** Current traces showing WT- or W401G-CFTR channels locked open by PPi with ATP or PATP. **(C)** Comparison of current decay traces shown in B. **(D)** The current relaxation time constant upon washout of PPi + ATP (blue bars) or PATP (green bars) for CFTR channels with different W401 mutations.

only ~1% of the maximal Po induced by ATP (Bompadre et al., 2005; Bompadre et al., 2007). Fig. 4-1A also shows that PATP increased the basal activity of G551D-CFTR by ~6-fold. Because this effect was diminished when the conserved aromatic residue that stacks against the adenine ring of ATP in NBD1 (W401) but not in NBD2 (Y1219) was mutated (Lewis et al., 2005; Zhou et al., 2006), we reported previously that PATP potentiates G551D channels by interacting with NBD1 (Bompadre et al., 2008). (Note: the ATP binding site of a monomeric NBD is at the head subdomain.) These findings led to an intriguing question: what's the factor that determines whether or not a ligand can activate G551D-CFTR upon binding to NBD1?

High affinity binding of nucleotides in NBD1 improves the function of G551D channels

As PATP may assume a much higher affinity than ATP in CFTR's NBDs (Zhou et al., 2005; Tsai et al., 2009), we hypothesized that high-affinity binding in NBD1 is essential for a nucleotide ligand to activate G551D channels. If this hypothesis is correct, one would predict that mutations that enhance nucleotide binding in NBD1 will confer ATP-dependent activation and a stronger response to PATP for G551D channels. Identifying such gain-of-function mutations however presents a challenge as an altered ATP affinity in NBD1 is not well reflected by the ATP dose-response relationship of CFTR (Powe et al., 2002; Zhou et al., 2006), due to the fact that gating of WT-CFTR is mainly controlled by ATP binding/hydrolysis in site 2 (Gadsby et al., 2006; Chen and Hwang, 2008).

An opportunity to overcome this difficulty lies in our recent findings that WT channels can be locked open in a configuration where the non-hydrolytic ligand pyrophosphate (PPi) occupies NBD2 (site 2) while ATP or its analogues bind in NBD1 (site 1), and that the stability of this lock-open state is correlated with the strength of nucleotide-NBD1 interactions (Tsai et al., 2009). This idea is recapitulated by the current traces shown in Fig. 4-1B, where the lock-open duration (i.e., current decay constant calculated from traces in Fig. 4-1C) of WT channels elicited by ATP and PPi (left) was shortened by the W401G mutation in NBD1 (middle) but was prolonged when PATP, instead of ATP, was used (right). Thus, by identifying mutations that stabilize the lock-open state, we could design strategies to tighten nucleotide binding in NBD1.

W401 was the first target for mutagenesis as it directly contacts ATP through a ring-ring stacking interaction (Lewis et al., 2005). It is also interesting to note that the equivalent residue at this position in most other ABC proteins is a tyrosine (Ambudkar et al., 2006), raising the possibility that a tyrosine substitution may improve the stacking interaction. Fig. 4-1D summarized the mutational effects of W401 on the mean lock-open duration induced by PPi with ATP or PATP (some of the original traces shown in Fig. 4-S1). As expected, non-conservative substitutions of W401 with Ile or Gly (W401I & W401G), which is unable to stack with ATP, facilitated channel closure from the lock-open state. Not surprisingly either, when applied with PPi, the high affinity ligand PATP was more capable than ATP in maintaining W401 mutants in the lock-open state. Interestingly, we found that phenylalanine (W401F) appeared better than tyrosine (W401Y), which was in turn

superior to tryptophan in stabilizing the lock-open state, suggesting that W401Y and W401F might enhance nucleotide-NBD1 interactions. Supporting this notion, we have shown in our previous report that the W401Y mutation may lead to a prolonged binding of ATP in NBD1 of WT-CFTR (Tsai et al., 2010).

We then incorporated W401Y or W401F mutations into G551D channels, intending to help G551D-NBD1 to bind nucleotide more tightly. The resulting double mutant channels indeed became ATP-responsive and were potentiated to an even greater extent by PATP (Fig. 4-2A). The fold-increase of basal current, as high as ~30-fold, was presented in Fig. 4-2B. It can be seen that W401F, which yielded a more stable lock-open state in the WT background (Fig. 4-1D), was also more effective than W401Y in conferring ATP-dependent activation of G551D channels. Furthermore, in both double mutants, PATP induced more robust potentiation than ATP did. Plotting the lock-open duration shown in Fig. 4-1D with the nucleotide response in Fig. 4-2B yielded a positive correlation (Fig. 4-S2), consistent with our hypothesis that high-affinity binding in NBD1 is critical for a nucleotide to activate G551D channels.

Two concerns over this proposition have to be addressed carefully. First, the response to ATP seen in W401Y (F)/G551D channels could be due to an altered ligand-NBD1 interaction as proposed or alternatively is a result of a restored ability for ATP to gate CFTR through binding to NBD2. We argue that the former is more likely the case since mutating the W401-equivalent residue in NBD2 (Y1219G), which greatly decreases NBD2's ATP affinity (Zhou et al., 2006), had little effect on

FIGURE 4-2

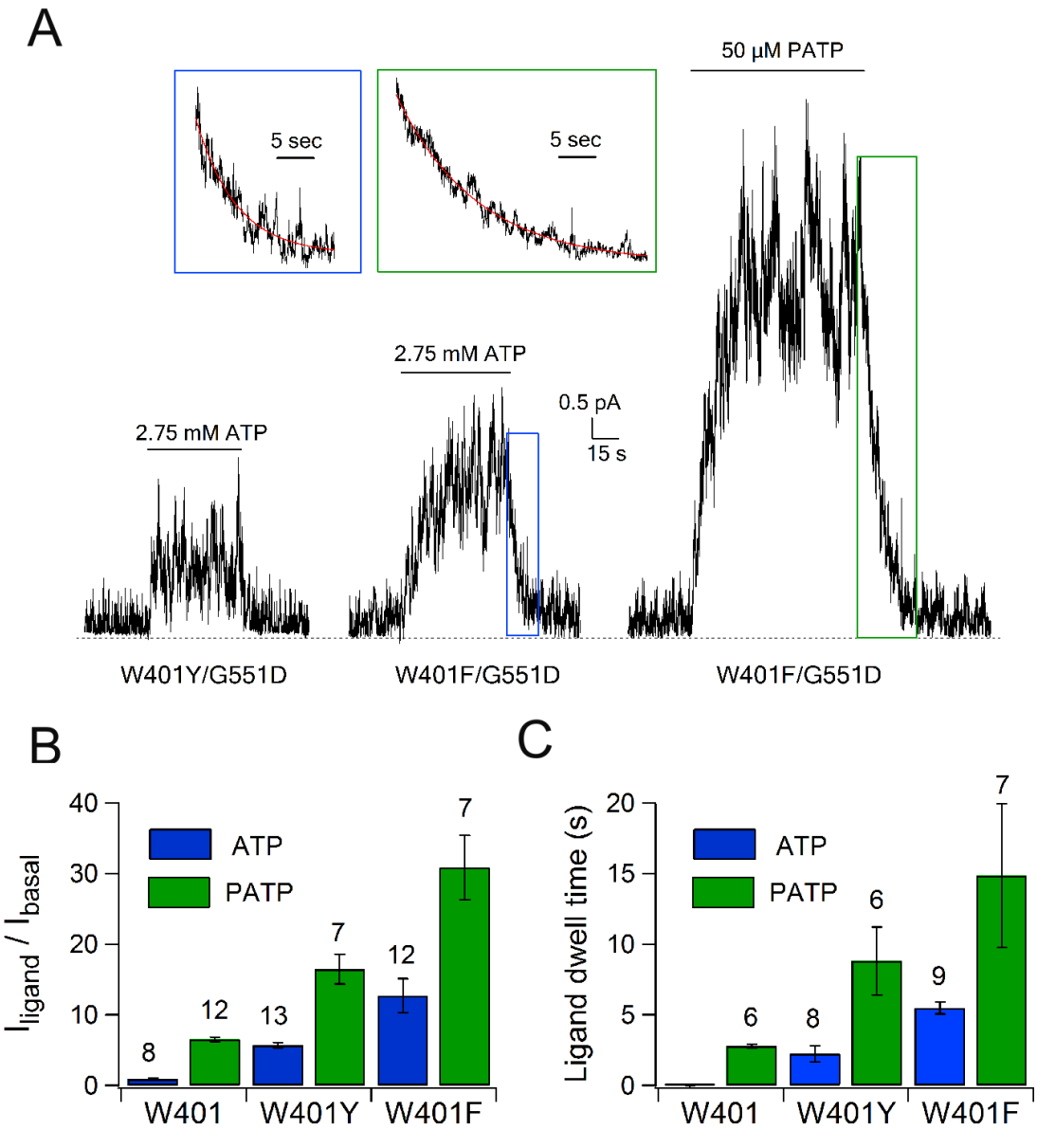
A
50 µM PATP
5 sec
5 sec
2.75 mM ATP
2.75 mM ATP
0.5 pA
15 s
W401Y/G551D
W401F/G551D
W401F/G551D
B
C
ATP
PATP
I ligand / I basal
Ligand dwell time (s)
W401
W401Y
W401F
8
12
13
7
12
7
6
8
6
9
7

Figure 4-2. W401Y and W401F mutations confer ATP dependent activation of G551D channels. (A) Application of ATP or PATP significantly increased currents of W401Y (F)/G551D channels. Inlets, current relaxation traces recorded after the removal of ATP (blue box) or PATP (green box) for W401F/G551D-CFTR. **(B)** The ratio of ATP or PATP induced current over the basal current for G551D channels with or without W401 mutations. **(C)** Fitting current decay traces upon withdrawal of ATP or PATP with a single exponential function yielded time constants reflecting ATP or PATP dwell time in different mutants.

ATP-mediated activation of W401Y (F)/G551D channels (Fig. 4-S3). Second, a more direct way to gauge nucleotide affinity is needed to address whether W401Y/F mutations indeed tighten nucleotide binding in G551D-NBD1. We therefore fitted the current relaxation traces of W401Y (F)/G551D channels upon removal of the nucleotide (Fig. 4-2A, inlet), as the resulting time constants report the mean nucleotide dwell time in NBD1 of these channels. From the data summarized in Fig. 4-2C, it's clear that the two W401 mutations do help G551D-NBD1 to bind nucleotides for a longer period. A comparison of Figs. 4-2B and 4-2C reveals that a longer nucleotide resident time is related to a stronger G551D channels' response to nucleotides (Fig. 4-S2), thus again supporting our proposition that the function of G551D channels can be improved when a nucleotide can bind tightly in NBD1.

G551D channels gain higher activity when NBD1's head and NBD2's tail are tightly connected

We then sought to answer the question: why is tight nucleotide binding in NBD1 so critical for increasing the open probability (Po) of G551D channels? It's noted that the ATP-responsive W401Y (F)/G551D channels had nucleotide dwell times of several seconds (Fig. 4-2C), unusually long for the well exposed ATP binding site in a monomeric NBD1 (Lewis et al., 2004; Lewis et al., 2005). We thus speculated that for these channels, the ATP binding site may be closed by NBD2's signature motif (LSHGH from position 1346 to 1350) so that the ATP molecule can be buried in site 1 without being exposed to the bulk solution (Fig. 4-3A). If this is the case, mutating NBD2's signature motif is expected to facilitate ATP dissociation from NBD1 if the

mutation promotes the disengagement of the two NBDs. We started our experiments by altering S1347 in that its corresponding residue can form a hydrogen bond with ATP's γ-phosphate in dimeric NBD structures of ABC proteins (Smith et al., 2002; Chen et al., 2003). Indeed, the S1347G mutation drastically shortened the mean nucleotide dwell time in NBD1 by ~80% for W401F/G551D channels (Fig. 4-S4). Similar phenomenon was also observed when the conserved L1346 and G1349 residues were mutated (Fig. 4-S4), corroborating the hypothesis that the W401F/G551D channels can adopt conformations where the NBD1's head and NBD2's tail subdomains are engaged to trap nucleotide in site 1 for seconds (Fig. 4-3A).

To relate this conclusion to our original question (see above), it's noted that L1346Q, S1347G (Fig. 4-3B), and G1349I mutations also demolished the nucleotide-dependent activation of W401F/G551D channels. For example, ATP and PATP, which increased the basal activity of W401F/G551D-CFTR by ~12-fold (blue dash line in Fig. 4-3E) and ~30-fold (green dash line) respectively, led to only ~2.5- and ~6-fold current increases when the S1347G mutation was present (Fig. 4-3E). Therefore, the engagement of site 1's two components (NBD1's head and NBD2's tail subdomains) is essential for nucleotide-dependent gating of G551D channels. It follows that W401Y and W401F mutations grant a better function (higher Po) to G551D channels because they favor conformational states where the two constituents of site 1 are connected. This conclusion is consistent with the idea that ATP serves as a molecular glue and thus a stronger ATP-NBD1 interaction (e.g., by W401Y/F) is expected to make ATP stickier for connecting two NBDs together.

FIGURE 4-3

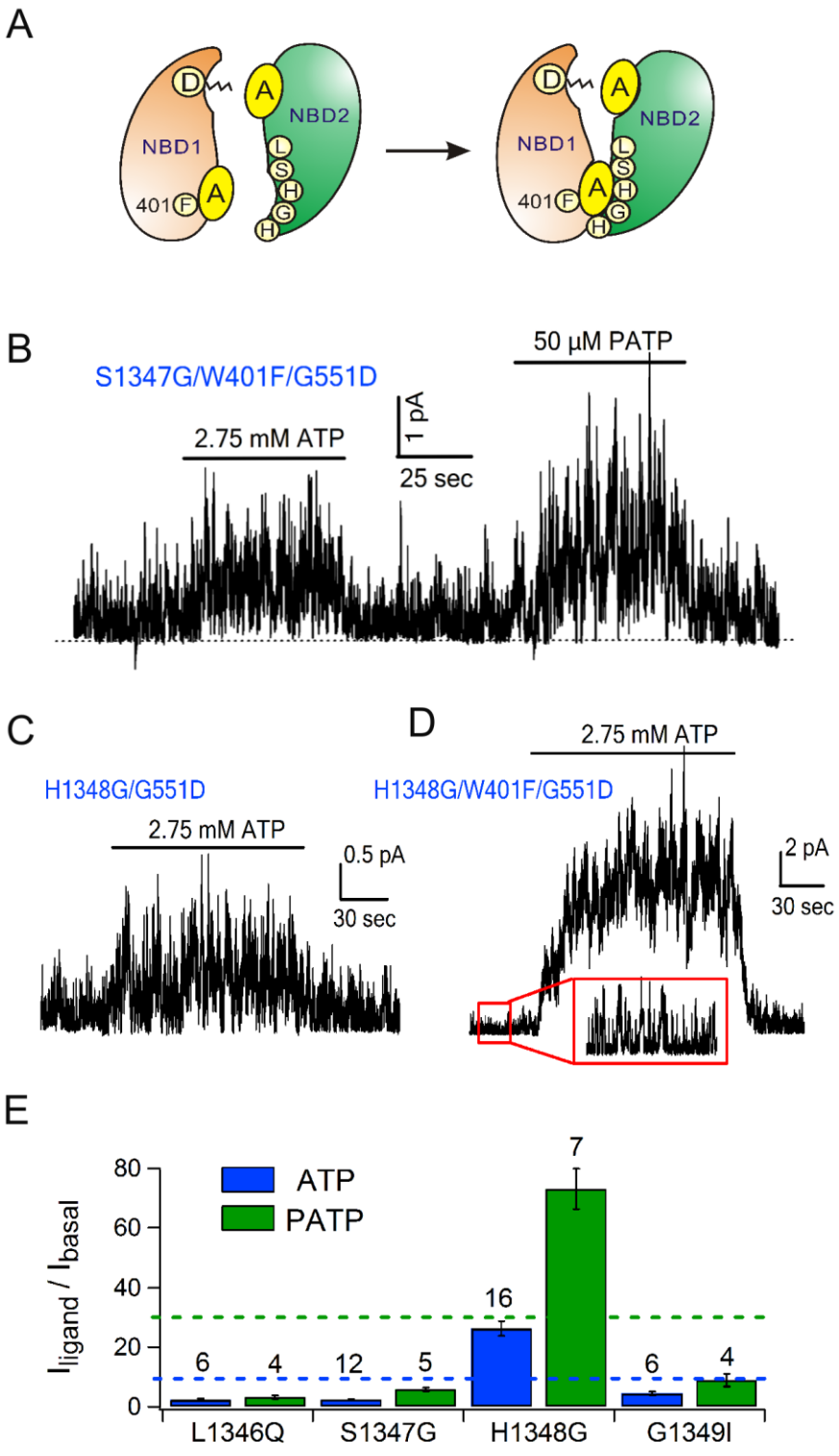
A
NBD1
NBD2
401
B
S1347G/W401F/G551D
2.75 mM ATP
50 µM PATP
1 pA
25 sec
C
H1348G/G551D
2.75 mM ATP
0.5 pA
30 sec
D
H1348G/W401F/G551D
2.75 mM ATP
2 pA
30 sec
E
ATP
PATP
I ligand / I basal
80
60
40
20
0
6
4
12
5
16
7
6
4
L1346Q
S1347G
H1348G
G1349I

Figure 4-3. The role of NBD2's signature motif in mediating ATP-response of optimized G551D channels. (A) A cartoon showing NBD1's ATP binding site closed by NBD2's signature motif. **(B)** The S1347G mutation diminished the response of W401F/G551D channels to ATP or PATP. **(C)** Incorporating the H1348G mutation into G551D-CFTR led to ATP-dependent gating of the mutant channel. **(D)** H1348G enhanced W401F/G551D-CFTR's response to ATP. **(E)** Histogram summarizing the ratio of ATP (blue bars)- or PATP (green bars)-induced current over basal current for W401F/G551D channels combined with a mutation in NBD2's signature motif as marked. Dash lines, the ratio of I_{ATP}/I_{basal} (blue) and I_{PATP}/I_{basal} (green) for W401F/G551D channels.

Here, it should be emphasized again that the nucleotide dependent gating of W401Y (F)/G551D-CFTR is distinct from that of WT-CFTR in that the former is sorely mediated by the nucleotide bound in site 1 without the need of nucleotide-site 2 interactions (Fig. 4-S3).

The idea that both the head of NBD1 and the tail of NBD2 are involved in ATP-dependent activation of W410Y (F)/G551D channels predicts that optimizing ATP's interactions with NBD2's tail subdomain might also improve the function of G551D-CFTR. H1348, the third amino-acid in NBD2's signature motif, is of particular interest as its equivalent residue in most ABC proteins is a glycine. Since this glycine is so close to ATP's phosphate groups in crystal structures of NBD dimers (Smith et al., 2002; Chen et al., 2003), a bulky H1348 side chain may cause a steric clash (Procko et al., 2006) upon closing of the NBD interface. We thus introduced the H1348G mutation into G551D channels. The resulting mutant channel was indeed responsive to ATP and the current in the presence of ATP was 3.9 ± 0.3-fold higher than the basal activity (n = 9, Fig. 3C). Moreover, the H1348G mutation further improved the function of W401F/G551D channels so that the application of ATP and PATP increased the basal activity by ~25- and ~75-fold respectively (Figs. 4-3D-E, 4-S5), again supporting the idea that the response of optimized G551D channels to nucleotides is a result of tight connection between the head of NBD1 and the tail of NBD2.

"Optimized" G551D channels enter into long open bursts

We next examined the channel kinetics for those compound mutants. Current traces in Figs. 4-4A-D show discernible openings and closings of G551D channels with W401 or H1348 mutations, recorded in the presence (upper traces) or absence (lower traces) of ATP. In all cases, an increase of the open time with ATP is apparent by eye inspection. Kinetic analysis (Fig. 4-4E) further revealed that mutants with more robust nucleotide response tend to have a longer mean open time. On the other hand, all tested mutant channels appeared to have a similarly low opening rate (see *Material and Methods* for details of measurements), only becoming ~1.5-fold faster when exposed to ATP (Fig. 4-4F). Therefore, mutations that optimize nucleotide-site 1 interactions only exert slight effects on the opening rate but greatly stabilize the open state once the channel passes through the opening transition process. Possible mechanisms and implications for these observations will be discussed.

W401F and H1348G mutations improve the function of WT and ΔF508 channels

To this point, we have demonstrated that optimizing ATP's interactions with site 1 components, NBD1' head (W401Y & F) and NBD2's tail (H1348G), ameliorates the functional defects of G551D channels. However, it's unclear whether the same maneuver is also effective for other CFTR channels, such as WT- or ΔF508-CFTR, whose opening and closing are mainly controlled by ATP binding and hydrolysis in site 2. A clue came from our previous report showing an allosteric communication

FIGURE 4-4

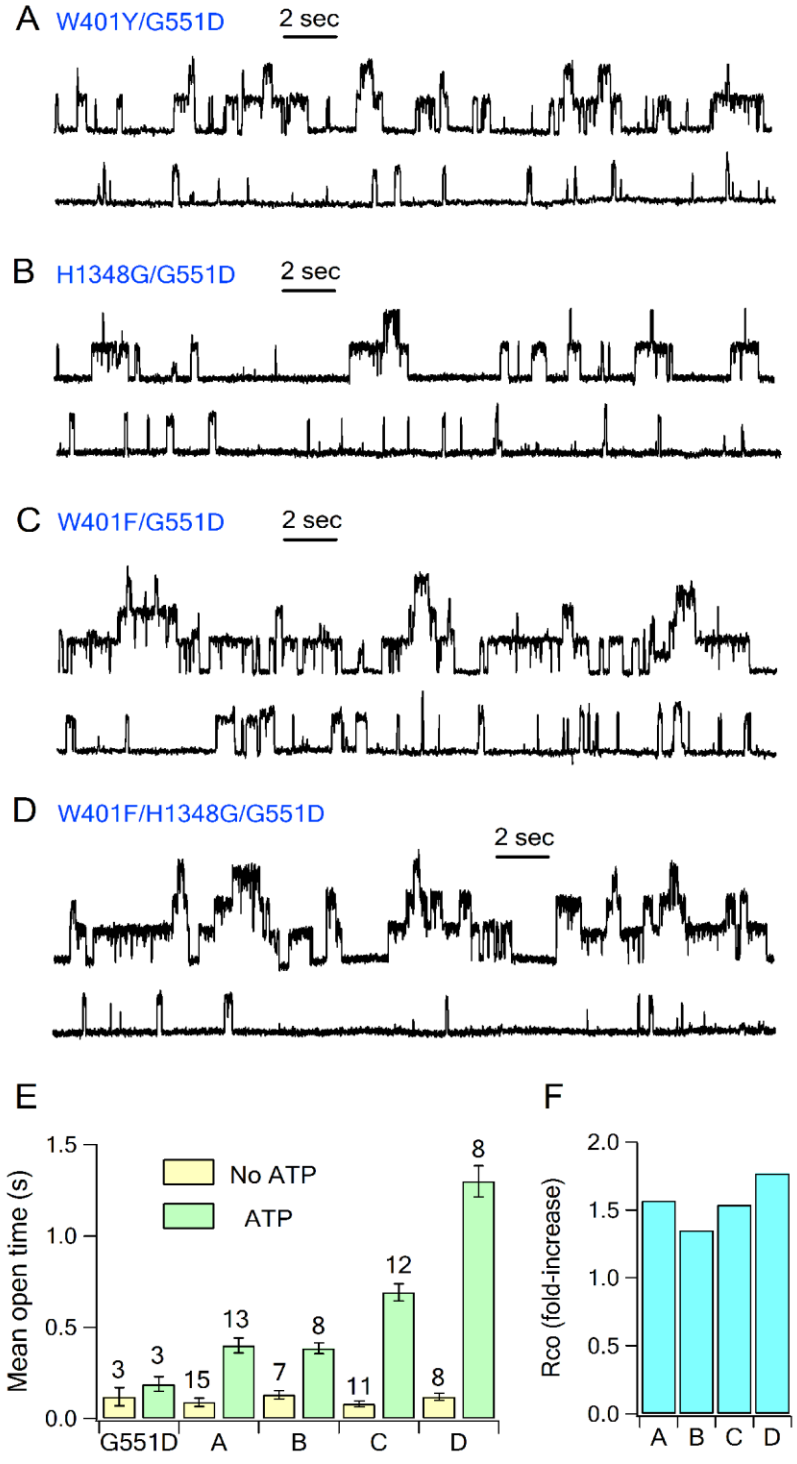
A W401Y/G551D
2 sec
B H1348G/G551D
2 sec
C W401F/G551D
2 sec
D W401F/H1348G/G551D
2 sec
E
Mean open time (s)
1.5
1.0
0.5
0.0
No ATP
ATP
3
3
15
13
7
8
11
12
8
8
G551D
A
B
C
D
F
Rco (fold-increase)
2.0
1.5
1.0
0.5
0.0
A
B
C
D

Figure 4-4. Single channel kinetics of G551D channels with W401Y/F or H1348G mutations. (A-D) Current traces for optimized G551D channels, recorded in the presence (top) or absence (bottom) of 2.75 mM ATP. **(E)** Mean open time for G551D channels and those mutant channels in (A-D). **(F)** Estimated increase of the opening rate upon the application of ATP for mutant channels in (A-D). It's noted that some short openings could be observed for these optimized G551D channels, implicating that ATP-independent openings may still be present. Therefore, it's possible that our kinetic analysis, by lumping all opening events into one single population, could underestimate the true open time of ATP-induced openings. If so, the subsequent calculation (see Materials and Methods) for the opening rate could overestimate the effect of ATP. Nevertheless, these analytic imprecisions do not affect our conclusion that ATP increases the Po of optimized G551D channels mainly by prolonging the channel open time.

between site 1 and site 2: closure of WT-CFTR timed by ATP hydrolysis in site 2 can be delayed by the high affinity ligand PATP bound in site 1 (Zhou et al., 2005). We thus reasoned that optimizing site 1 for ATP binding may slow down closure of WT- and ΔF508-CFTR channels and leads to an increased overall Po. Indeed, when W401F and H1348G mutations were engineered into WT channels (Fig. 4-5A), the mean open time of WT-CFTR was more than quadrupled (Fig. 4-5C) with the already high Po (~0.4) almost doubled (~0.78, Fig. 4-5D). Furthermore, these two mutations similarly prolonged the mean open time of ΔF508 channels (Figs. 4-5B-C) and increased its Po from ~0.03 to ~0.22 (Fig. 4-5D), reaching ~50% of WT activity. In either case, W401F/H1348G mutations did not significantly alter the opening rate (Fig. 4-5E). Therefore, the strategy to restore G551D-CFTR's function by strengthening nucleotide-site 1 interactions also works to augment WT or ΔF508 channels activity.

FIGURE 4-5

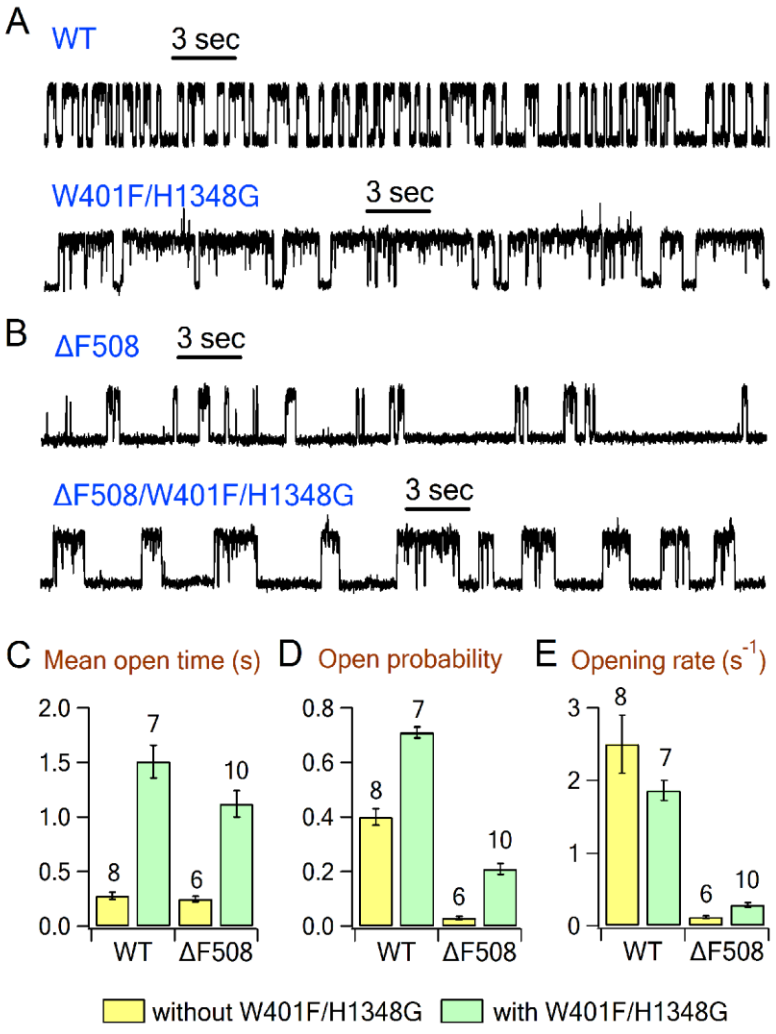

Figure 4-5. Effects of W401F/H1348G mutations on WT and ΔF508 channels. **(A)** 30-s single channel recordings of WT and W401F/H1348G channels exposed to 2.75 mM ATP. **(B)** Current recordings of ΔF508 and ΔF508/W401F/H1348G channels in the presence of 2.75 mM ATP. **(C-E)** Mean open time (C), open probability (D), and opening rate (E) extracted from single channel experiments in (A-B).

4-5. Discussion

The current study was inspired by a puzzling observation that the ATP-irresponsive G551D channel could be activated by PATP, a high-affinity ATP analog. By introducing several gain-of-function mutations that likely strengthen nucleotide-site 1 interactions into G551D-CFTR, we were able to confer ATP responsiveness for this CF-associated mutant. Importantly, this strategy to improve CFTR function is not limited to G551D-CFTR with a disabled site 2; optimization of site 1 is also effectively increasing the Po for WT and ΔF508 channels that rely mostly on site 2 for gating control.

Structural and functional implications for CFTR gating

For WT-CFTR, gating is mainly controlled by ATP binding/hydrolysis in site 2. Several studies have suggested that NBD dimerization induced by ATP binding to NBD2's core subdomain is coupled to the conformational changes in TMDs that open the CFTR pore (Gadsby et al., 2006; Chen and Hwang, 2008). Hydrolysis of the same ATP molecule, now buried in site 2, reverses this process by separating NBD2's core and NBD1's helical subdomains resulting in a partially opened NBD dimer (Tsai et al., 2010). We've shown before that for WT-CFTR this partial dimer state is very stable with NBD1's head and NBD2's tail connected for tens of seconds trapping an ATP molecule in site 1 (Tsai et al., 2010). Here we reported that W401F/H1348G mutations in site 1 prolonged the mean open time of WT-CFTR. Since this compound mutation stabilizes the open state to a similar extent no matter channels close via

hydrolytic (Fig. 4-5C) or non-hydrolytic pathway (Fig. 4-S6), we conclude that an elevated energy barrier for partial NBD separation, rather than an altered ATP hydrolysis rate in site 2, accounts for the stabilized open state. Thus, a tight ATP binding in site 1 can allosterically affect the tightness of connection between the two NBD components in site 2.

For G551D channels, it's anticipated that ATP-induced closure of the interface between NBD2's head and NBD1's tail is energetically unfavorable due to the presence of a negatively charged D551 side chain in NBD1's signature motif. However, it's interesting to ask whether the other interface between NBD1's head and NBD2's tail could close upon ATP binding. Our previous study exploiting a ligand exchange protocol has already suggested that once site 2 is disabled by the G551D mutation, ATP binding at NBD1 either failed to close this interface or only closed it loosely (Tsai et al., 2010). Here, our data provided another level of evidence in support of this proposition. We've noticed a positive correlation between the nucleotide response of an optimized G551D channel and the ATP dwell time in its site 1 (Fig. 4-S2). Thus, the ATP resident time of ~1 s for the S1347G/W401F/G551D channel, which exhibits the weakest response to ATP in the current study, should set the upper limit for the duration when the NBD1's head and NBD2's tail can remain engaged for the G551D channel that fails to respond to ATP. Comparing this short duration with that of WT-CFTR for tens of seconds clearly suggests that an intact site 2 is necessary for a tight interaction between the components of site 1. Therefore, the allosteric communication between site 1 and

site 2 appears to be bi-directional and investigating the underlying mechanism should greatly advance our knowledge toward the dynamics between the two NBDs.

The most drastic result presented here is probably the restored ATP response for G551D channels by W401Y/F and H1348G mutations. Kinetic analysis further showed that in the presence of ATP, these optimized G551D channels exhibited a slow opening rate (Fig. 4-4F) similar to that of ATP-independent gating but a prolonged open time (Fig. 4-4E) comparable to that of site 1-optimized WT-CFTR. As site 2, which mediates rapid channel opening in WT-CFTR, is disabled by the G551D mutation, the slow opening rate is an expected observation. However, it's puzzling how ATP binding in site 1 can induce stabilized open bursts, which led to an increased Po for optimized G551D channels. Three tentative conclusions drawn from the current results may provide a rough picture for the underlying structural mechanism.

First, as the ATP-induced mean channel open time can be modulated by mutations at both the head of NBD1 and the tail of NBD2 (Fig. 4-4E), it's likely that these two subdomains are connected by ATP in the open state. Second, since the ATP dwell time in site 1 (Fig. 4-2C) was much longer than the mean channel open time (Fig. 4-4E), we reasoned that the channel can close without the disengagement of site 1's two NBD constituents (see Fig. 4-S8 for details). Here, if we take one step further in hypothesizing that the open state for optimized G551D channels, like WT-CFTR, also represents an NBD dimer, we can explain the ATP-elicited long open bursts by the same argument used for site 1-optimized WT-CFTR; that is, the tight

ATP-site 1 interaction allosterically delays partial separation of NBDs. However, this NBD dimer state, if exists, may have an unoccupied site 2 to avoid a possible steric clash between ATP and the D551 residue, an idea consistent with our third conclusion that NBD2 could remain vacant during ATP-dependent gating of optimized G551D channels, because the Y1219G mutation, which disrupts ATP binding in NBD2, posed no functional impacts on these channels (Fig. 4-S3). Further experiments will be needed to test the hypothesis that even for G551D-CFTR, NBD dimerization constitutes the fundamental mechanism for coupling NBDs and the gate.

Pharmacological implications for cystic fibrosis

Past few decades have witnessed tremendous progresses on symptom-oriented CF therapeutics that have been translated to the drastically improved life expectancy and quality for patients with CF. Now, the main challenge for the ultimate goal of turning CF into a curable disease is probably to develop therapies that treat the underlying defects of CFTR. To accomplish this, it's necessary to identify chemical compounds called correctors that improve membrane expression of CFTR and potentiators that restore defective CFTR function (Verkman and Galietta, 2009). In the current study, we have demonstrated the impacts of modulating composite site 1 on the function of WT and CF-related mutant CFTR channels. For G551D-CFTR whose maximal Po is only ~1% of that for WT-CFTR (Bompadre et al., 2007), the reported ~75-fold increase of basal current (Fig. 4-3E) implicates that the mutant's activity may potentially be restored to ~75% of WT

level. Similarly, in the presence of site 1 mutations, the Po of ΔF508 channels can approach ~50% of that for WT-CFTR (Fig. 4-5B), thus suggesting that site 1 can be a target for high efficacy CFTR potentiators. An important property for a small molecule drug is its selectivity: the ability to recognize the desired target from hundreds of similar proteins. Site 1 provides a unique opportunity for the design of highly specific drugs as it differs from its catalysis-competent homologues of other ABC proteins by numerous non-canonical substitutions in ATP-interacting motifs. That site 1 of CFTR is not optimized for ATP binding also implicates that a pharmacological reagent of higher affinity than ATP can be practically designed and employed for this particular site.

Two lines of research efforts may help rational drug design targeting CFTR's site 1 in the future. First, as the high-resolution structure of human CFTR-NBD1 is now available for public (Lewis et al., 2005) and the structure for NBD2 has already been determined (PDB code: 3GD7), it can be envisioned that an accurate structural model of CFTR's site 1 could be generated to guide *in silico* screening and synthesis of chemical compounds as candidates of CFTR potentiators. Second, high-throughput screening strategies in the past decade have led to the discovery of numerous CFTR potentiators (Verkman and Galietta, 2009). Examining whether some of these compounds share the same mechanism as H1348G & W401Y/F mutations to potentiate CFTR mutants may provide information about necessary structural properties a molecule must possess to act on site 1. In this regard, VX-770, a potentiator currently in phase III clinical trials in CF patients carrying G551D-CFTR, is of particular interest in that the prolonged open time of G551D-CFTR

channels in the presence of VX-770 appears to be reminiscent of the ATP-dependent gating with gain-of-function mutations described in the current study (Van Goor et al., 2009).

4-6. Supplemental information

FIGURE 4-S1

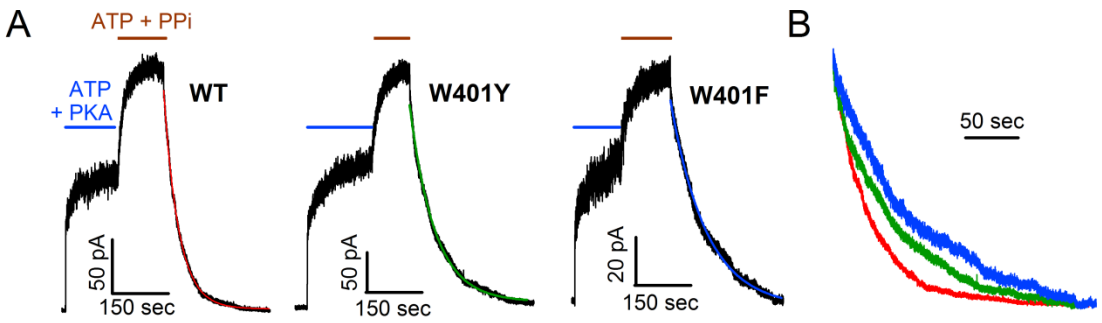

Figure 4-S1. Stabilization of the lock-open state by W401Y and W401F mutations. (A) Current recordings showing WT, W401Y, and W401F channels locked open by ATP and PPi. The same trace of WT-CFTR shown in Fig. 1B is presented for comparison. **(B)** The current decay traces upon removal of ATP and PPi in (A) were compared (red: WT; green: W401Y; blue: W401F). The relaxation time constant follows an order of W401F > W401Y > WT.

FIGURE 4-S2

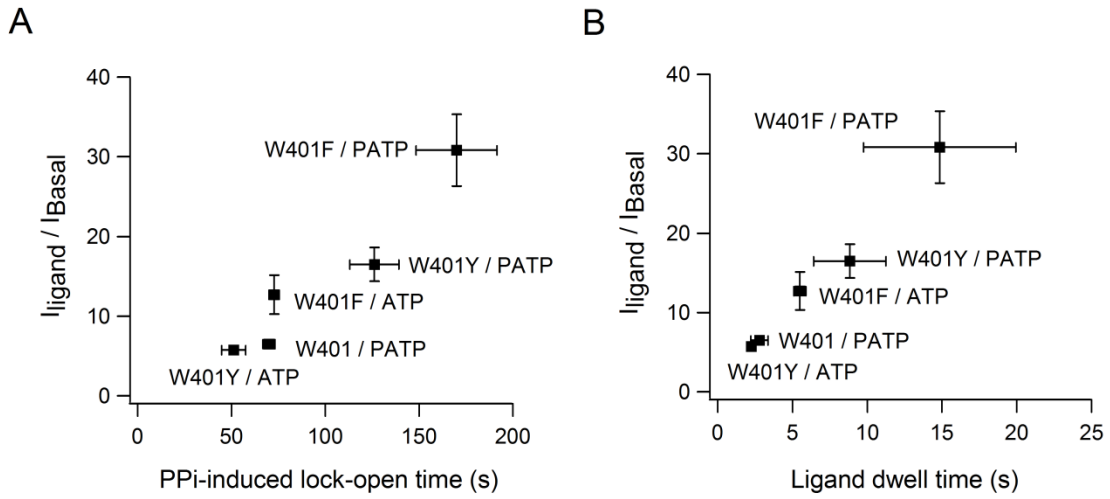

Figure 4-S2. Positive correlations between the nucleotide response of G551D-CFTR and various compound mutants as marked (Y-axes) and the binding strength of the ligand in NBD1 (X-axes). Two different assays were employed to assess ligand binding strength in NBD1: duration of the PPi-induced lock-open state under the WT background (**A**) and nucleotide dwell time measured in NBD1 of G551D or W401Y (F)/G551D channels as shown in Fig. 2C (**B**).

FIGURE 4-S3

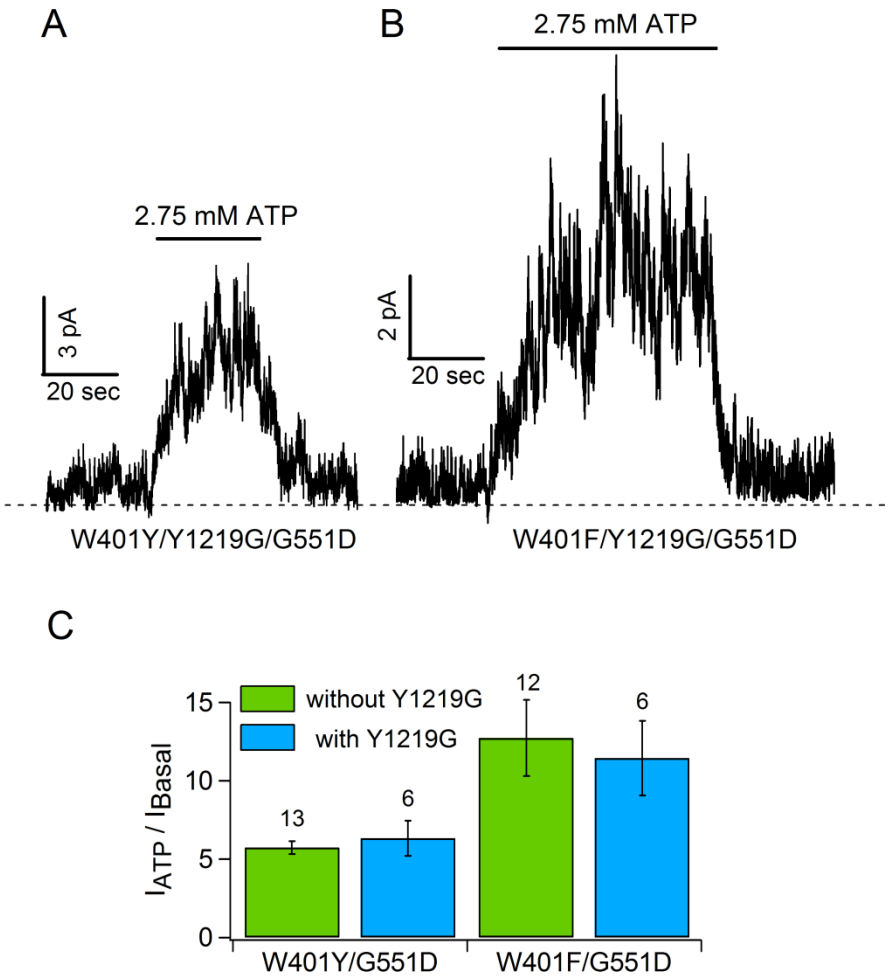

Figure 4-S3. The effect of the Y1219G mutation on the ATP response of W401Y (F)/G551D-CFTR. (A-B) Current recordings showing the response of W401Y (F)/Y1219G/G551D-CFTR to ATP. **(C)** Histogram summarizing the results in (A-B). The Y1219G mutation, which drastically decreases nucleotide binding affinity at the head of NBD2, had little effects on the nucleotide dependent gating of optimized G551D channels.

FIGURE 4-S4

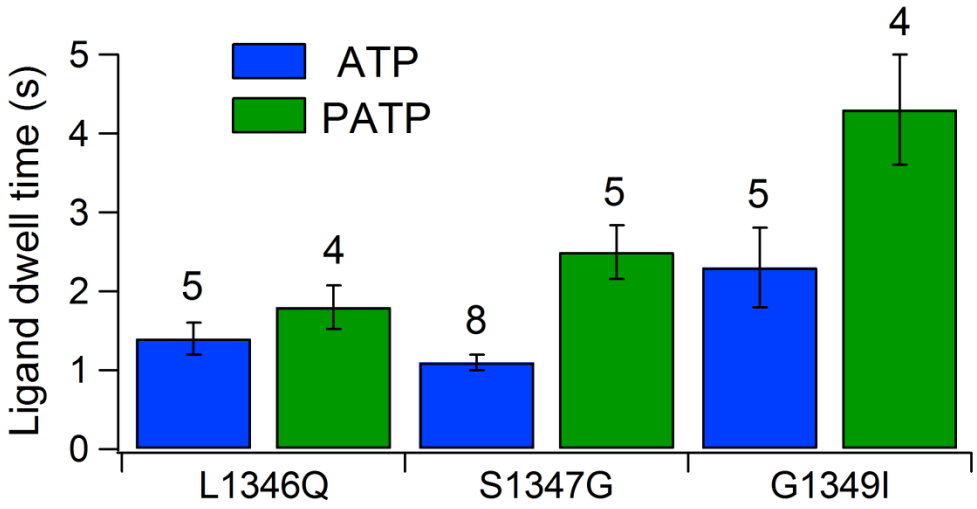

Figure 4-S4. The effect of mutations in NBD2's signature motif (L1346Q, S1347G, and G1349I) on the ligand (ATP or PATP) dwell time in NBD1 of W401F/G551D channels. The dwell times, measured as shown in Fig. 4-2A, were significantly shortened ($P < 0.001$) by all the mutations tested.

FIGURE 4-S5

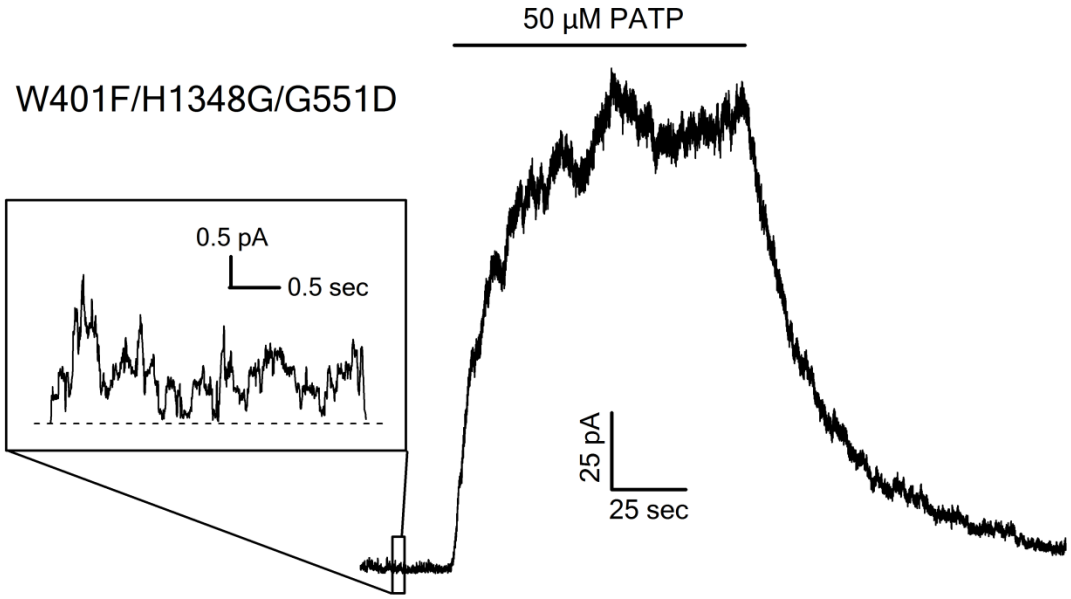

Figure 4-S5. PATP increased the basal current (inlet) of W401F/H1348G/G551D-CFTR by 73.1 ± 10.8-fold (n = 7).

FIGURE 4-S6

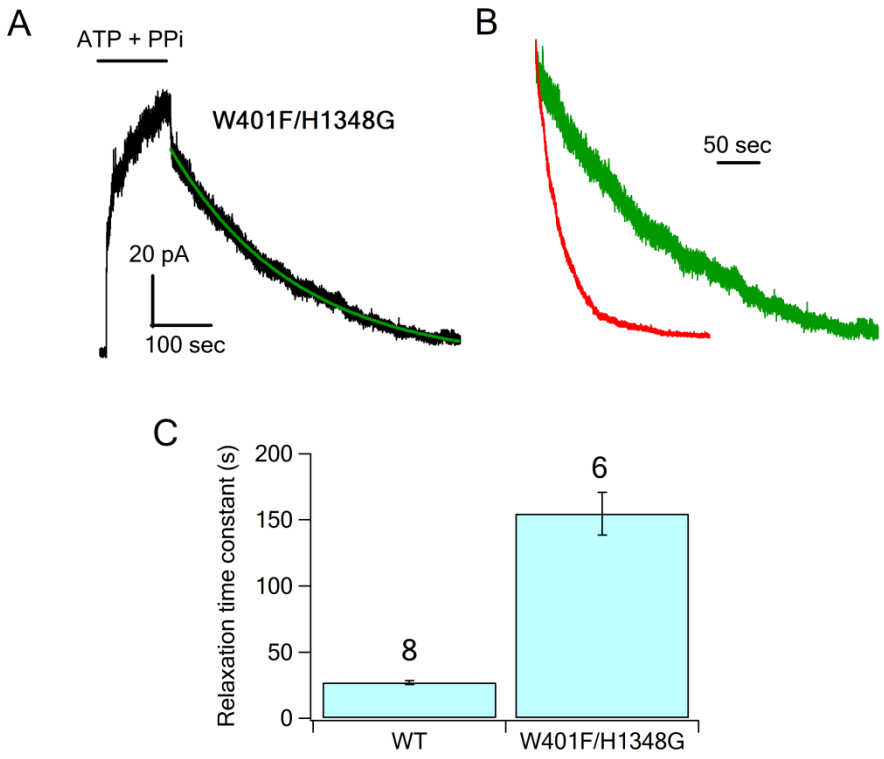

Figure 4-S6. Prolongation of the lock-open time by the compound mutation, W401F/H1348G. (A) A real-time current recording showing a slow current decay upon removal of ATP and PPi for W401F/H1348G channels. **(B)** The current relaxation traces for W401F/H1348G (green) and WT (red) channels upon withdrawal of ATP and PPi were compared. **(C)** Histogram showing the relaxation time constants, which reflect the mean lock-open duration, for WT and W401F/H1348G channels ($P<0.001$).

FIGURE 4-S7

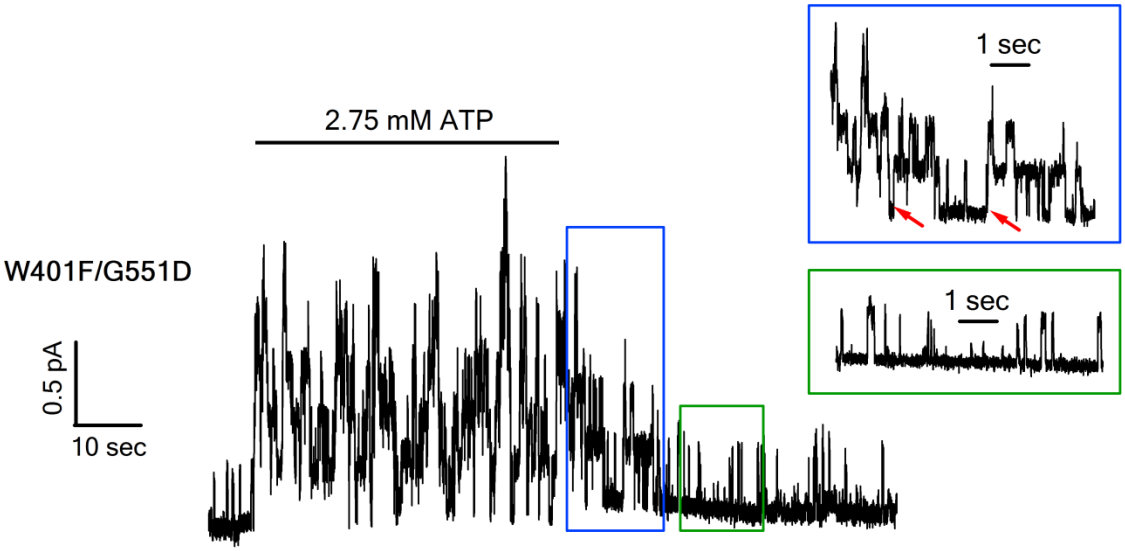

Figure 4-S7. Although the measured open time for optimized G551D channels (Fig. 4E) is much shorter than the ATP dwell time, as described in the legend of Fig. 4, we may have underestimated the true open time for ATP-induced openings due to the presence of some short-lived ATP-independent openings in our current recordings. The current trace shown here provides another level of evidence suggesting that ATP can indeed remain bound in optimized site 1 when the channel is closed. It can be seen that in the initial phase of current decay upon removal of ATP (blue box), the closed W401F/G551D channels can re-enter into long open bursts (red arrows in the blue box). Since there was no continuous supply of ATP, the ATP molecule bound in site 1 before the withdrawal of the ATP solution has to stay in the closed state so as to stabilize any new openings. As a control, we observed that these long

openings disappeared after the ATP-containing solution was removed for several seconds (green box), which is long enough for ATP to dissociate from site 1 (Fig. 4-2C). It's noted that we have assumed here that NBD1's head and NBD2's tail are connected in the closed state to trap ATP in site 1. However, one could argue that it's also possible that the two subdomains may separate in the closed state, where ATP stays bound in NBD1 tightly. This is unlikely the case as the closed time for G551D channels was estimated to be several seconds, too long for an ATP molecule to stay in an exposed NBD1 site. In fact, we've demonstrated that the S1347G mutation, which is expected to weaken the connection between NBD1's head and NBD2's tail, decreased the ATP dwell time in site 1 for W401F/G551D channels to ~1 s, implicating that ATP resident time in the monomeric NBD1 should be even shorter than 1 s.

4-7. References

Ambudkar, S.V., I.W. Kim, D. Xia, and Z.E. Sauna. 2006. The A-loop, a novel conserved aromatic acid subdomain upstream of the Walker A motif in ABC transporters, is critical for ATP binding. *FEBS Lett*. 580:1049-1055.

Bompadre, S.G., T. Ai, J.H. Cho, X. Wang, Y. Sohma, M. Li, and T.C. Hwang. 2005. CFTR gating I: Characterization of the ATP-dependent gating of a phosphorylation-independent CFTR channel (DeltaR-CFTR). *J Gen Physiol*. 125:361-375.

Bompadre, S.G., M. Li, and T.C. Hwang. 2008. Mechanism of G551D-CFTR (cystic fibrosis transmembrane conductance regulator) potentiation by a high affinity ATP analog. *J Biol Chem*. 283:5364-5369.

Bompadre, S.G., Y. Sohma, M. Li, and T.C. Hwang. 2007. G551D and G1349D, two CF-associated mutations in the signature sequences of CFTR, exhibit distinct gating defects. *J Gen Physiol*. 129:285-298.

Chen, J., G. Lu, J. Lin, A.L. Davidson, and F.A. Quiocho. 2003. A tweezers-like motion of the ATP-binding cassette dimer in an ABC transport cycle. *Mol Cell*. 12:651-661.

Chen, T.Y., and T.C. Hwang. 2008. CLC-0 and CFTR: chloride channels evolved from transporters. *Physiol Rev*. 88:351-387.

Csanady, L. 2000. Rapid kinetic analysis of multichannel records by a simultaneous fit to all dwell-time histograms. *Biophys J*. 78:785-799.

Davidson, A.L., and J. Chen. 2004. ATP-binding cassette transporters in bacteria. *Annu Rev Biochem*. 73:241-268.

Davidson, A.L., E. Dassa, C. Orelle, and J. Chen. 2008. Structure, function, and evolution of bacterial ATP-binding cassette systems. *Microbiol Mol Biol Rev*. 72:317-364, table of contents.

Gadsby, D.C., P. Vergani, and L. Csanady. 2006. The ABC protein turned chloride channel whose failure causes cystic fibrosis. *Nature*. 440:477-483.

Kanelis, V., R.P. Hudson, P.H. Thibodeau, P.J. Thomas, and J.D. Forman-Kay. 2010. NMR evidence for differential phosphorylation-dependent interactions in WT and DeltaF508 CFTR. *EMBO J*. 29:263-277.

Lewis, H.A., S.G. Buchanan, S.K. Burley, K. Conners, M. Dickey, M. Dorwart, R. Fowler, X. Gao, W.B. Guggino, W.A. Hendrickson, J.F. Hunt, M.C. Kearins, D. Lorimer, P.C. Maloney, K.W. Post, K.R. Rajashankar, M.E. Rutter, J.M. Sauder, S. Shriver, P.H. Thibodeau, P.J. Thomas, M. Zhang, X. Zhao, and S. Emtage. 2004. Structure of nucleotide-binding domain 1 of the cystic fibrosis transmembrane conductance regulator. *EMBO J*. 23:282-293.

Lewis, H.A., X. Zhao, C. Wang, J.M. Sauder, I. Rooney, B.W. Noland, D. Lorimer, M.C. Kearins, K. Conners, B. Condon, P.C. Maloney, W.B. Guggino, J.F. Hunt, and S. Emtage. 2005. Impact of the deltaF508 mutation in first nucleotide-binding domain of human cystic fibrosis transmembrane conductance regulator on domain folding and structure. *J Biol Chem*. 280:1346-1353.

Miki, H., Z. Zhou, M. Li, T.C. Hwang, and S.G. Bompadre. 2010. Potentiation of disease-associated CFTR mutants by hydrolyzable ATP analogs. *J Biol Chem*.

Ostedgaard, L.S., C.S. Rogers, Q. Dong, C.O. Randak, D.W. Vermeer, T. Rokhlina, P.H. Karp, and M.J. Welsh. 2007. Processing and function of CFTR-DeltaF508 are species-dependent. *Proc Natl Acad Sci U S A*. 104:15370-15375.

Oswald, C., I.B. Holland, and L. Schmitt. 2006. The motor domains of ABC-transporters. What can structures tell us? *Naunyn Schmiedebergs Arch Pharmacol*. 372:385-399.

Powe, A.C., Jr., L. Al-Nakkash, M. Li, and T.C. Hwang. 2002. Mutation of Walker-A lysine 464 in cystic fibrosis transmembrane conductance regulator reveals functional interaction between its nucleotide-binding domains. *J Physiol*. 539:333-346.

Procko, E., I. Ferrin-O'Connell, S.L. Ng, and R. Gaudet. 2006. Distinct structural and functional properties of the ATPase sites in an asymmetric ABC transporter. *Mol Cell*. 24:51-62.

Procko, E., M.L. O'Mara, W.F. Bennett, D.P. Tieleman, and R. Gaudet. 2009. The mechanism of ABC transporters: general lessons from structural and functional studies of an antigenic peptide transporter. *FASEB J*. 23:1287-1302.

Riordan, J.R., J.M. Rommens, B. Kerem, N. Alon, R. Rozmahel, Z. Grzelczak, J. Zielenski, S. Lok, N. Plavsic, J.L. Chou, and et al. 1989. Identification of the cystic fibrosis

gene: cloning and characterization of complementary DNA. *Science*. 245:1066-1073.

Serohijos, A.W., T. Hegedus, A.A. Aleksandrov, L. He, L. Cui, N.V. Dokholyan, and J.R. Riordan. 2008. Phenylalanine-508 mediates a cytoplasmic-membrane domain contact in the CFTR 3D structure crucial to assembly and channel function. *Proc Natl Acad Sci U S A*. 105:3256-3261.

Smith, P.C., N. Karpowich, L. Millen, J.E. Moody, J. Rosen, P.J. Thomas, and J.F. Hunt. 2002. ATP binding to the motor domain from an ABC transporter drives formation of a nucleotide sandwich dimer. *Mol Cell*. 10:139-149.

Tsai, M.F., M. Li, and T.C. Hwang. 2010. Stable ATP binding mediated by a partial NBD dimer of the CFTR chloride channel. *J Gen Physiol*. 135:399-414.

Tsai, M.F., H. Shimizu, Y. Sohma, M. Li, and T.C. Hwang. 2009. State-dependent modulation of CFTR gating by pyrophosphate. *J Gen Physiol*. 133:405-419.

Van Goor, F., S. Hadida, P.D. Grootenhuis, B. Burton, D. Cao, T. Neuberger, A. Turnbull, A. Singh, J. Joubran, A. Hazlewood, J. Zhou, J. McCartney, V. Arumugam, C. Decker, J. Yang, C. Young, E.R. Olson, J.J. Wine, R.A. Frizzell, M. Ashlock, and P. Negulescu. 2009. Rescue of CF airway epithelial cell function in vitro by a CFTR potentiator, VX-770. *Proc Natl Acad Sci U S A*. 106:18825-18830.

Verkman, A.S., and L.J. Galietta. 2009. Chloride channels as drug targets. *Nat Rev Drug Discov*. 8:153-171.

Zhou, Z., X. Wang, M. Li, Y. Sohma, X. Zou, and T.C. Hwang. 2005. High affinity ATP/ADP analogues as new tools for studying CFTR gating. *J Physiol*. 569:447-457.

Zhou, Z., X. Wang, H.Y. Liu, X. Zou, M. Li, and T.C. Hwang. 2006. The two ATP binding sites of cystic fibrosis transmembrane conductance regulator (CFTR) play distinct roles in gating kinetics and energetics. *J Gen Physiol*. 128:413-422.

CHAPTER 5

Future Directions

5-1. Outline

In the past few years, we have witnessed rapid progress of structural and functional mechanisms of CFTR and other ABC proteins. A dynamic picture of CFTR's channel gating has since begun to emerge while at the same time more challenging questions also arise. For instance, we've discussed that closure of CFTR is accompanied with a partial separation of the NBDs at the dimeric state. Nonetheless, it remains largely unclear about why evolution creates a static portion of the NBD interface (i.e. around site 1), about the exact moving trajectory of NBDs upon separation, and about how this NBD motion is transmitted to the CFTR gate. More difficult questions include how ATP binding in one NBD recruits the partner NBD for dimerization, how each submolecular moiety of ATP regulates CFTR gating, what role the energy of ATP hydrolysis plays in the functional cycle of CFTR, etc.

In sections 5-2 and 5-3, I will point out how electrophysiological experiments based on the results presented in previous chapters might help to address a small portion of the aforementioned issues. It's stressed here that I strongly believe that to tackle all these tough issues effectively, we will have to rely on a multidisciplinary approach combining electrophysiological, biochemical, and structural biological

methodologies. It can also be foreseen that computational methods for data-mining and molecular dynamic simulation will play an increasingly more important role in the following years.

One noble goal for studying CFTR is to discover novel strategies for the treatment of CFTR-associated diseases. Although present symptomatic treatment of CF has lengthened the median life of survival for CF patients to over 35 years, treatments that can cure CF are yet to be developed. Recent efforts on high throughput screening of CFTR potentiators and correctors have pushed some pharmaceutical reagents into clinical trials. On the other hand, our identification of site 1 as a potential target for developing CFTR potentiators may also help rational design of CFTR potentiators. In section 5-4, I will discuss possible directions to extend the current research efforts.

5-2. Unidentified intermediate closed states of CFTR

We have demonstrated in chapters 2-4 the power of the patch clamp technique to resolve intermediate states of CFTR channels that are not previously identified by crystallographic studies of ABC proteins mainly because they are less energetically stable compared with other possible conformational states under crystallization conditions. The immediate impact of identifying these intermediates is a better understanding of the structure-function relationship of CFTR channels. Importantly, the information could also provide incentives and guidance for crystallographers to determine the structure of the intermediate state. For instance, based on our

understanding of the partial NBD dimer of CFTR, we've proposed that the NBDs of classical ABC proteins could be crystallized in the partial dimer state once the catalytic residues in only one of the two composite sites are mutated. This section is therefore devoted to *a discussion of theoretically existed, but yet-to-be indentified and characterized intermediate closed states of CFTR as well as possible approaches to investigate these states*.

In chapter 2, we summarized our results with a multiple step channel closing scheme:

$$O_{ATP}^{ATP} \xrightarrow{1} C_{ATP}^{ADP} \xrightarrow{2} C_{ATP} \xrightarrow{3} C$$

where steps 1 and 2 represent rapid ATP hydrolysis and releasing of hydrolytic products from site 2, while step 3 involves a slow dissociation of ATP from site 1. The rates of steps 1 and 2 are faster than 1 s^{-1} as in the presence of ATP at a saturating concentration, a gating cycle of CFTR is completed within 1 second (i.e. the process O →→ C_{ATP} →→ O takes less than 1 second). To determine the rate of step 3, the strategy was to apply PPi at different time points after CFTR channels were closed upon removal of ATP (O →→ C_{ATP}). The concept was that PPi can report the proportion of channels with ATP remained bound in site 1 by re-opening them into the lock-open state. We found that PPi locked open fewer and fewer closed CFTR channels as the duration of washout became longer (Fig. 2-3). In other words, more and more channels lost ATP from site 1 (C_{ATP} → C) with a prolonged washout

time. As the number of channels being locked open by PPi decreased along an exponential curve with a time constant of ~30 s (Fig. 2-4), the rate of step 3 was estimated to be ~0.03 s^{-1}. It's noted that this rate is similar to that derived from ligand exchange experiments described in chapter 3.

Although the kinetic scheme appears to reasonably explain all data presented, a careful re-examination of raw recording traces reveals some problems. In Fig. 5-1 A, it can be seen that a direct switch of solution from 2 mM ATP to 10 mM PPi resulted in a rapid current drop for a duration of ~0.6 s due to channel closure by ATP hydrolysis (Fig. 5-1 A, inlet) and a subsequent slow current increase due to openings of CFTR channels by PPi. The current rising phase can be fitted with an exponential function yielding a time constant of 8.8 ± 2.1 s (n = 5), which presumably reflects the rate (~0.11 s^{-1}) by which 10 mM PPi brings CFTR into the lock-open state. With this slow rate, it's estimated that in a 0.6 s duration, PPi can lock open at most 5% of all channels in the membrane patch. However, it was noticed that in Fig. 5-1A that 0.6 s after solution changes from ATP to PPi, ~25 % of channels has entered the lock-open state (see Y-axis)! Thus, it appears that shortly after ATP/PPi solution exchanges, there are at least two groups of closed channels with site 2 vacated but site 1 occupied by ATP: one group (C_{ATP-F}) can respond to PPi rapidly while another group (C_{ATP-S}) responds to PPi much slowly. Corroborating this proposition, after 5 s of washout of ATP and all CFTR channels were closed, the application of PPi in fact induced a slow (τ = 7.6 ± 1.3 s, n = 3) and a fast (τ = 0.9 ± 0.4 s, n = 3) phases of current increase (Fig. 5-1B).

FIGURE 5-1

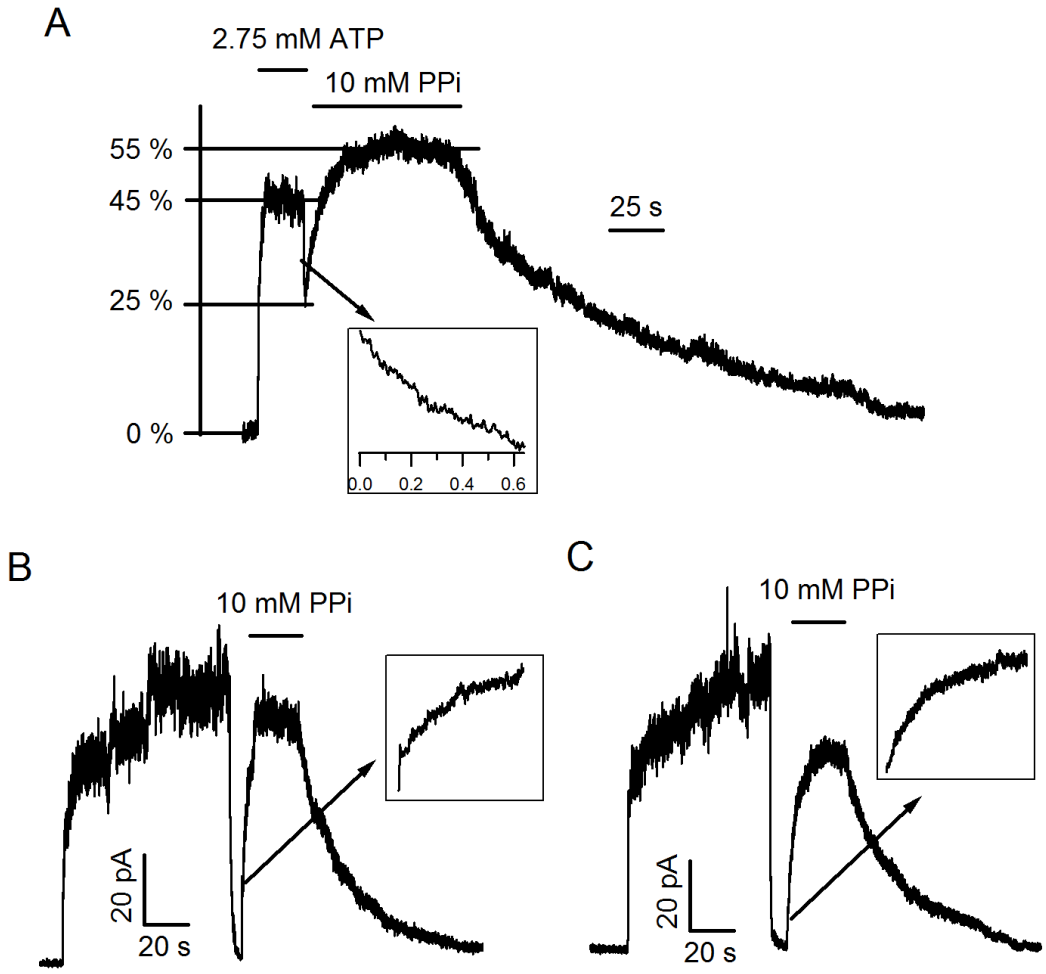

Figure 5-1. Clues for unidentified closed states of CFTR. **(A)** ATP solution was switched to 10 mM PPi, resulting in a current drop (inlet) and then a slow current increase. The left hand axis shows the percentage of all channels in the open state, assuming that ATP induced a Po of 0.45. **(B)** PPi was applied 5 s after the removal of ATP. Pay attention to the biphasic current rising (inlet). **(C)** 10 s after washing of ATP, PPi no longer induced fast openings (inlet).

In addition to their different speeds of responding to PPi, it was also observed that the C_{ATP-F} state is much short-lived than the C_{ATP-S} state. Fig. 5-1C shows that the fast current increase phase seen in Fig. 5-1B disappeared when PPi was applied 10 or 20 s after the withdrawal of ATP, indicating that once the supply of ATP is discontinued, the C_{ATP-F} state dissipates within 10 s! For a further investigation of the C_{ATP-S} and C_{ATP-F} states, it's desirable to identify other more distinguishable properties between these two states. One possible difference might be the mean burst duration of the lock-open states induced by PPi's interactions with the two states. This could be readily tested by removing PPi solution right or long after solution changes from ATP to PPi and measuring the time constant of the subsequent current decay.

Of course, the more interesting question is: what is the structural basis underlying the different responses of the C_{ATP-S} and C_{ATP-F} states to PPi? More experiments are certainly needed to tackle this challenging issue. Here, I want to point out that first of all, one has to ask how the C_{ATP-F} state is related to other identified states of CFTR. For example, two possible scenarios are:

Scheme 5-1.

$$C_{ATP-F} \leftarrow O_{ATP}^{ATP} \rightarrow C_{ATP-S}$$

Scheme 5-2.

$$O_{ATP}^{ATP} \rightarrow C_{ATP-F} \rightarrow C_{ATP-S}$$

To differentiate these two schemes, one should take advantage of the power of the fast solution change system to observe channels' response to PPi 1 s, 2 s, up to 5 s after the removal of ATP. Scheme 5-1 predicts that the amplitude of the slow component (see Fig. 5-1B) of PPi-induced current rising phase will only decrease as the washout duration is extended. On the other hand, scheme 5-2 predicts that the amplitude of the slow component will increase as a longer washout time is accompanied by more channels entering into the C_{ATP-S} state from the C_{ATP-F} state. Here, I would like to stress that our thinking should not be limited by schemes 5-1 and 5-2, as there are certainly more possible kinetic schemes that could relate the C_{ATP-F} state to those known states. Once we are able to incorporate the C_{ATP-F} state into the current kinetic model of CFTR gating, interpretation of mutational effects of NBD residues will be easier.

There are more mysteries surrounding the ligand PPi that our current model fails to explain. For example, it can be seen in Fig. 5-1A that ATP/PPi exchange resulting in only **~55 %** of channels in the membrane patch locked in the open state. This is in conflict with our kinetic model:

$$C \xleftarrow{0.03\ s^{-1}} C_{ATP} \xrightarrow{0.12\ s^{-1}} O_{ATP}^{PPi}$$

which leads to the estimation that **80 %** of channels should eventually enter the lock-open state! (It's noted that leaving of the channel from the O_{ATP}^{PPi} state can be neglected during modeling as experimental results have shown that a continuous

application of PPi maintained the channels in this state.) Thus, to account for this result, it's needed to have a more complicated kinetic model involving more states.

From the above mentioned "odd" results, it becomes more and more certain that our understating to the intermediate closed states of CFTR is still very limited. However, it's also fortunate that we have PPi as a tool which has already taught us so much and now even given us clues about how and what to explore in the near future.

5-3. The need of a re-examination of site 1 functions

We have concluded in early sections that the NBD interface around site 1 is relatively static compared with that around site 2, likely due to the impaired ATPase activity of CFTR's site 1. This proposition raises some interesting questions: Why does CFTR lose catalytic ability of a composite site during evolution? Is the stationary NBD interface around site 1 simply a by-product when site 1's ATPase activity is lost or does it represent an evolutionary adaptation and thus actually have an important functional role in supporting CFTR gating?

It's a great challenge to come up with a definitive answer for the first question as it's unlikely to figure out all possible benefits a non-catalytic ATPase site could bring to an ABC protein. Nonetheless, it seems reasonable to speculate that disabling ATPase funtion can help an organism to improve its energy efficiency, if the energy

for hydrolyzing one ATP molecule is sufficient to support the function of ABC proteins. This advantage could be quite significant at least for prokaryotes, as the genes that encoding ABC proteins may occupy up to one fourth of their whole genome.

The literature has already provided some clues about how ABC proteins with a degenerated ATPase site may have evolved. It has been reported that the yeast mitochondrial ABC transporter Mdl1P hydrolyzes two ATP molecules for a transport cycle (Janas et al., 2003) while it takes only one ATP hydrolysis for human P-glycoprotein (PgP), which resided at the cell membrane (Urbatsch e al., 1995). Since both Mdl1P and PgP are classical ABC proteins with two functional ATPase sites, one may wonder why there are different energy requirements for transport. I envisage that the primordial ABC proteins, such as those resided in mitochondria, may evolve to improve energy efficiency, resulting in a group of ABC proteins, like PgP, that could extract sufficient energy from one ATP molecule to perform their functions. Once these ABC proteins have evolved, one of the two ATPase sites can become degenerated without having a major impact to protein functions, thus leading to the birth of atypical (or asymmetrical) ABC proteins. Indeed, phylogenic studies have shown that the classical ABC protein human PgP (ABCB1) is a close relative to several atypical human ABC proteins, such as TAP1 (ABCB2), TAP2 (ABCB3), MRPs (ABCC1-6), CFTR (ABCC7), and etc (see procko et al., 2006). This hypothesis could be further tested by systemic biochemical studies of ATPase activity for different ABC proteins in the phylogenic trees, which have long been established (Davidson et al., 2008).

If a dead ATPase site was selected purely for energy saving, it might be thought that the stationary NBD interface around site 1 is merely a by-product of the evolutionary process without having a significant functional relevance. This idea can theoretically be tested by mutating residues, such as K464, W401, or LSHGH, that are critical for maintaining the connection between two NBD constituents of site 1. In fact, our group has previously reported that the W401G and K464A mutations pose only slight effects on the overall CFTR open probability (<10 %). This result appears to indicate that CFTR can function normally without a need of a stable connection between NBD1's head and NBD2's tail.

The structure of human PgP solved in the apo form (Aller et al., 2009), however, raises a red flag for this line of thoughts. The two monomeric NBDs of PgP was reported to separate for a distance of >10 Å! It can be envisioned that if there exists such a distance between CFTR's NBDs, it might require much more work for two NBDs to form a dimer from the resting state than from the partial dimer state, where the two NBDs has already been partially connected. Furthermore, the findings that the G1349D (Bompadre et al., 2007) and S1347G (chapter 3) mutations in NBD2's signature motif (in the tail subdomain) significantly decrease CFTR opening rate by ~10- and ~3-fold respectively also corroborate the idea that a tightly closed NBD interface around site 1 is required for normal CFTR function.

To solve the mystery, the first task is to reconcile the conflicting experimental results that mutations at NBD2's tail (S1347G and G1349D) and NBD1's head (W401G and K464A) have quite different impacts on CFTR function. As CFTR gating

is severely impaired with a glycine to aspartate mutation at position 1349 (G1349D), it's possible that less drastic substitutions, such as W401G and K464A, may not destabilize the NBD interface around site 1 sufficiently to yield detectable changes of CFTR gating. This idea could be tested by studying the function of K464D-CFTR, W401D-CFTR, or a complex mutant W401G/K464A-CFTR. In fact, I have observed that PATP elicited a current ~4-fold higher than that induced by ATP for K464D channels, indicating that the Po for this mutant gated by ATP cannot be higher than 0.25, a number already ~50% lower than the maximal Po of ~0.45 for WT-CFTR treated with ATP.

Even if the above mentioned conflicting results can be successfully reconciled, there exist many other challenges. For instance, as the direct effect of mutations at W401 or K464 is presumably a disrupted ATP binding in NBD1's head subdomain, which then causes a destabilized connection between the NBD1 head and NBD2 tail, it is unclear whether these mutations impair CFTR gating by affecting ATP binding or the NBD1 interface around site 1. Using a crosslinker, instead of ATP, to connect the two NBD subdomains that form site 1 might be a possible approach to deal with this issue.

The ultimate question here is that if a stationary NBD interface around site 1 is essential for CFTR opening and closing, why is it essential at all? I cannot see a clear overall strategy to tackle this difficult issue at the current moment before more experimental results materialize and would like to leave this question as a major challenge for readers who are interested in pursuing this direction of research.

5-4. Toward rational design of CFTR potentiators

In chapter 4, we have pointed out that site 1 of CFTR can serve as a potential target for developing CFTR potentiators. Nonetheless, compared with random screening, knowledge based drug design is very technically challenging in nature and it's therefore very important to learn from those few successful examples and to be aware of what knowledge we currently have and don't have.

There are two major approaches for drug design. One is referred to as ligand-based drug design. This strategy involves iterative modifications of the structure of known ligands relying on knowledge about the necessary structural properties a molecule must possess to act on the biological target of interest. The second is called structure-based drug design. This method relies on 3D structures of the molecular target to predict chemical compounds with desired pharmaceutical properties. It's noted that the two approaches are not mutually exclusive and can in fact become complementary to each other when there are well established knowledge bases for both the ligand and the biological target (for example, see Tran et al., 2009).

What strategy should be adopted to design potentiators targeting CFTR's site 1? As there is currently no established method to crystallize CFTR's NBDs in the dimeric state, the power of structure-based approach is greatly reduced. Modeling site 1 using monomeric NBD structures of CFTR or dimeric structures of other ABC proteins may serve as an alternative, while the degree of accuracy for computational methods might be a potential problem in the long run. On the other hand, it's also

quite disappointing that we have very limited information about structural characteristics that are necessary for a chemical compound to bind in site 1 as a potentiator. However, it's fortunate that random screenings in the past several years have led to the identification of many CFTR potentiators. If some of these potentiators exert their effects by interacting with site 1, they could reasonably serve as initial compounds for structural modifications.

I therefore propose that the first step toward rational design of CFTR potentiator is to examine whether some of those existent potentiators may act on site 1. This task could readily be done by testing for competition between a potentiator and ATP on G551D channels, where ATP can be considered as a competitive inhibitor for the potentiator's action on G551D-site 1. If this step fails to yield desired results, it's the authors believe that the efforts to design a potentiator working on site 1 should be seized and it'll be more cost efficient to perform random structural modifications of existent potentiators or simply initiate a new round of high throughput drug screening.

If an initial compound described above can be discovered, chemical modifications of this compound by a synthetic chemist and testing of the newly synthesized chemicals by an electrophysiologist should greatly advance our knowledge toward the chemistry at site 1. With more experimental data about site 1-ligand interactions and with solved NBD structures of ABC proteins, a computational chemist should be able to build more accurate structure-based model, which can provide valuable

information guiding further modifications of existent pharmaceuticals or even predicting new drug candidates.

5-5. References

Aller, S.G., J. Yu, A. Ward, Y. Weng, S. Chittaboina, R. Zhuo, P.M. Harrell, Y.T. Trinh, Q. Zhang, I.L. Urbatsch, and G. Chang. 2009. Structure of P-glycoprotein reveals a molecular basis for poly-specific drug binding. *Science*. 323:1718-1722.

Bompadre, S.G., Y. Sohma, M. Li, and T.C. Hwang. 2007. G551D and G1349D, two CF-associated mutations in the signature sequences of CFTR, exhibit distinct gating defects. *J Gen Physiol*. 129:285-298.

Davidson, A.L., E. Dassa, C. Orelle, and J. Chen. 2008. Structure, function, and evolution of bacterial ATP-binding cassette systems. *Microbiol Mol Biol Rev*. 72:317-364, table of contents.

Janas, E., M. Hofacker, M. Chen, S. Gompf, C. van der Does, and R. Tampe. 2003. The ATP hydrolysis cycle of the nucleotide-binding domain of the mitochondrial ATP-binding cassette transporter Mdl1p. *J Biol Chem*. 278:26862-26869.

Procko, E., I. Ferrin-O'Connell, S.L. Ng, and R. Gaudet. 2006. Distinct structural and functional properties of the ATPase sites in an asymmetric ABC transporter. *Mol Cell*. 24:51-62.

Tran, C., S. Ouk, N.J. Clegg, Y. Chen, P.A. Watson, V. Arora, J. Wongvipat, P.M. Smith-Jones, D. Yoo, A. Kwon, T. Wasielewska, D. Welsbie, C.D. Chen, C.S. Higano, T.M. Beer, D.T. Hung, H.I. Scher, M.E. Jung, and C.L. Sawyers. 2009. Development of a second-generation antiandrogen for treatment of advanced prostate cancer. *Science*. 324:787-790.

Urbatsch, I.L., B. Sankaran, J. Weber, and A.E. Senior. 1995. P-glycoprotein is stably inhibited by vanadate-induced trapping of nucleotide at a single catalytic site. *J Biol Chem*. 270:19383-19390.

VITA

Ming-Feng Tsai was born April 20, 1985, in Kaohsiung county, Taiwan. He attened elementary and high schools in Kaohsiung city near his hometown. In 2003, he moved to Taipei city, the capital city of Taiwan, for college education in Natioanl Yang-Ming University, where he majored in Medicine. In 2007, he was admitted into the PhD program in the Department of Medical Pharmacology and Physiolgy in the University of Missouri. He expects to graduate in July, 2010 and will continue his academic career as a postdoctoral researcher.